การระบุโปรตีนเป้าหมายของแอลฟา-2-แมคโครโกลบูลินของกุ้งขาว *Litopenaeus vannamei* โดยเทคนิคทางชีวเคมีและการจำลองแบบเชิงโมเลกุล

นายวิศว์ชนนท์ วงศ์บัวชื่น

วิทยานิพนธ์นี้เป็นส่วนหนึ่งของการศึกษาตามหลักสูตรปริญญาวิทยาศาสตรมหาบัณฑิต
สาขาวิชาชีวเคมีและชีววิทยาโมเลกุล ภาควิชาชีวเคมี
คณะวิทยาศาสตร์ จุฬาลงกรณ์มหาวิทยาลัย
ปีการศึกษา 2557

IDENTIFICATION OF TARGET PROTEIN OF ALPHA-2-MACROGLOBULIN FROM WHITE SHRIMP *Litopenaeus vannamei* BY BIOCHEMICAL AND MOLECULAR MODELING TECHNIQUES

Mr. Witchanon Wongbaucheun

A Thesis Submitted in Partial Fulfillment of the Requirements
for the Degree of Master of Science Program in Biochemistry and Molecular Biology
Department of Biochemistry
Faculty of Science
Chulalongkorn University
Academic Year 2014

Thesis Title	IDENTIFICATION OF TARGET PROTEIN OF ALPHA-2-MACROGLOBULIN FROM WHITE SHRIMP *Litopenaeus vannamei* BY BIOCHEMICAL AND MOLECULAR MODELING TECHNIQUES
By	Mr. Witchanon Wongbaucheun
Field of Study	Biochemistry and Molecular Biology
Thesis Advisor	Professor Anchalee Tassanakajon, Ph.D.
Thesis Co-Advisor	Assistant Professor Kunlaya Somboonwiwat, Ph.D.
	Thanyada Rungrotmongkol, Ph.D.

Accepted by the Faculty of Science, Chulalongkorn University in Partial Fulfillment of the Requirements for the Master's Degree

.....Dean of the Faculty of Science
(Professor Supot Hannongbua, Dr.rer.nat.)

THESIS COMMITTEE

.....Chairman
(Assistant Professor Manchumas Prousoontorn, Ph.D.)

.....Thesis Advisor
(Professor Anchalee Tassanakajon, Ph.D.)

.....Thesis Co-Advisor
(Assistant Professor Kunlaya Somboonwiwat, Ph.D.)

.....Thesis Co-Advisor
(Thanyada Rungrotmongkol, Ph.D.)

.....Examiner
(Assistant Professor Kanoktip Packdibamrung, Ph.D.)

.....External Examiner
(Associate Professor Apinunt Udomkit, Ph.D.)

วิศว์ชนนท์ วงศ์บัวชื่น : การระบุโปรตีนเป้าหมายของแอลฟา-2-แมคโครโกลบูลินของกุ้งขาว *Litopenaeus vannamei* โดยเทคนิคทางชีวเคมีและการจำลองแบบเชิงโมเลกุล (IDENTIFICATION OF TARGET PROTEIN OF ALPHA-2-MACROGLOBULIN FROM WHITE SHRIMP *Litopenaeus vannamei* BY BIOCHEMICAL AND MOLECULAR MODELING TECHNIQUES) อ.ที่ปรึกษาวิทยานิพนธ์หลัก: อัญชลี ทัศนาขจร, อ.ที่ปรึกษาวิทยานิพนธ์ร่วม: กุลยา สมบูรณ์วิวัฒน์, ธัญญดา รุ่งโรจน์มงคล, 174 หน้า.

แอลฟา-2-แมคโครโกลบูลิน (A2M) เป็นตัวยับยั้งโปรติเอสที่มีความอนุรักษ์ในสายวิวัฒนาการ ในสัตว์ไม่มีกระดูกสันหลังรวมถึงกุ้ง A2M มีบทบาทที่สำคัญอย่างมากในการตอบสนองทางภูมิคุ้มกัน ในที่นี้ A2M ในกุ้งขาว *Litopenaeus vannamei* (*Lv*A2M) ได้นำมาศึกษาหน้าที่ในระบบภูมิคุ้มกันในการยับยั้งโปรติเอสจากเชื้อแบคทีเรีย โดยทำการผลิตโปรตีนรีคอมบิแนนท์ *Lv*A2M (r*Lv*A2M) ซึ่งจะมีน้ำหนักโมเลกุล และค่า pI เท่ากับ 166.9 กิโลดาลตัน และ 5.77 ตามลำดับ ในแบคทีเรีย *Escherichia coli* แต่ไม่สามารถทำบริสุทธิ์โปรตีนด้วยเทคนิคนิเกิลคอลัมน์โครมาโทกราฟี ต่อมาทำการแยกโปรตีน *Lv*A2M ที่บริสุทธิ์บางส่วนโดยตรงจากน้ำเลือดของกุ้งขาว (native *Lv*A2M) เพื่อนำมาใช้ในการศึกษาหน้าที่ของ *Lv*A2M ต่อไป เมื่อทดสอบแอคติวิตีของ native *Lv*A2M พบว่า native *Lv*A2M มีแอคติวิตีสูงกว่า r*Lv*A2M โดยสามารถยังยั้งทริปซินและค่าแอคติวิตีแปรตามปริมาณ จากนั้นทำการยืนยันตำแหน่งตัดโดยทริปซินที่บริเวณ bait ของ *Lv*A2M โดยวิธีโมเลคิวลาร์ ด็อกกิ้ง จากนั้นศึกษาแอคติวิตีและการยับยั้งโปรติเอสที่หลั่งออกมานอกเซลล์ของเชื้อ *Vibrio harveyi* ของ native *Lv*A2M โดยอาศัยวิธี disc diffusion พบว่า native *Lv*A2M สามารถยับยั้งโปรติเอสดังกล่าวได้ และยังพบว่า native *Lv*A2M สามารถยับยั้งแอคติวิตีของโปรติเอสที่หลั่งออกมานอกเซลล์จากเชื้อแบคทีเรียอื่นๆ ได้แก่ *Staphylococcus aurues, Micrococcus luteus, Escherichia coli* และ *Vibrio parahaemolyticus* ได้เช่นกัน อย่างไรก็ดีไม่สามารถระบุโปรติเอสเป้าหมายของ native LvA2M ได้ด้วยเทคนิค co-immunoprecipitation และ zymography ได้ จากการศึกษาก่อนหน้านี้ที่ระบุว่า A2M สามารถยับยั้งซีรีนโปรติเอสและเมเทิลโลโปรติเอสที่หลั่งจากเชื้อแบคทีเรีย *V. harveyi* ได้ ดังนั้นจึงทำการโคลนยีนของเมเทิลโลโปรติเอส PAP6 แบบสมบูรณ์ (PAP6F) และแบบบางส่วน (PAP6P) จากเชื้อ *V. harveyi* เพื่อแสดงออกโปรตีนรีคอมบิแนนท์ ซึ่งมีน้ำหนักโมเลกุล เท่ากับ 75 กิโลดาลตันและ 59 กิโลดาลตัน ตามลำดับ ในระบบ *E. coli* เมื่อนำมาทดสอบแอคติวิตีพบว่าโปรตีนรีคอมบิแนนท์โปรตีนทั้งสองไม่มีแอคติวิตี และเมื่อทดสอบความสามารถในการจับกับ native *Lv*A2M พบว่าสามารถโปรตีนรีคอมบิแนนท์ PAP6F และ PAP6P จับกับ native *Lv*A2M ได้โดยมีค่าคงที่การแตกตัว (Kd) เท่ากับ 8.1×10^{-7}M และ = 1.1×10^{-6}M ตามลำดับ มีรายงานก่อนหน้านี้ A2M จับกับท็อกซินจากเชื้อก่อโรค ดังนั้นเราจึงการทดสอบ *Lv*A2M สามารถลดความเป็นพิษของโปรตีนสารพิษ Pir ที่หลั่งออกมาจากเชื้อแบคทีเรีย*V. parahaemolyticus* ซึ่งเป็นสาเหตุสำคัญของโรคตายด่วน (EMS) การทดสอบปฏิสัมพันธ์ระหว่างโปรตีน แสดงให้เห็นว่า ในการทดลอง *Lv*A2M สามารถจับกับโปรตีนสารพิษ PirA และ PirB มีค่า Kd เท่ากับ 3.6×10^{-7}M และ 5.8×10^{-7}M ตามลำดับ ทำการยืนยันผลการจับกันด้วยวิธีโมเลกุลด็อกกิ้ง นอกจากนี้ *Lv*A2M มีความสามารถในการลดความเป็นพิษของโปรตีนสารพิษ Pir ได้ ซึ่งส่งผลทำให้อัตราการตายของกุ้งลดลง จากเหตุผลดังที่กล่าวมานี้ ชี้ให้เห็นว่า *Lv*A2M อาจมีส่วนในการตอบสนองต่อระบบภูมิคุ้มกันต่างๆ ที่จะยับยั้งโปรติเอสเป้าหมายและสารพิษที่แตกต่างกันของแบคทีเรียที่บุกรุก เช่นเดียวกันกับการควบคุมระบบภูมิคุ้มกันของโฮสต์

ภาควิชา	ชีวเคมี	ลายมือชื่อนิสิต .....
สาขาวิชา	ชีวเคมีและชีววิทยาโมเลกุล	ลายมือชื่อ อ.ที่ปรึกษาหลัก .....
ปีการศึกษา	2557	ลายมือชื่อ อ.ที่ปรึกษาร่วม .....
		ลายมือชื่อ อ.ที่ปรึกษาร่วม .....

5472055123 : MAJOR BIOCHEMISTRY AND MOLECULAR BIOLOGY
KEYWORDS: ALPHA-2-MACROGLOBULIN / VIBRIO HARVEYI / VIBRIO PARAHAEMOLYTICUS / LITOPENAEUS VANNAMEI / PHOTORHABDUS INSECT-RELATED (PIR) TOXIN

WITCHANON WONGBAUCHEUN: IDENTIFICATION OF TARGET PROTEIN OF ALPHA-2-MACROGLOBULIN FROM WHITE SHRIMP *Litopenaeus vannamei* BY BIOCHEMICAL AND MOLECULAR MODELING TECHNIQUES. ADVISOR: PROF. ANCHALEE TASSANAKAJON, Ph.D., CO-ADVISOR: ASST. PROF. KUNLAYA SOMBOONWIWAT, Ph.D., THANYADA RUNGROTMONGKOL, Ph.D., 174 pp.

Alpha-2-macroglobulin (A2M) is an evolutionarily conserved protease inhibitor. In invertebrates including shrimp, A2M has been shown to be crucially involved in immune responses. Herein, A2M from the Pacific white shrimp *Litopenaeus vannamei* named *Lv*A2M was characterized for its immune function against bacterial proteases. The recombinant *Lv*A2M protein (r*Lv*A2M) with the predicted molecular mass and pI of 166.9 kDa and 5.77, respectively, was produced in *Escherichia coli* but was not successfully purified by Ni-NTA column chromatography. Then, the native *Lv*A2M was partially purified from the plasma of *P. vannamei* and exhibited inhibitory activity against trypsin in a dose-dependent manner. The cleavage site on bait region of *Lv*A2M by trypsin was confirmed by molecular docking. Using agar disc diffusion method, the inhibitory activity against *Vibrio harveyi* proteases of native *Lv*A2M was found to be much higher than r*Lv*A2M. Moreover, native *Lv*A2M also inhibited other bacterial secreted proteases from *Staphylococcus aurues, Micrococcus luteus, Escherichia coli and Vibrio parahaemolyticus*. Unfortunately, the specific protease of *Lv*A2M could not be identified by co-immunoprecipitation and zymography techniques. Consequently, the full length (PAP6F) and the partial sequence (PAP6P) of PAP6 gene encoding a metalloprotease from *V. harveyi* were cloned and expressed in *E. coli* system to investigate whether PAP6 is the target protease of *Lv*A2M. The recombinant proteins of PAP6F and PAP6P did not exhibit protease activity but both bound to native *Lv*A2M with the dissociation constant (Kd) of 8.1×10^{-7}M and 1.1×10^{-6}M, respectively. Since A2M has been reported to bind toxin produced from pathogens, so we tested if *Lv*A2M could neutralize Pir toxins secreted from *V. parahaemolyticus*, the causative agent of the deadly disease Early mortality Syndrome (EMS). The binding assay showed that *Lv*A2M could interact with PirA and PirB toxins *in vitro* with the Kd of 3.6×10^{-7}M and 5.8×10^{-7}M, respectively. This binding was confirmed by molecular docking. Furthermore, *Lv*A2M also neutralized toxic effect of the crude Pir toxins resulting in a decrease of cumulative mortality of shrimp. Taken together, our results suggested that *Lv*A2M might participate in many immune responses to inhibit different target proteases and toxins of invading bacteria as well as controlling the host immune reactions.

Department:	Biochemistry	Student's Signature	.....
Field of Study:	Biochemistry and Molecular Biology	Advisor's Signature	.....
Academic Year:	2014	Co-Advisor's Signature	.....
		Co-Advisor's Signature	.....

ACKNOWLEDGEMENTS

On the completion of my thesis, I would like to appreciate for excellent, supports, guidance, encouragement and supervision throughout my four-year study from my advisor, Professor Dr. Anchalee Tassanakajon, and from my co-advisors, Assistant Professor Dr. Kunlaya Somboonwiwat. The great discussion and suggestion have become important keys for developing my research outcome. Exceptionally, I have to thank you very much for your hard attempt to teach, inspire and improve me into a researcher. To my co- advisors Dr. Thanyada Rungrotmongkol thank you very much for supports all the time while I was studying in this Chulalongkorn University. Moreover, I did not only gain so much knowledge of science from you but I also have your worth experiences of science that you kindly shared to me.

My appreciation is also to Associate Professor Dr. Vichien Rimpanitchayakit, Dr. Premruethai Supungul for helping and instruction. I would like to thank Dr. Grace Chu-Fang Lo from National Cheng Kung University, Taiwan for for providing toxin protein and antibody for A2M study. Her kindness was greatly appreciated. Thankfulness are also extended to all members at Center of Excellence for Molecular Biology and Genomics of Shrimp laboratory for their help and for friendship that allow me enjoy throughout my study. Thanks to every friends in the Department of Biochemistry.

I express my gratitude to Assistant Professor Dr. Manchumas Prousoontorn., Assistant Professor Dr. Kanoktip Packdibamrung and Associate Professor Dr. Apinunt Udomkit for giving me your time on being my thesis's defense committee and for useful suggestions and valuable comments.

Finally, I would like to express my deepest thankfulness to indispensable people including my parents and my family for their endless love, encouragement, guide, understanding, care and support along my lifetime.

CONTENTS

Page

Page

Page

Page

Page

Page

Page

LIST OF TABLES

LIST OF FIGURES

LIST OF ABBREVIATIONS

%	percentage
℃	degree Celcius
µg	microgram
µl	microliter
µM	micromolar
A	absorbance
A2M	Alpha-2-macroglobulin
AMP	antimicrobial peptide
amp	ampicillin
bp	base pair
cDNA	complementary deoxyribonucleic acid
CFU	colony forming unit
CL	carapace length
CP	clottable protein
C-terminus	carboxyl terminus
CVPs	crude *Vibrio harveyi* proteases
d	day
DEPC	diethylpyrocarbonate

DNA	deoxyribonucleic acid
DNase	deoxyribonuclease
ELISA	enzyme-linked immunosorbent assay
EMS	early mortality syndrome
EST	expressed sequence tag
h	hour
HL	hemolymph
HLS	hemocyte lysate supernatant
hpi	hour post infection
iELISA	indirect enzyme-linked immunosorbent assay
IgG	immunoglobulin G
IPTG	isopropyl-beta-D-thiogalatopyranoside
kana	kanamycin
kb	kilobase pair
Kd	dissociation constant
kDa	kilodalton
LB	Luria broth
Lv	*Litopenaeus vannamie*
M	molar

mg	milligram
min	minute
ml	milliliter
mM	millimolar
mm	millimeter
Mw	molecular weight
ng	nanogram
N-terminus	amino terminus
OD	optical density
ORF	open reading frame
PAGE	polyacrylamide gel electrophoresis
PAP6	metalloproteinase from *Vibrio harveyi* strain AP6
PAP6F	full-length of metalloproteinase from *Vibrio harveyi* strain AP6
PAP6P	partail-length of metalloproteinase from *Vibrio harveyi* strain AP6
PBS	phosphate buffer saline
PCR	polymerase chain reaction
pI	isoelectric point

Pir	*Photorhabdus* insect-related
pmol	picomole
proPO	prophenoloxidase
r	recombinant protein
RNA	ribonucleic acid
RNAi	ribonucleic acid interference
rpm	round per minute
RT	reverse transcription
s	second
SDS-PAGE	sodium dodecyl sulfate polyacrylamide gel electrophoresis
SPH	serine proteinase homolog
TGase	transglutaminase
TSB	tryptic soy broth
TSV	Taura syndrome virus
v/v	volume by volume
w/v	weight by volume
WSSV	white spot syndrome virus
YHV	yellow head virus

CHAPTER I
INTRODUCTION

1.1 General introduction

Over the last few decades, aquafarming such as fish farming, oyster farming, shrimp farming, and aquaculture has become one of the most rapidly growing sources of food animal protein in the world. Decreasing stocks within wild fisheries and increasing demand for seafood are driving this inclined growth mostly from the United States, Europe, and Japan. More recently demand in developing economies has grown at a rapid tempo. One of the fastest growing market segments within aquaculture is farm-raised shrimp. According to data from the United Nations Food and Agriculture Organization (FAO), shrimp farming is a very important agro-industry in many countries.

Since 1970 it has developed into a multi-billion-dollar industry and thereby has become one of the most economically significant farming in many countries in Asia, especially China and Thailand, which share up to 75% of the world shrimp trade (Source FAO database, 2012) (Fig. 1.1). The other 25% is produced mainly in Latin America such as Brazil, Ecuador, and Mexico. Shrimp farming provides approximately 30% of the shrimp supplied to the world market. Many species of shrimp are cultured in several parts of the world. The eight important shrimp species are the giant tiger shrimp, *Penaeus monodon*, the pacific white shrimp, *Litopenaeus vannamei*, the Chinese white shrimp, *Fenneropenaeus chinensis*, the northern brown shrimp,

Farfantepenaeus aztecus, the yellow leg shrimp, *Farfantepenaeus californiensis*, the Indian white shrimp, *Fenneropenaeus indicus*, the western blue shrimp, *Penaeus stylirostris*, and the Japanese kuruma prawn, *Marsupenaeus japonicas* (Conklin 2003). Thailand has been the world leader in farmed shrimp exportation since 1990s, and used to be the biggest shrimp exporter of the world market (Wyban 2007). Dispersively located along the eastern and sounthern coastal areas of Thailand.

In the past few decades, the shrimp farming industry in Southeast Asia was plagued by many problems in cultural management of the shrimp bloodstock, environmental image, and the outbreaks of diseases caused by pathogens such as the white spot syndrome virus (WSSV), Taura syndrome virus (TSV) and Yellow head virus (YHV) and the *Vibrios* spp. (Flegel 2007). The luminescent bacteria *Vibrio harveyi* has been the recognized as deadly infectious pathogens causing main loss in majority of the shrimp production (Austin, 2006) and Acute hepatopancreatic necrosis disease (AHPND, also known as early mortality syndrome, EMS) has caused severe mortalities (up to 100%) in farmed populations of marine shrimp *L. vannamei* and *P. monodon*. The causative agent was determined to be the unique strains of the bacterium *Vibrio parahaemolyticus* (Tran et al., 2013)

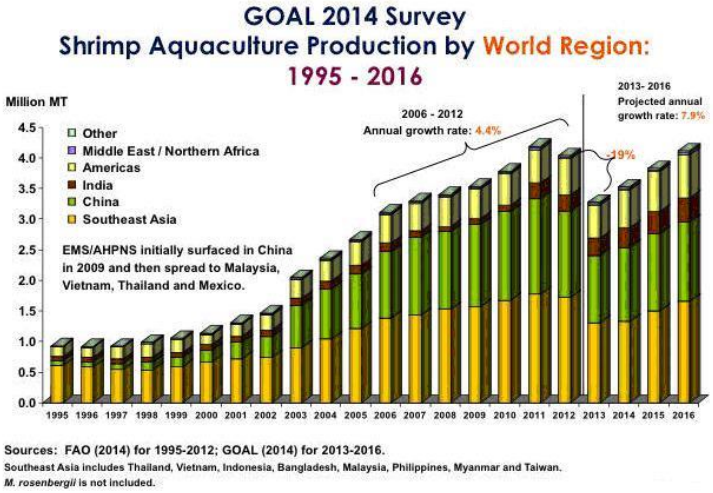

(Source: http://aseanseafood.asia/ca339-n28826-global-shrimp-production-trends.htm #sthash.hEKenhWd.dpuf)

Figure 1.1 Shrimp aquaculture production in the world since 1995-2012 (FAO (2014) for 1995 – 2012; GOAL (2014) for 2013-2016)

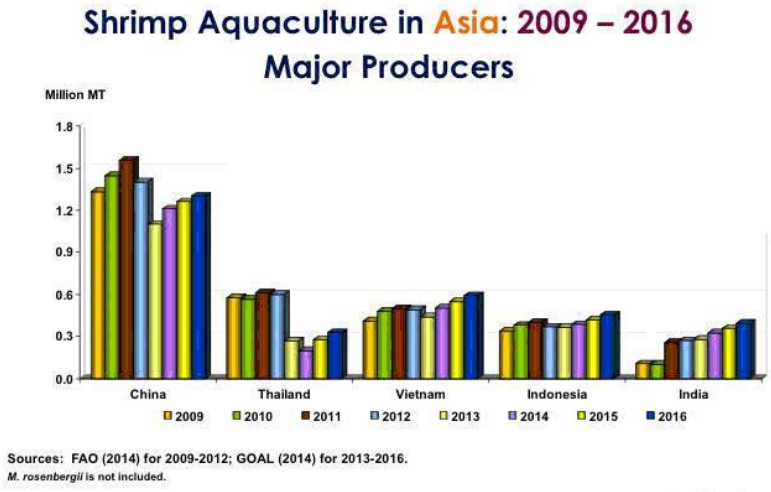

Figure 1.2 Shrimp aquaculture production in major producer of Asia since 2009 – 2012 (FAO (2014) for 2009 - 2012; GOAL (2014) for 2013 – 2016)

Since 2013, shrimp production in Southeast Asia has undergone considerable changes including in Thailand. Understanding in shrimp immune system is required to improve its pathogen resistance, developing better cultural management, and inventing the effective means to control these infectious diseases.

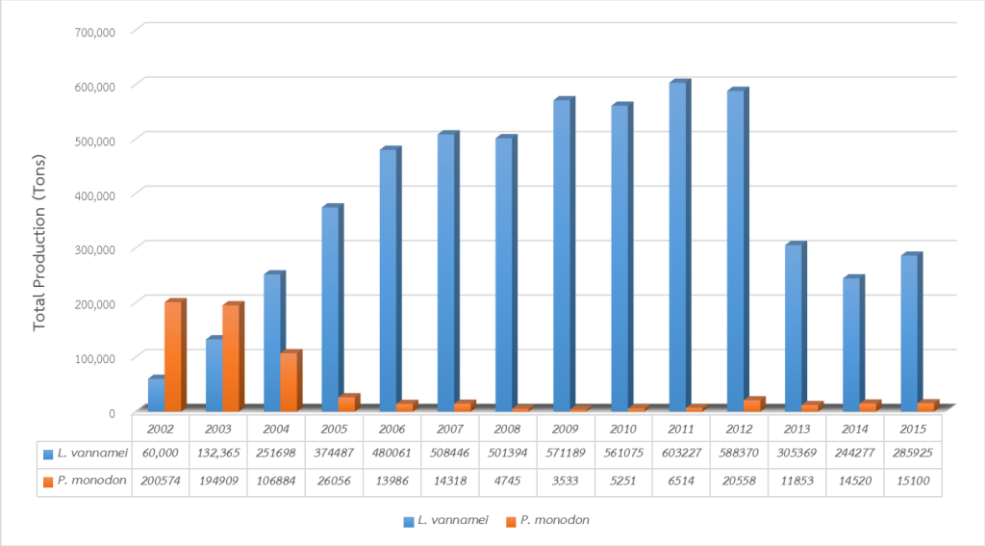

	2002	2003	2004	2005	2006	2007	2008	2009	2010	2011	2012	2013	2014	2015
L. vannamei	60,000	132,365	251698	374487	480061	508446	501394	571189	561075	603227	588370	305369	244277	285925
P. monodon	200574	194909	106884	26056	13986	14318	4745	3533	5251	6514	20558	11853	14520	15100

(Modified from source: the United Nations Food and Agriculture Organization (FAO) and Office of Agriculture Economics(OAE))

Figure 1.3 The shrimp *Litopenaeus vannamei* and *Penaeus monodon* production in Thailand between 2002-2015

1.2 Taxonomy of the Pacific white shrimp, *Litopenaeus vannamei*

(Source: http://www.oliveto.com/this-just-in-georgia-white-shrimp)

Figure 1.4 The Pacific white shrimp *(Litopenaeus vannamei)*

The Pacific white shrimp, *L. vannamei* are catergorized into the largest kingdom, Animalia (Young 1959), Arthropoda phylum (Bowman and Abele 1982). The presences of protective exoskeletons covering the whole body of animals and pair of jointed appendages are obvious characteristics of the animals classified into this phylum. The Crustacea subphylum (Ahyong et al. 2011) consist of approximately 42,000 aquatic species belonging to ten classes. Shrimp, crab, lobster, and crayfish belong to Decapoda order which is under Malacostraca class (Schweitzer and Feldmann 2000). *P. vannamei* is classified into Dendrobranchiata suborder (Tavares and Martin 2010), Penaidae family (Vazquez-Bader et al. 2004), and *Litopenaeus vannamei* (Ponce-Palafox et al. 1997) by the general characteristics such as pair appendages and protective cuticle or exoskeleton.

Table 1.1 The taxonomic definition of the Pacific white shrimp *(Litopenaeus vannamei)*

Scientific classification	
Kingdom	Animalia
Phylum	Arthropoda
Subphylum	Crustacea
Class	Malacostraca
Subclass	Eumalacostraca
Superorder	Eucarida
Order	Decapoda
Suborder	Dendrobranchiata
Superfamily	Penaeoidea
Family	Penaeidae
Genus	*Litopenaeus*
Species	*vannamei*

Scientific name: *Litopenaeus vannamei*

Common Name(s): camarón patiblanco **[Spanish]**

crevette pattes blanches **[French]**

whiteleg shrimp **[English]**

FAO name : *Penaeus vannamei*

1.3 The biological features of shrimp

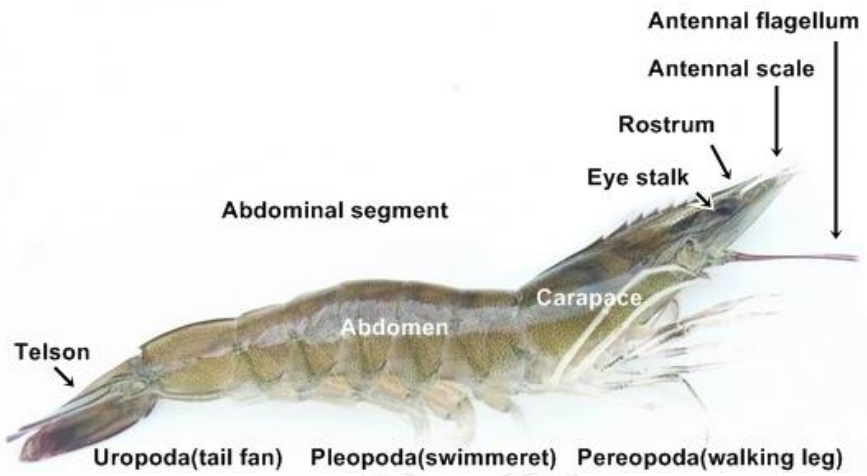

(Modified from source: http://siamintersea.co.th/product.php)

Figure 1.5 External anatomy of *Litopenaeus vannamei*

The color of *L. vannamei* is typically translucent-white. The body can display a bluish hue that is due to a predominance of blue chromatophores which are concentrated near the margins of the telson and uropods (Eldred and Hutton 1960). Colour variations are also shown in cases of nutritional deficiencies. The legs of *L. vannamei* can often appear white; hence the common name, white-legged shrimp. The external morphology of *L. vannamei* contains three parts, Carapase (head), abdomen, and Telson (tail) in Figure 1.5

1.4 Distribution and life cycle of *Litopenaeus vannamei*

Whiteleg shrimp are native to the eastern Pacific Ocean, from the Mexican state of Sonora as far south as northern Peru. It is restricted to areas where the water temperature remains above 20 °C (68 °F) for at least one grow out period and in which salinity does not rapidly change within 2-45 ppt. *L. vannamei* has also been introduced to Asia. The first introduction apparently occurred in 1980 in the Philippines, followed by Taiwan in 1981. In 2002, Thailand started commercial production of *L. vannamei*. *L. vannamei* has six nauplius stages, three protozeal stages, and three mysis stages in its pelagic larval life history (Kitani 1986) Subsequently, it becomes a post-larvae and adopts a benthic lifestyle. The carapace length (CL) of *L. vannamei* post-larvae ranges from 0.88 to 3.00 mm (Kitani 1993). The larval stages (1.95-2.73 mm of CL) can be recognized by the lack of a thoracic spine on the seventh sternite, and relative rostral length against the length of eye plus eye stalk ranges from 2/5 to 3/5, rarely 4/5 (Kitani 1994). The most distinguishable morphological character is the development of supraorbital spines in the second and third protozoea (Kitani 1986).

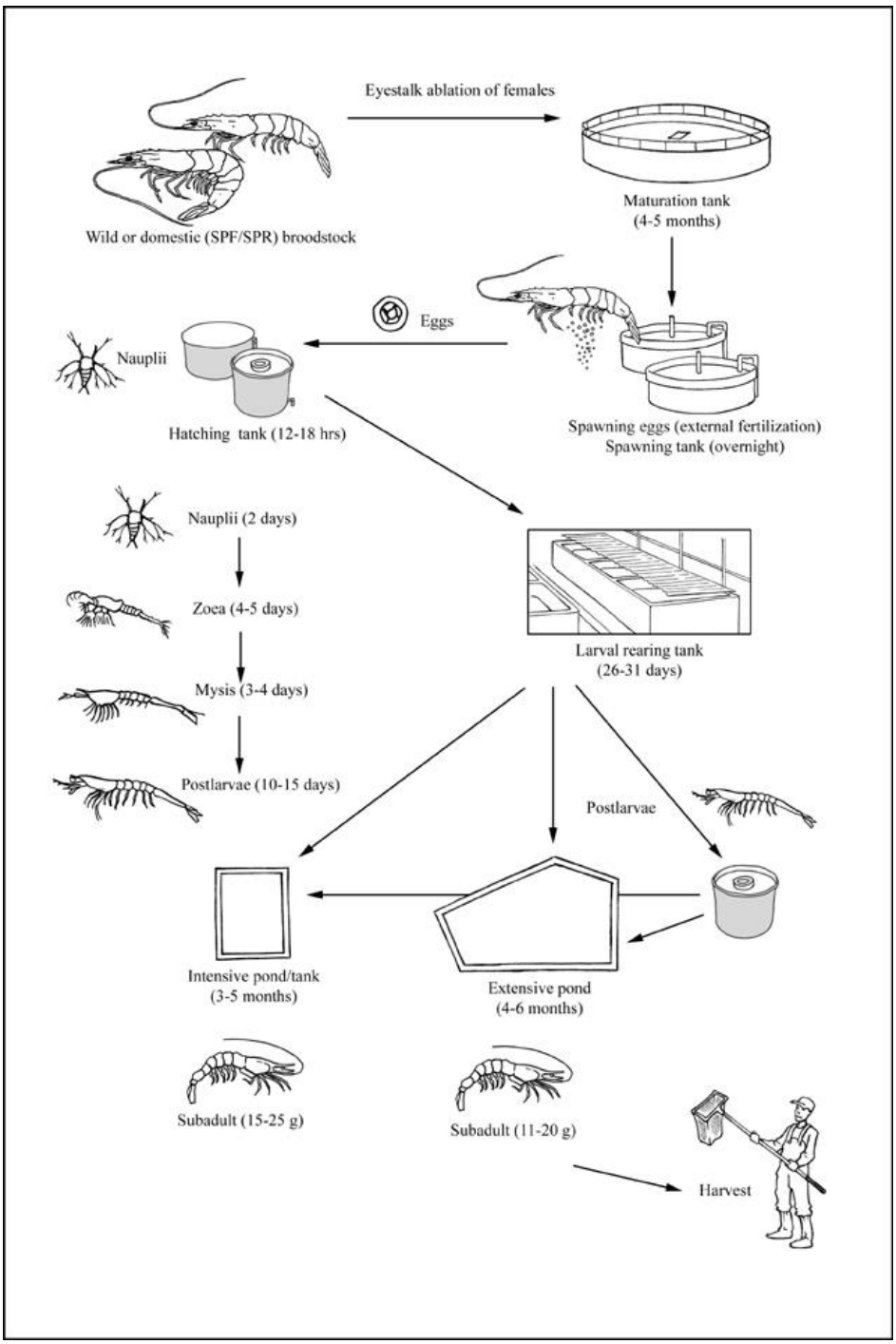

(Source : http://www.fao.org/fishery/culturedspecies/Penaeus_vannamei/en)

Figure 1.6 The life cycle of *Litopenaeus vannamei* production

1.4 Shrimp disease

Viruses and bacteria are the major cause of the infectious diseases in *L. vannamei* Because of the artificial conditions in the shrimp farms where water quality, microbiological flora and nutrition are immensely difference from those in the natural habitat. Although the shrimp diseases caused by severe viral pathogens such as White Spot Syndrome Virus (WSSV), Yellow Head Virus (YHV) and Taura Syndrome Virus (TSV) viruses are much more pandemic than others, the shrimp diseases caused by bacteria belonging to the genus *Vibrio* also contribute to morbidity and even mass mortality in the shrimp. Caused by *Vibrio spp*., vibriosis is notably known as a lethal shrimp disease resulting in almost 100% cumulative mortality of the infected hosts (Alvarez et al. 1998; Flegel 2006). The apparent characteristics of the genus *Vibrio* are Gam-negative, motile, and bioluminescent bacteria possessing a rod shape of around 0.5 μm in width and 1.4 μm in length. Normally found in seawater, *Vibrio spp.* are facultative anaerobes and most of them are mortal pathogenic strains in a wide spectrum of hosts such as *Vibrio harveyi* and *Vibrio parahaemolyticus* found in aquaculture (Rao 2002).

1.4.1 Viral diseases

The major viral pathogens in shrimp are caused by TSV, WSSV and YHV and hematopoietic necrosis virus (IHHNV). There are 7 families of viral pathogens including Parvoviridae, Bacuroviridae, Iridoviridae, Picornaviridae, Rhabdoviridae, and Togaviridae identified in penaeid shrimp (Jittivadhna 2000).

1.4.1.1 Taura syndrome virus (TSV)

The Taura syndrome virus, TSV was first reviewed by Jimenes in 1992 as a shrimp disease that caused by Taura virus. The Taura virus is a cytoplasmic, nonenveloped icosahedral virus containing a single-stranded positive sense RNA genome of 10,205 nucleotides of 32 nm diameter (Bonami et al. 1997; Mari et al. 2002). It was classified as a possible member of the family Picornaviridae based on biological and physical characteristics. It was later reclassified in the Dicistroviridae family, genus Cripavirus (Mayo 2002, 2005). It has since been reassigned to a second genus in the same family - the Aparavirus. Seriously, this disease is a causative of shrimp mortality in *P. monodon* and *L. vannamei*. In 2004, Taura syndrome virus was hit to Thailand shrimp farm, it made a lot of damages and the farmers have to change from cultivation of *P. monodon* to *L. vannamei.* The symptoms of Taura syndrome virus in shrimp are tail fan and pleopods particularly were red (Fig. 1.7), shell soft, darkening of body from infection.

(Source : http://www.aquatoyou.com/index.php/2013-05-14-08-19-43/10-2013-02-20-06-42-05/814-taura-syndrome)

Figure 1.7 The presenting symptom of the Taura syndrome in black tiger shrimp. The tail fan and pleopods partially present in red.

1.4.1.2 White spot syndrome virus (WSSV)

White spot syndrome virus (WSSV) is a virus that can infect crustacean species such as penaeid shrimps and crabs (Lo et al. 1996; Peng et al. 1998; Chen et al. 2000). Firstly, it caused severe death of shrimp in Taiwan (Chiang and Lo 1995) and further reported in Thailand (Lo et al. 1996). The disease is highly lethal and spreads and kills shrimps quickly. The outbreaks of this disease have cleared within a few days the whole populations of many shrimp farms throughout the world. WSSV is an envelope with double stranded DNA. This virus was classified in Whispovirus genus, Nimaviridae family (Mayo 2002; Westenberg et al. 2005). The clinical signs of this disease are lethargy, a pink to reddish-brown discoloration. The typical symptom of this disease is

presenting the white spot of 0.5-2 nm on shrimp's carapace of the cephalothorax (Figure. 1.8) (Chiang and Lo 1995).

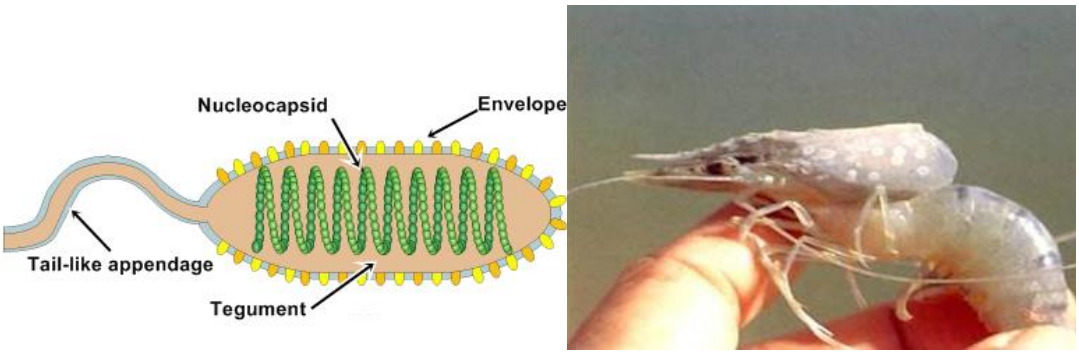

(Source: https://shrimpdiseases.wordpress.com/wssv/)

Figure 1.8 The morphology of the WSSV viral particle and gross signs of white spot on shrimp carapace

1.4.1.3 Yellow-head virus (YHV)

Yellow-head virus (YHV) caused the economic losses in Thailand shrimp aquaculture since 1992 (Limsuwan 1991; Boonyaratpalin et al. 1993; Chantanachookin et al. 1993). Moreover, this shrimp disease was found in shrimp farm in the Asia (Walker et al. 2001). YHV is a positive-sense single-stranded RNA virus with rod-shaped and enveloped viral particle of about 40-60 nm 150-200 nm. This virus was classified in Okavirus genus, Roniviridae family and Nidovirales order (Wonteerasupaya et al. 1995; Fauquet et al. 2005). The symptoms of this disease can be observed as abnormally high rate feeding, yellow light at cephalothorax and hepatopancreas and dramatrically increase shrimp mortality to 100% in 3-5 days (Figure. 1.9) (Chantanachookin et al. 1993).

(Source: http://thailandshrimp.org/data/eng_white_shrimp_p1_files)

Figure 1.9 Yellow head disease in the Pacific white shrimp (*L. vannamei*). The yellow heads of infected shrimp was shown on the left-hand side and normal shrimp was shown on the right-hand side.

1.4.1.4 Infectious Hypodermal and Hematopoietic Necrosis Virus (IHHNV)

Infectious hypodermal and hematopoietic necrosis virus (IHHNV) is one of the most important DNA viruses infecting penaeid shrimp. IHHNV is an icosahedral, non-enveloped, parvovirus with a single-stranded, 4.1 kb, DNA genome comprised of three large open reading frames (ORFs) (Bonami et al. 1990; Shike et al. 2000). Natural infection by IHHNV has been reported for most shrimp (*Penaeus spp.*). In shrimp aquaculture, the most commercially important species of shrimp are *P. stylirostris, L. vannamei* and *P.monodon. P. stylirostris* is highly susceptible to IHHNV, and the virus causes lethal disease (up to 90% mortality) in *P. stylirostris* juveniles (Lightner et al. 1983). However, the virus does not cause lethal infection in *L. vannamei* and *P.monodon*; instead, it causes reduction in growth and a variety of cuticular deformities

of the rostrum, antenna, and other thoracic and abdominal areas. This disease is commonly known as runt deformity syndrome. Losses of revenue due to runt deformity syndrome range from 10 to 50% depending on the level of infection.

(Source : http://www.shrimpex.in/aquaculture/aqua-services-diagnostics-IHHNV.html)

Figure 1.10 Infectious hypodermal and haematopoietic necrosis (IHHN) disease in the Pacific white shrimp (*Litopenaeus vannamei*).

1.4.2 Bacterial diseases

1.4.2.1 Vibriosis

Vibrio is a genus of gram-negative, motile, bioluminescent bacteria with morphology of rod shape, 0.5-0.8 μm in width and 1.4-2.6 μm in length. *Vibrio* is anaerobic bacteria usually found in seawater and do not form spores. There are several pathogenic strains including *Vibrio harveyi*, *Vibrio splendidus*, *Vibrio parahaemolyticus*, *Vibrio alginolyticus*, *Vibrio anguillarum*, *Vibrio vulnificus*, *Vibrio campbelli, Vibrio fischeri, Vibrio damsella, Vibrio pelagicus, Vibrio orientalis, Vibrio ordalii, Vibrio mediterrani, and Vibrio logei* (Rao 2002). *V. harveyi* is a major shrimp pathogenic species causing Vibriosis. Among the *V. harveyi* isolates, some are virulent and some are not,

suggesting a great deal of genetic variation in this species. The *Vibrio spp*. infection in shrimp can occur at all life stages, but mostly in hatcheries. The clinical signs of this disease in adult shrimp are appear hypoxic, show reddening of the body with red to brown gills, reduce feeding and may be observed swimming lethargically at the edges and surface of ponds. The bacteria are able to emit a bluegreen color light by luciferase catalysis reaction. The luminescence can be visible on the head and pectoral part of infected shrimp (Fig. 1.11). *Vibrio* infection alone may cause shrimp mortality for up to 95%. It was also evidenced that shrimps co-infected with *Vibrio harveyi* and white spot syndrome virus has faster and higher mortality rates than shrimp infected with *Vibrio harveyi* alone (Phuoc et al. 2008).

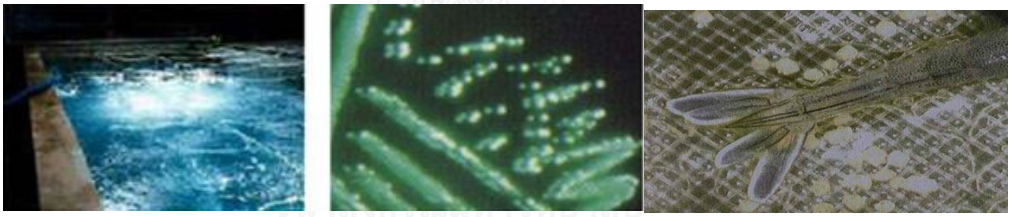

Figure 1.11 Luminescence of *Vibrio* on selective medium plate and *Litopenaeus vannamei* with greenish fluorescence on the tail (Rao, 2008)

1.4.2.2 Early Mortality Syndrome, EMS

Since 2009, Acute hepatopancreatic necrosis disease (AHPND, also known as early mortality syndrome, EMS) has caused severe mortalities (up to 100%) in farmed populations of marine shrimp *L. vannamei* and *P. monodon*. The disease has led to significant production and economic losses to shrimp farms, and to the aquaculture industry in general, in affected regions (Flegel 2012; Leaño and Mohan 2012; Lightner

et al. 2012). The disease develops quickly, starting approximately 8 d after the ponds are stocked, and severe mortalities occur during the first 20 to 30 d of culture. Clinical signs of the disease in infected shrimp include an empty gastrointestinal tract, milky appearance of the stomach, whitish atrophied hepatopancreas, lethargy, and a soft exoskeleton. The causative agent was determined to be the unique strains of the bacterium *Vibrio parahaemolyticus* (Tran et al. 2013). *Vibrio parahaemolyticus* is a common inhabitant of coastal and estuarine environments all over the world. Hence they are often found naturally associated with shrimp aquaculture systems. Certain environmental conditions may be more favourable for the establishment, survival and growth of the organism such as temperature, salinity, zooplankton, tidal flushing and dissolved oxygen. *V. parahaemolyticus* is closely related to shrimp pathogenic luminous bacteria such as *V. harveyi, V. campbelli* and *V. owensii*. These along with other closely related *Vibrio* spp form a "*V. harveyi* clade" (Cano-Gomez et al. 2009). Bacteria within this clade have a very high degree of similarity at phenotypic and genotypic level. Certain strains of *V. parahaemolyticus* can cause gastroenteritis in humans and clinical strains are characterised by the ability to produce a thermostable direct hemolysin (TDH) or a TDH-related hemolysin (TRH). The genes encoding these hemolysins (tdh and trh genes) are generally used as markers for human pathogenic strains of *V. parahaemolyticus*. Human pathogenic strains possessing these markers account for 1–2 percent of environmental strains of *V. parahaemolyticus*.

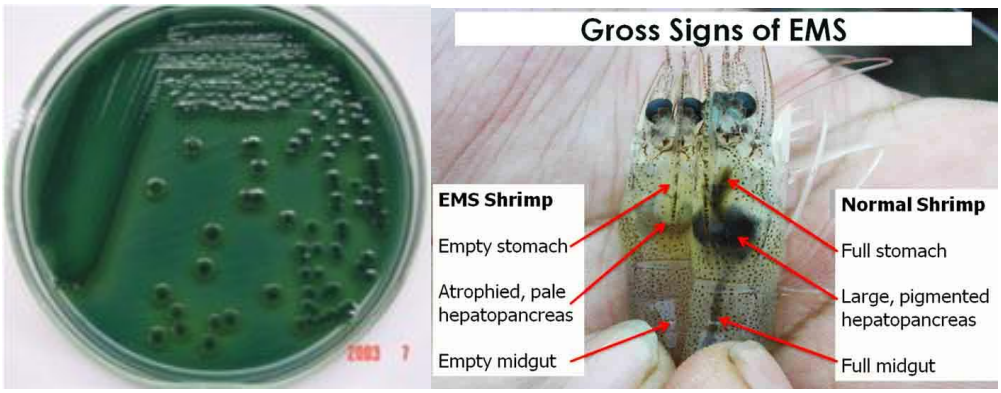

(Source:http://www.shrimpnews.com/FreeReportsFolder/NewsReportsFolder/VietnamGAAwe binarEMS.html)

Figure 1.12 Green colony of *V. parahaemolyticus* on thiosulfate citrate bile salt (TCBS) agar and *Litopenaeus vannamei* showing gross signs of EMS/AHPND, specifically a pale atrophied hepatopancreas and an empty stomach and midgut.

Comparison of genome sequences among strains of *V. parahaemolyticus* revealed that a plasmid containing genes homologous with *Photorhabdus* insect-related (Pir) toxin genes was found in all pathogenic strains but was absent in non-pathogenic strains (Kondo et al. 2014). Pir toxins were first identified in *P. luminescens*, a bacterium that maintains a symbiotic relationship with entomopathogenic nematodes of the family Heterorhabditidae (Ffrench-Constant et al. 2000; Duchaud et al. 2003)

The Pir toxins act as binary proteins; they are encoded by the PirA and PirB genes, and both proteins are necessary for oral toxicity in moths and mosquitoes. (Blackburn et al. 2006; Ahantarig et al. 2009). The pathogenic bacteria harbors a 69-kb plasmid, on average of 33 copies per cell, that contains 2 genes homologous with the

Photorhabdus insect-related (Pir) toxin genes, PirA and PirB (Fig 1.13) (Han et al. 2015; Yang et al. 2014).

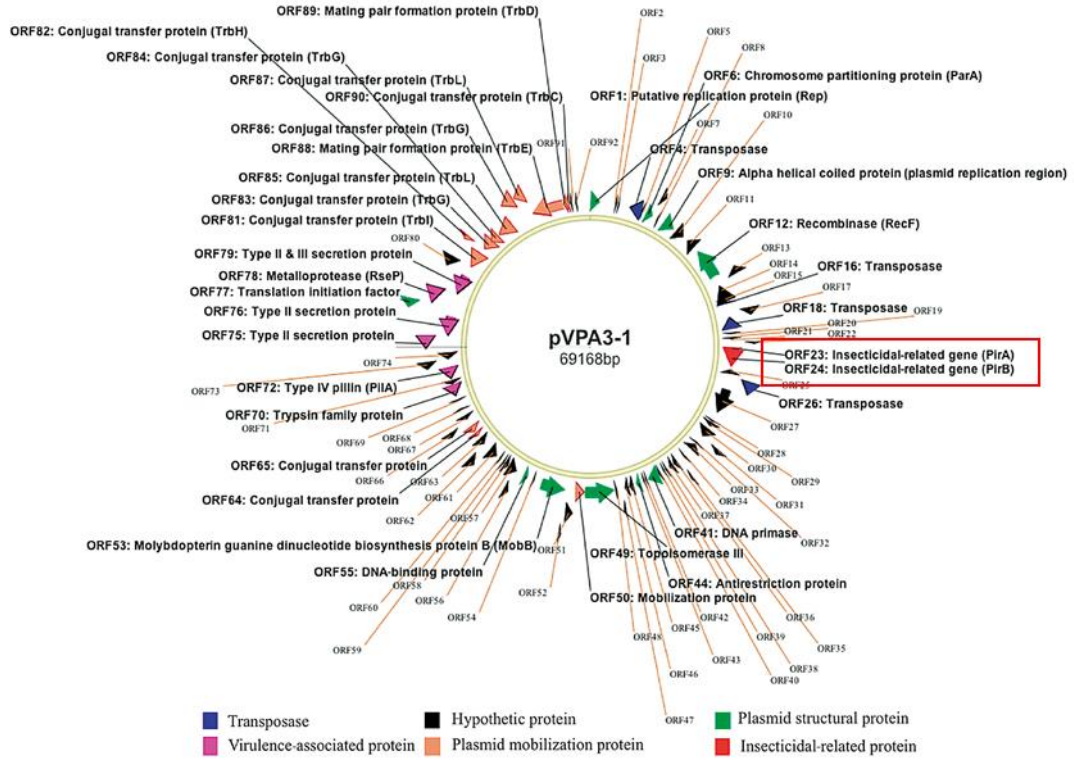

Figure 1.13 Plasmid pVPA3-1 map. Two genes homologous with the *Photorhabdus* insect-related (Pir) toxin in red box (Han et al. 2015) are shown.

1.5 Invertebrate immunity

All living organisms have developed immune system for defending themselves against microbial invasion or other foreign substances. Immune system can be evolutionarily classified into two types: adaptive (acquired) and innate (natural) immunity. Vertebrates possess both adaptive and innate immune systems, whereas invertebrates have only innate immune system. The adaptive immune response provides the vertebrate immune system with the ability to recognize and remember

specific pathogens (to generate immunity), and to mount stronger attacks each time the pathogen is encountered. It is adaptive immunity because the body's immune system prepares itself for future challenges. The innate immune system is a more phylogenetically ancient defense mechanism found in all multicellular microorganisms. This first line of defense helps to limit infection at an early stage and relies on germline-encoded receptors recognizing conserved pathogen-associated molecular patterns (PAMPs) that are present on the microorganisms such as bacterial lipopolysaccharide (LPS), peptidoglycan and β-1, 3-glucan (Fig. 1.14) (Medzhitov and Janeway Jr 1998).

This immune defense comprises of two major responses; cellular mediated and humoral immune responses (Jiravanichpaisal et al. 2006). The defense mechanism in which host hemocytes directly participate are catagorized in the cellular mediated reponses including phagocytosis, nodule formation and encapsulation. Otherwise, the humoral immune reponses defines as the defense mechanism without any direct participations of immune related cells, but immune effectors originally synthesized from those cells mainly involve in activation of signal transduction to initiate immune cascades. These effectors are varied in biological functions and act as potential biomolecules, such as soluble substances, enzymes, and proteins, involved in prophenoloxidase system, hemolymph coagulation system, agglutination, proteases, proteinase inhibitors, and antimicrobial peptides (Hoffmann et al. 1999; Iwanaga and Lee 2005; Soderhall 1999). There is, however, an overlap between both types of the

immune responses because several humoral effectors involve the hemocytic responses as well as the blood cells are a principle source of a number of humoral molecules (Elrod-Erickson et al. 2000; Lavine and Strand 2002).

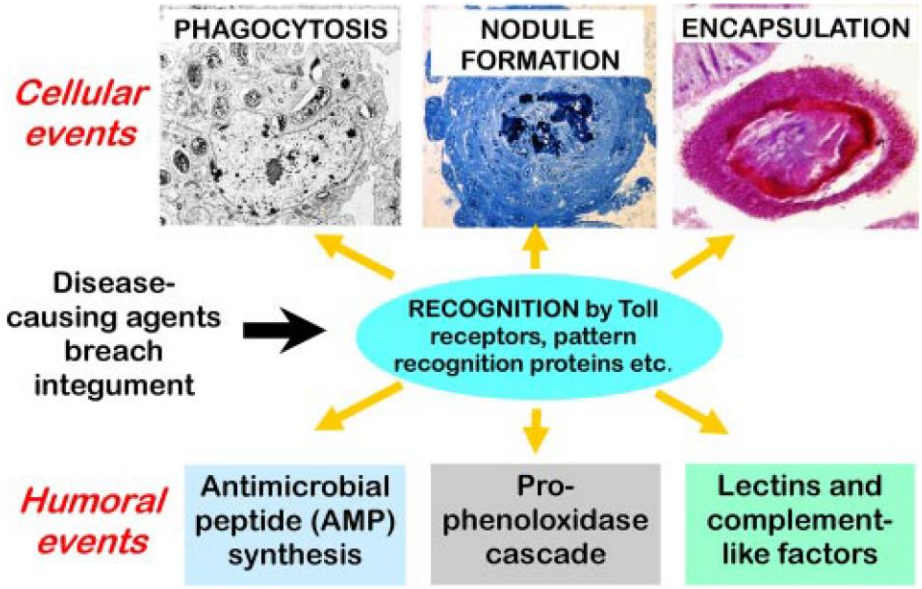

Figure 1.14 Schematic overview of the innate immune defense mechanism of invertebrate (Powell and Rowley 2007).

1.6 The shrimp immune response

In the last decade, a series of papers about shrimp immunity were published and a batch of related data accumulated, which are very useful for understanding the interaction between shrimp and pathogens to enrich the immune theory of invertebrates. Recently, several review papers summarized the achievements in shrimp immunity including EST sequencing and database construction (Leu et al. 2011), microarray analysis of shrimp immune response (Aoki et al. 2011), shrimp molecular responses to viral pathogen (Flegel and Sritunyalucksana 2011), the cationic antimicrobial peptides in penaeid shrimp (Tassanakajon et al. 2010) and immune molecules and their crucial functions in shrimp immunity (Tassanakajon et al. 2013). Obviously understanding the shrimp immunology is necessary to develop an effective strategy for disease control.

The hemocytes in crustaceans are a major immune related cells because they can involve both cellular mediated immune responses and humoral immune responses. These immune responsive cells, hemocytes, are fundamentally classified into three groups; hyaline cell (agranular), semigranular cell (small granular) and granular cell (large granular). The hyaline hemocytes serve potential roles in phagocytosis and in initiation of the blood clotting via cytolysis (Smith and Soderhall 1983; Vargas-Albores et al. 1998), while the granular hemocytes generally function in

apoptosis, encapsulation, melanization and nodulation via exocytosis (Kobayashi et al. 1990; Pech and Strand 2000; Sung et al. 1998).

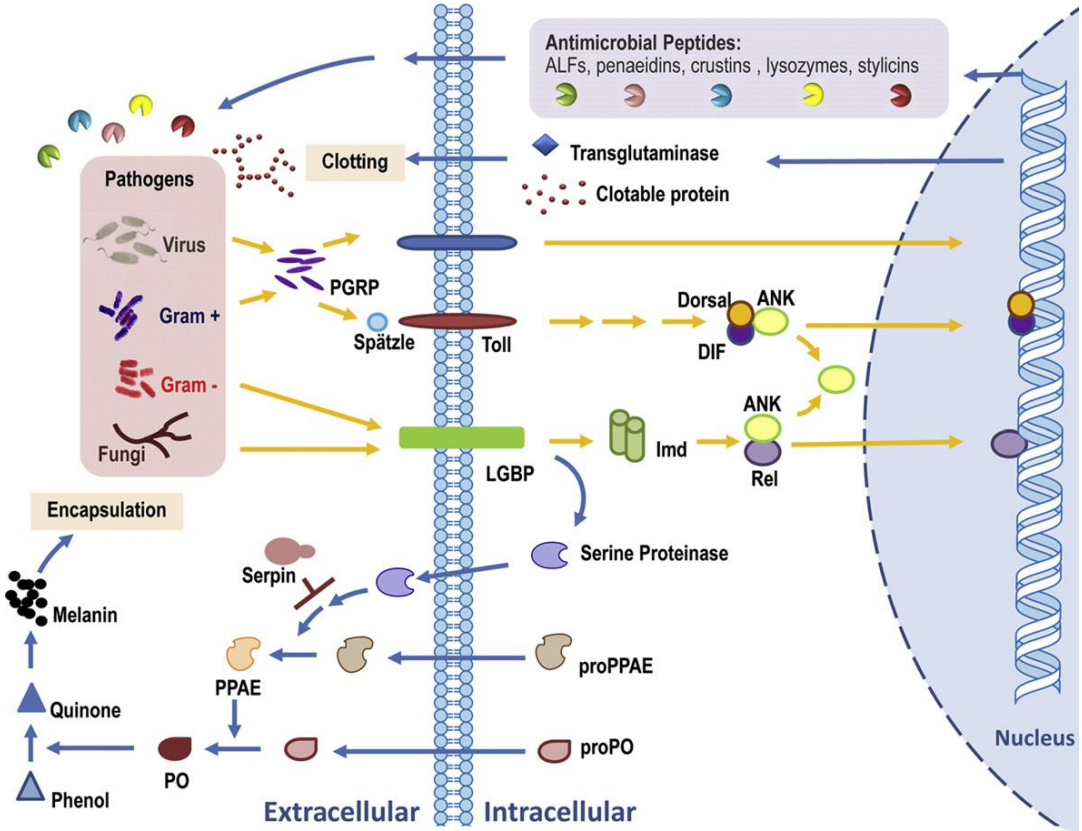

Figure 1.15 A schematic model of the shrimp immune system (Tassanakajon et al. 2013)

1.7 Shrimp immunity

The immunity of shrimp immediately acts against pathogen invading. Their immune system mainly involves in the 3 types of hemocytes, which are able to carry out encapsulation, nodule formation, and phagocytosis in removing microorganisms (Kobayashi et al. 1990; Pech and Strand 2000; Sung et al. 1998). Moreover, several plasma components such as antimicrobial peptides, histones, lysosomal enzymes,

recognition molecules (Lee and Soderhall 2002), lipopolysaccharide- and β-1, 3-glucanbinding proteins (Amparyup et al. 2012) are importants in penaied shrimp defense reactions. Among immune reactions in shrimp innate immunity, prophenoloxidase (proPO) activating system is one of major immune reaction in shrimp.

1.7.1 Cellular-mediated defense mechanisms

The cellular response is the cell-mediated reaction against pathogen invasion including phagocytosis, encapsulation, and nodule formation. Circulating hemocytes are important effector cells in crustacean immunity. Phagocytosis is the cellular process of engulfing solid particles, closing up, and pinching of the membrane to be an internal phagosome which internalizes the solid particles such as bacteria (Jeon et al., 2010). It is a major mechanism of removing the pathogens and cell debris. The mechanism of phagocytosis includes three stages that are recognition the microbes with lectins, ingestion, and killing (Sharon and Lis 2004). Cellular encapsulation is an immune response, occurs when a microbe is too large to phagocytosis (Gillespie et al. 1997). It protects host by attracting the host hemocytes to a foreign invader and aggregating on its surface. The microbes in capsule occurring from cell encapsulation process are harmless. This reaction occurs against a wide range of pathogens and parasites resulting in the formation of multiple layers of dead hemocytes. When the number of invader is high, nodule formation occurs from cellular aggregation involving

in cell-cell co-operation. The forming nodule includes central core of entrapped foreign particles. The nodule trapped microorganisms will be killed by physiological stresses such as nutrients reactive oxygen species that produced by the prophenoloxidase activating system (Jiravanichpaisal et al. 2006).

1.7.2 Pattern recognition proteins

When the pathogenic microorganisms invade animals, cell surfaces components of the pathogens will be detected and recognized by the first line of the innate immune response of the hosts. These factors are referred to as pathogen-associated molecular patterns (PAMPs) which vary among groups of the invading pathogens; for instance, lipopolysaccharides (LPS) of Gram-negative bacteria, lipoteichoic acids (LTA) of Gram-positive bacteria, peptidoglycan of of microbial cell wall, β-1,3-glucan of fungi, mannans of yeasts, glycolipids of mycobacteria, and double-stranded RNA of viruses (Hoffmann et al. 1999). The recognition processes to these PAMPs are mediated by a variey of receptors or proteins of the host immune system, so-called Pattern Recognition Receptors or Proteins (PRRs or PRPs). The interactions between these recognition proteins and their partners are able to trigger a number of distinct immune casecades in response to the invading microorganisms (Fig. 1.15). In crustaceans, several pattern recognition proteins have been recently identified such as LPS binding proteins (LBPs), β-1,3-glucan-binding proteins (bGBPs), peptidoglycan recognition protein, lectins, and hemolin (Lee and Soderhall 2002). Additionally, many

LPS or/and ß-glucan binding proteins (bGBPs or/and LGBPs) has been found in penaeid shrimp (Amparyup et al. 2012).

1.7.3 Antimicrobial peptides (AMPs)

Found in a variety of organisms including mammals and invertebrates, antimicrobial peptides (AMPs) are evolutionarily conserved elements of the innate immune defense. The AMPs are originated from many immune related tissues and various cell types. These peptides have a broad range of microorganism killing such as Gram-negative and Gram-positive bacteria, fungi, enveloped viruses, and even antibiotic resistant strains, so-called host defense peptide. They are generally small in size, approximately less than 200 amino acid residues, with total cationic charge and amphipathic structure; however, a few of anionic peptides are also found. Due to these properties, not only the AMPs can be simply synthesized and rapidly translocated to the wound sites, but also they can attach and insert themselves into membrane bilayers to form pores. The pore forming on the membranes will destroy the membrane permeability barrier and completely lyse the cells resulting in the leakage of cellular components. Different mechanisms of bacterial killing are purposed (Fig. 1.16). The first one is a Barrel-stave pore model. Peptides insert perpendicularly in the bilayer, associate and form a pore. The peptides line the pore lumen in a parallel direction relative to the phospholipid chains, which remain perpendicular to the bilayer plane. The second model is the Carpet mechanism. Peptides adsorb parallel to the

bilayer and after reaching sufficient coverage, they produce a detergent-like effect that causes membrane disintegration. Thirdly, in the Toroidal model, peptides insert perpendicularly in the bilayer and induce a local membrane curvature in such a way that the pore lumen is lined partly by peptides and partly by phospholipid head groups. A continuity between inner and outer leaflets is established. The last model is disordered toroidal pore. A recent modification to the toroidal pore proposes that less-rigid peptide conformations and orientations are formed; the pore lumen is lined by the phospholipid head groups (Melo et al. 2009).

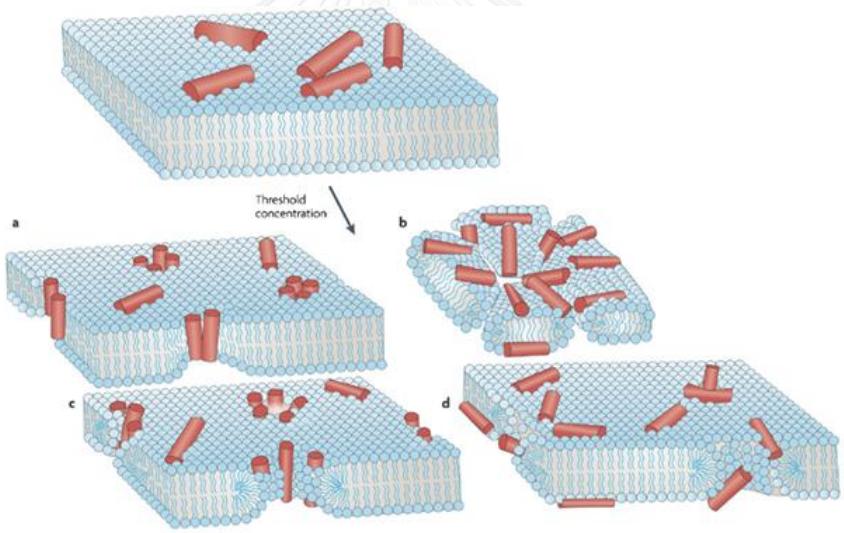

Figure 1.16 Overview of pore forming mechanisms of antimicrobial peptides (AMPs). A) Barrel-stave pore model. B) Carpet mechanism model. C) The toroidal model and D) Disordered toroidal pore (Melo et al. 2009)

1.7.4 The prophenoloxidase (proPO) activating system

The prophenoloxidase (proPO) activating system is one of the most important innate immune sytems in crustaceans. This system comprises of several proteases participating in the immune cascade in order to generate cytotoxic products and melanin as final products. It is believed that the proPO acitivating system involves in phagocytosis, encapsulation and cell adhesion as well (Soderhall and Cerenius 1998). Initially stimulated by pathogen-associated molecular patterns (PAMPs) such as microbial cell wall elements (LPS, LTA and peptidoglycan of bacteria) and β-1,3-glucan of fungi via pattern recognition proteins, prophenoloxidase-activating factor, enzyme or proteinases (ppA, PPAEs, PPAFs, PPAPs) which are stored as a zymogen, an inactive form, will be activated and transformed to phenoloxidase-activating factor, enzyme or proteinases (PAEs, PAFs, PAPs), an active form. This process leads to many active enzymes stepwise occured in the proPO cascade, which are controlled by serine proteases and their inhibitors, to eventually produce prophenoloxidase (PO) (Ariki et al. 2004). The melanin produced helps removing microorganisms by nodule formation (Soderhall and Cerenius 1998; Amparyup et al. 2012) (Fig. 1.17). The activation of proPO system should be tightly regulated to prevent host cell damage. The presence of proPO system has been reported in arthropod immune system, such as crayfish *Pacifastacua leniusculus, Manduca sexta, Bombyx mori*, and *Drosophila melanogater* (Aspan et al. 1995; Fujimoto et al. 1995; Hall et al. 1995; Kawabata et al. 1995). In penaeid shrimp, enzymes in the proPO system are localized in the semigranular and

granular cells (Perazzolo and Barracco 1997). Moreover, PPAE gene (as *Lv*PPAE1) knockdown reduces the survival of *L. vannamei* after *V. harveyi* infection, supporting an important role shrimp PPAE in the defense against bacterial invasion (Jang et al. 2011). The previous study showed that *P. monodon* proPO and PPAE mRNAs as well as a *L. vannamei* proPO mRNA are expressed only in hemocytes (Ai et al. 2009; Amparyup et al. 2009; Sritunyalucksana and Söderhäll 2000; Charoensapsri et al. 2011, 2009). In *L. vannamei*, the function of proPO-II contributes earlier to the acute-phase defence mechanism, and proPO-I is the major type of prophenoloxidase involved in the follow-up defence in white shrimp challenged with *Vibrio alginolyticus* (Ai et al. 2009). Overall, the molecular investigations suggest that the proPO system is critical for the defense against pathogenic infections (Amparyup et al. 2013).

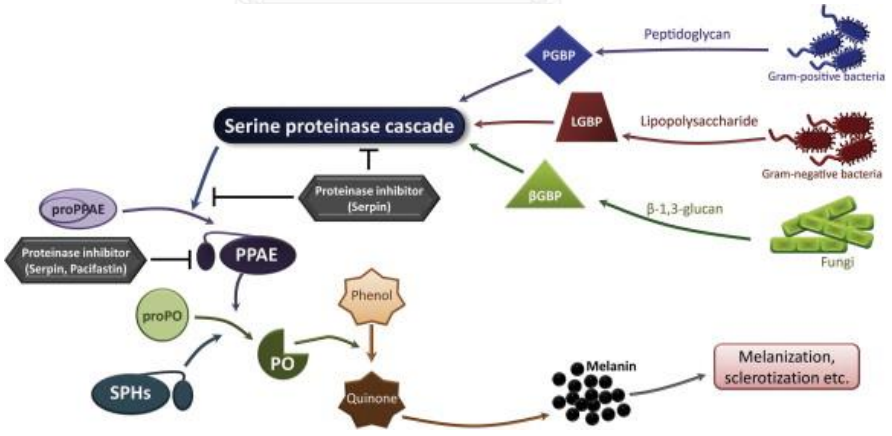

Figure 1.17 Serine proteinase cascade of the prophenoloxidase (proPO) activating system in arthopods (Amparyup et al., 2013)

1.7.5 Blood coagulation system

Due to the fact that invertebrates have an open circulatory system, hemolymph coagulation system, one of the most fundamental innate immune defense, therefore, becomes necessary. The blood clotting serves important roles in preventing hemolymph bleeding at the wound sites as well as obstructing pathogen dissemination throughout the body (Martin et al. 1991). In many organisms including crustaceans, plasma clotting occurs in hemolymph without direct involvement of circulating hemocytes. During an acitivation of the clotting, the reaction of cross-linking of coagulation-associated proteins in plasma is catalyzed by hemocyte-derived factors (Cerenius and Soderhall 2011). In invertebrates, two distinct blood clotting reactions of horseshoe crab and crayfish have been most extensively studied (Fig. 1.18). The plasma coagulation process of horseshoe crab is much more complicated than that of the crayfish. Upon stimulation of pathogen-associated molecular patterns (PAMPs) through pattern recognition proteins, hemocyte derived factors involved in the clotting are released via exocytosis and they are then coverted to proteolytically active forms. These enzymes are responsible for activation of proclotting enzyme to clotting enzyme which can transform coagulogen to coagulin. The coagulin, coagulation-associated proteins, can non-covalently polymerize itself to form a large insoluble gel. Even though tranglutaminase (TGase) is not involved in the coagulin formation, it is yet necessay in cross-linking proxin and stablin onto the coagulin gel for more productive

bacterial immobilization (Cerenius and Soderhall 2011; Kawabata et al. 2009). Unlike horseshoe crab, blood clotting in crayfish and shrimp results from the polymerization between free glutamine and lysine residues of clottable proteins (CPs) which is catalyzed by a calcium ion-dependent TGase (Chen et al. 2005; Hall et al. 1999; Wang et al. 2001). The CP in the white shrimp, *L. vannamei*, is a 380 kDa homodimeric glycoprotein linked by a disulfide bond and is mainly produced in the subcellular epidermis and heart. (Cheng et al. 2008). In *P. monodon*, there have been three isoforms of TGase which are PmSTG I (Huang et al. 2004) and two members of *Pm*STG II (Chen et al. 2005; Young 1959). These *Pm*STG IIs exert the polymerization activity using CPs as a substrate; while *Pm*STG I lacks the blood coagulation activity. In addition, alpha-2-macroglobulin (A2M), a broad range proteinase inhibitor, was previously found to be decorated on the blood clots in both horseshoe crab and crayfish for some extra functions of the clotting system (Armstrong and Armstrong 2003). In previous study, *Pm*A2M interacted with structural elements of the extracellular blood clots by transglutaminase type II activity and so involved in the blood coagulation system of shrimp and protected the clot against bacterial protease-mediated fibrinolysis (Chaikeeratisak et al. 2012; Chaikeeratisak et al. 2014).

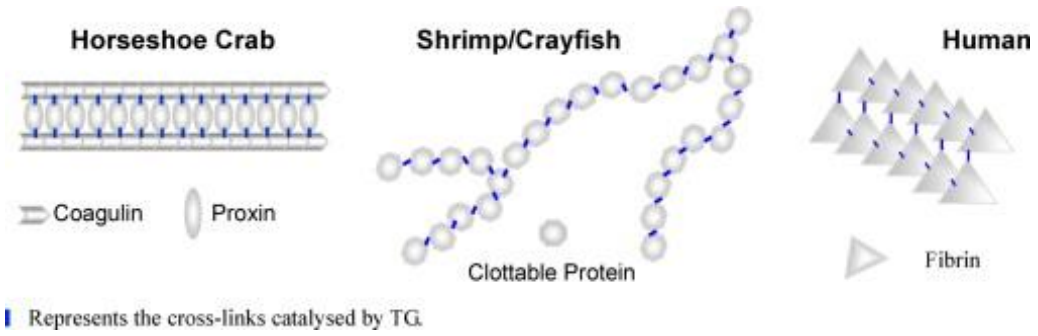

Figure 1.18 A comparative diagram of TG-catalysed cross-links in coagulation products between horseshoe crab, shrimp, crayfish and human (Chen et al. 2005).

1.7.6 Proteinases and their inhibitors in the immune system

Classified by the basis of their active-site catalytic residue, proteinases can be divided into main proteinase families as follows; i) metalloproteinase, ii) serine proteinase , iii) cysteine proteinase , iv) threonine proteinase , and v) aspartic proteinase, and vi) unidentified proteinase families. Although a variety of proteinases, such as serine proteinases, cysteine proteinases, and aspartic proteinases, serves major functions in the immunity in vertebrates, serine proteinases are supposed to be one of the most vital elements in the immune system of insects and arthropods due to the relatively high concentration of their inhibitors in these organisms' hemolymph (Kanost 1999; Tyndall et al. 2005; van Eijk et al. 2003). Otherwise, proteinases produced by pathogenic parasites are virulence factors playing various roles in pathogenesis. It has been reported that almost all types of classified proteinases (serine, cysteine, metallo, and aspartyl proteinases) (Fig. 1.19) were found to associate in the pathogenic

evasions of the host immune system (Wladyka and Pustelny 2008; Armstrong et al. 2006).

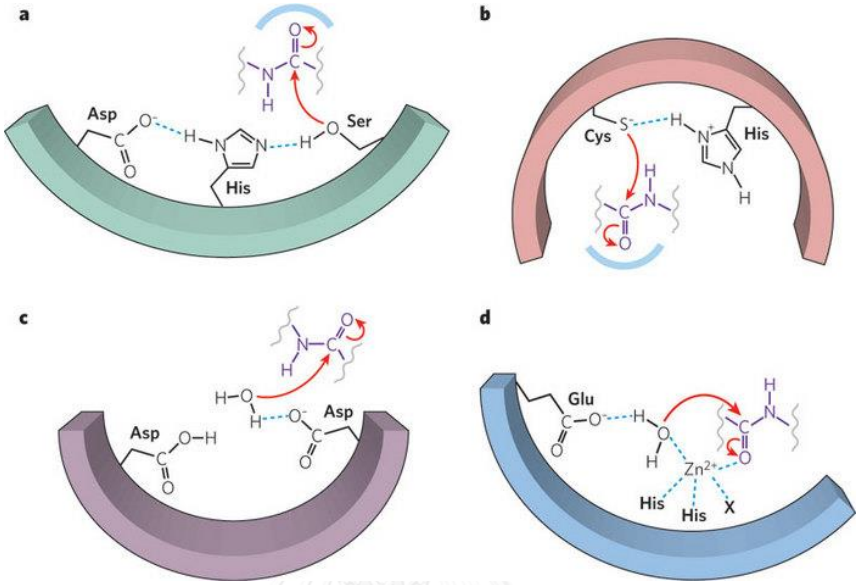

Figure 1.19 Schematic of protease mechanisms in active site of serine proteases (a); cysteine proteases (b); aspartyl proteases (c); and metalloproteases (d) (Neitzel 2010).

Expectedly, protease inhibitors are hence ubiquitously found in various creatures and consequentially become essential for controlling both exogenous and endogenous proteases. These proteinase inhibitors can be categorized by their inhibitory mechanisms into 2 major groups; active site inhibitors and alpha-2-macroglobulin (A2M). The inhibitory mechanism of the active site inhibitors is that the inhibitors directly interact with proteinases resulting in activity losses, while A2M possesses its distinctly unique mechanism to inhibit the proteinase activity (Laskowski and Kato 1980; Armstrong 2001). Since serine proteases and their inhibitors are a major

component in arthropod immunity, a specific classification of the serine proteinase inhibitors has also been reported. Based on their functions and three dimensional structures, the serine proteinase inhibitors in arthopods can be mainly divided to Serpins, Alpha-2-macroglobulin (A2M), Kunitz, Kazal, and Pacifastin (Kanost 1999).

1.8 Alpha-2-macroglobulin

Alpha-2-macroglobulin (A2M) is a broad range-protease inhibitory molecule and is an evolutionarily conserved component in the innate immunity. A2M possesses a unique mechanism to entrap a targeted proteinase inside its molecule without active site inactivation, so-called the physical entrapment mechanism (Figure 1.20) Alpha macroglobulins are composed of identical subunits, which could be monomeric (in rat and hamster, murinoglobulin in mice) or assembled in dimeric (human PZP, invertebrates) or tetrameric (vertebrates) structures.

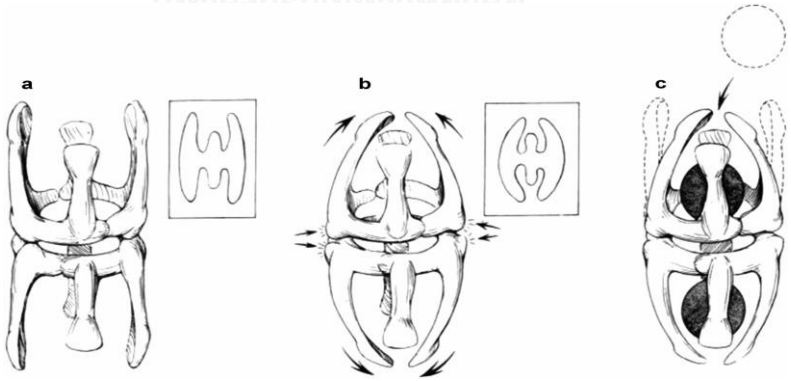

Figure 1.20 Model of A2M. (A) Normal A2M, (b) the conformational change of A2M (small arrows in the center indicate the positions for the receptor recognition sites), (c) proteinase trapping by A2M (Feldman et al. 1985)

Located near the middle of the polypeptide chain is a unique sequence of amino acids which is susceptible to cleavage by almost all endopeptidases. Cleavage of this region, termed the ‘‘bait’’ region, triggers a conformational change in the structure of alpha macroglobulin and consequent entrapment of the proteinase (Lin et al. 2012; Meyer et al. 2012). The cage formed by A2M for entrapment of proteinases is a unique molecular structure (Marrero et al. 2012) (Figure 1.21). Following the conformational change, an internal β-cystenyl-γ-glutamyl thiol ester bond is exposed which has the potential to bind covalently to the entrapped proteinase or other nucleophiles present (Barrera et al. 2007; Lin et al. 2008). There are some receptor recognition sites on A2M which are also exposed following cleavage of bait region and recognized by receptors present on several cell types. The inhibitor–proteinase complex is subsequently engulfed by these receptor-bearing cells and degraded, resulting in the clearing of proteinases from circulation (Rehman et al. 2013).

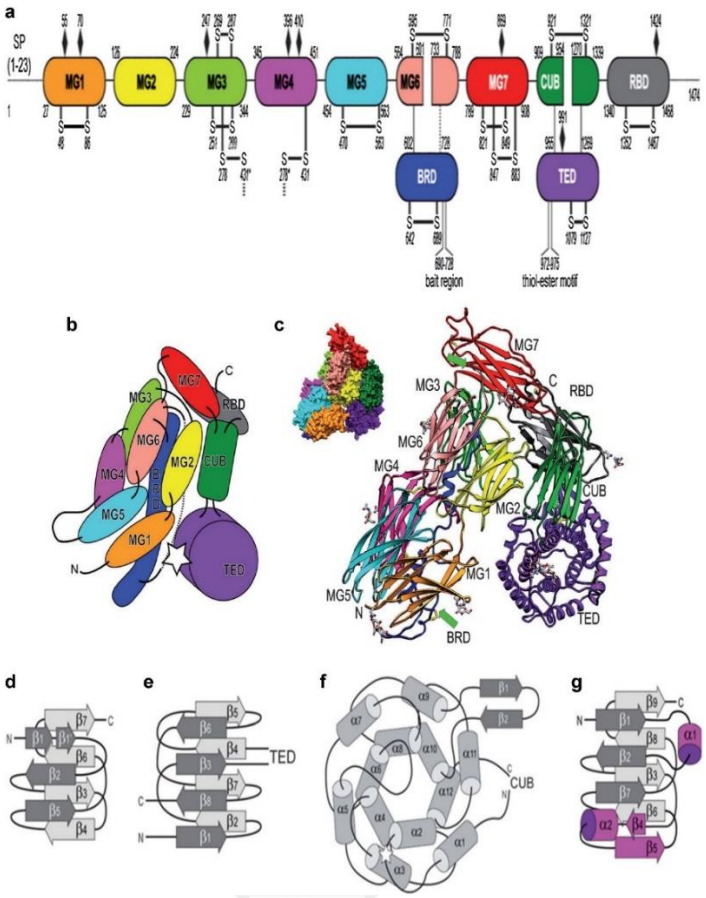

Figure 1.21 Molecular structure of A2M. (A) Domain organization of human A2M portraying the flanking residues of each domain, the disulfide bonds, the N-linked glycosylation sites, and the insertion sites of the bait region and the thioester. (b) Approximate arrangement of the domains constituting the A2M-methylamine (A2M-MA) monomer in front view (left) and back view (right). (c) Connolly surface and Richardson-type plot of A2M-MA monomer in front and back view. Green arrows represent the anchor points of the flexible bait region. (d) – (g) Topology scheme with secondary structure element nomenclature of the MGdomains (d), the CUB (Complement C1r/C1s, Uegf, Bmp1) domain (e), the TED (Thioester domain) domain (f), and the receptor RBD (Receptor binding domain) domain (g) (Marrero et al. 2012)

There have been a number of studies reporting that A2M serves crucial roles in the innate immune response in arthropods such as phagocytosis in the mosquito, *Anopheles gambiae* (Levashina et al. 2001) and the hard tick, *Ixodes ricinus* (Buresova et al. 2009), the blood clotting system in crayfish, *Pacifastacus leniusculus* (Hall et al. 1989) and the horseshoe crab, *Limulus polyphemus* (Armstrong et al. 1984), and the proPO activating system in the crayfish, *P. leniusculus* (Soderhall et al. 1990). In penaied shrimp, A2Ms from white shrimp, *L. vannamei* (Gollas-Galvan et al. 2003), the kuruma shrimp*, Marsupenaeus japonicus* (Rattanachai et al. 2004), the black tiger shrimp, *P. monodon* (Lin et al. 2007), and the chinese white shrimp, *Fenneropenaeus chinesis* (Ma et al. 2010) have been cloned and characterized. Interestingly, the shrimp A2M expression level is altered upon bacterial, viral and fungal infections at either the transcriptional or the translational levels (Perazzolo et al. 2011; Somboonwiwat et al. 2010; Ma et al. 2010). Functional analysis of the *P. monodon* A2M revealed that it can bind to syntenin, a cytosolic protein with diverse biological functions (Tonganunt et al. 2005). Also, A2M may facilitate the entry of the phagocytosis activating protein (PAP) into phagocytic cells and increase the survival rate of the shrimp after being infected by WSSV (Chotigeat et al. 2007). The protein expression profile of A2M in the major immune tissues of *V. harveyi* infected *P. monodon* indicated that it was the most strongly altered protein in hemocytes (Somboonwiwat et al. 2010) and lymphoid organ (Chaikeeratisak et al. 2012) following *V. harveyi* infection. *Pm*A2M was located on the shrimp clot and functioned as inhibitor of clot fibrinolysis**.** Recently, it has been shown

that the secreted proteases from *V. harveyi*, required for clot fibrinolysis were catergorized in the metalloprotease and the serine protease families (Chaikeeratisak et al. 2014; Chaikeeratisak et al. 2012). Therefore, it is possible that these *V. harveyi* secreted proteases are the *Pm*A2M target but this need further investigation.

1.9 Protein-protein interaction technologies

Protein-protein interactions have attracted much attention because they form the basis of a wide variety of biochemical reactions. The identification of proteins that interact with the known protein is an essential aspect of the protein-functional characterization. The study of interaction between two or more proteins can be elucidated in several different ways such as Yeast two-hybrid system and *in vitro* pull-down assay, and ELISA

1.10 Co-immunoprecipitation (co-IP)

Co-immunoprecipitation (co-IP) is a key technique for the analysis of protein–protein interactions, including interactions of subunits within a protein complex. The co-IP of proteins from cellular fractions is the most persuading proof that two or more proteins physically interact *in vivo* (Ren et al. 2003; Phee et al. 2006; Monti et al. 2005). Typically an antibody specific for one protein is incubated with a clarified homogenate or protein mixture to form an immune complex with the subject protein (antigen). A subject protein might interact with one or more other proteins in a complex. After

binding to the antibodies, the entire complex can be isolated from the mixture using immobilized protein A or protein G (protein A/G).

1.11 Enzyme-linked immunosorbent assay (ELISA)

ELISA is the abbreviation of enzyme-linked immunosorbent assay. It is a useful and powerful method in estimating ng/ml to pg/ml ordered materials in the solution, such as serum, urine, sperm and culture supernatant (Savige et al. 1998). ELISA has been widely used in the life science researches. The basic principle of an ELISA is to use an enzyme to detect the binding of antigen (Ag) antibody (Ab). The enzyme converts a colorless substrate (chromogen) to a colored product, indicating the presence of Ag:Ab binding. An ELISA can be used to detect either the presence of Antigens or Antibodies in a sample, depending on how the test is designed**.** ELISAs can provide a useful measurement of antigen or antibody concentration. There are two main variations on this method: The ELISA can be used to detect the presence of antigens that are recognized by an antibody or it can be used to test for antibodies that recognize an antigen. A general ELISA is a five-step procedure: 1) coat the microtiter plate wells with antigen; 2) block all unbound sites to prevent false positive results; 3) add primary antibody (e.g. rabbit monoclonal antibody) to the wells; 4) add secondary antibody conjugated to an enzyme (e.g. anti-mouse IgG); 5) reaction of a substrate with the enzyme to produce a colored product, thus indicating a positive reaction.

Indirect ELISA is a two-step ELISA which involves two binding process of primary antibody and labeled secondary antibody. The primary antibody is incubated with the antigen followed by the incubation with the secondary antibody in Figure 1.22 (Hnasko et al. 2011). However, iELISA technique has been applied for protein interaction assay such as In Glioblastoma of human cancer (GBM), iELISA was perform interaction between GBM and p53, Translocator Protein (TSPO), both acting as apoptosis inducers (Daniele et al. 2014).

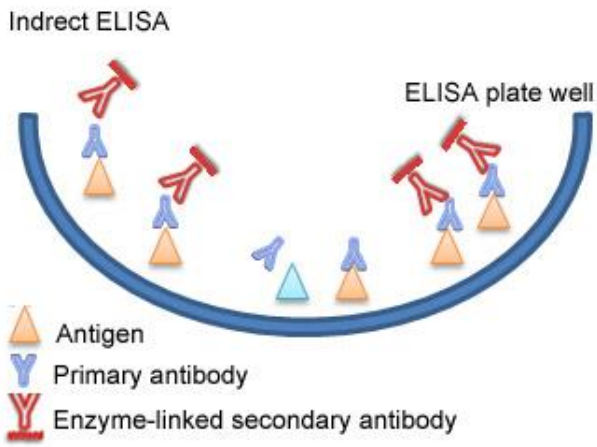

(Source: http://www.elisa-antibody.com/ELISA-Introduction/ELISA-types/indirect-elisa)

Figure 1.22 Schematic of indirect-ELISA technique.

1.12 *In vitro* pull-down assay

The pull-down assay is an *in vitro* method used to determine a physical interaction between two or more proteins. Pull-down assays are useful for both confirming the being of a protein-protein interaction predicted by other techniques and as an initial screening assay for identifying previously unknown protein-protein

interactions. In this technique, a bait protein is tagged and captured on an immobilized affinity ligand; for example, polyhistidine tag for Ni^{+} immobilized beads, and used to purify interacting proteins from a protein solution. The fusion protein and cell lysate are mixed in the presence of specific beads and incubated to allow protein associations to occur. The fusion proteins and any associated molecules are collected by centrifugation. The unbound proteins are washed out. The complexes are then eluted from the beads. Then, the protein-protein interactions are determined by SDS-PAGE (Figure. 1.23). In *P. monodon,* this technique was performed to identify several proteins involved in shrimp immune responses (Sengprasert et al. 2015) and pathogenic protein infection (Zhan et al. 2013; Youtong et al. 2011; Chen et al. 2008). The *in vitro* pull-down technique is especially useful for probing protein interactions in solutions that might go undetected in a membrane assay. This method of detecting interactions is determined by the availability of antibodies to the target protein.

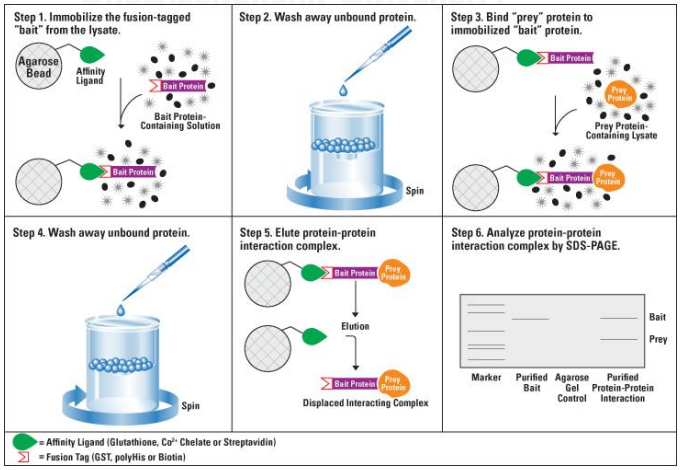

Figure 1.23 A schematic of *in vitro* pull-down assay

1.13 Molecular docking

Molecular docking is a method which predicts the preferred conformation and orientation of a ligand bound to a macromolecular target to form stable complex. Knowledge of the preferred orientation in turn may be used to predict the strength of stability or binding affinity between two molecules. Docking process has many algorithms but in this study use CDOCKER algorithm. The positions of the ligands are optimized in the binding site using rigid body rotations followed by simulated annealing. A CDOCKER algorithm is a grid-based molecular docking method that employs CHARMm. The receptor is held rigid while the ligands are allowed to be flexible during the refinement. Ligand conformations are randomly generated from the initial ligand structure through high temperature molecular dynamics, followed by random rotations. The random conformations are refined by grid-based simulated annealing and a final grid-based or full force field minimization

1.14 Objectives of the thesis

Even though, A2M was found to play role in the shrimp blood clotting system by protecting the shrimp clots against proteinase-mediated fibrinolysis and bacterial escape, little is known about the target protease of A2M in shrimp. Therefore, the aim of this study is to identify target protease of *Lv*A2M from the Pacific white shrimp, *P. vannamei.* First, the recombinant mature *Lv*A2M protein was successfully produced in *Escherichia coli*. The A2M activity of the native *Lv*A2M protein purified from shrimp

hemolymph and that of the purified recombinant *Lv*A2M was compared. The native *Lv*A2M protein was used for further experiments to identify the possible target proteins of *Lv*A2M. The inhibitory activity assay against crude bacterial proteinase using agar diffusion and binding and neutralizing assay on PirA-and PirB-like toxins from *V. paraheamolyticus* were performed to identify bacterial protease targets of *Lv*A2M. The binding of *Lv*A2M proteins and PirA and B-like proteins was confirmed by molecular docking. This studies on A2M target proteases will be fulfill and extend knowledge based on the shrimp immune defense and defense against pathogenic *Vibrio spp.* Infections.

CHAPTER II

MATERIALS AND METHODS

2.1 Materials

2.1.1 Equipments

Autoclave model # MLS-3750 (SANYO E&E Europe (UK Branch) (UK Co.)

Automatic micropipette P10, P20, P100, P200 and P1000 (Gilson Medical Electrical)

Peristaltic pump P-1 (GE Healthcare)

Balance PB303-s (Mettler Teledo)

Centrifuge 5804R (eppendrof)

Centrivap Concentrator (LABCONCO)

-20°C Freezer (Whirlpool)

-80°C Freezer (Thermo Electron Corporation)

Gel Documention System (GeneCam FLEX1, Syngene)

Gene pulser (Bio-RAD)

Imagescanner III (GE healthcare)

Incubator 30°C (Heraeus)

Incubator 37°C (Memmert)

Innova 4080 incubator shaker (New Brunswick Scientific)

Laminar Airflow Biological Safety Cabinets ClassII (NuAire, Inc., USA)

Microcentrifuge tube 0.6 ml and 1.5 ml (Axygen®Scientific, USA)

Nipro disposable syringes (Nissho)

PCR thin wall microcentrifuge tubes 0.2 ml (Axygen®Scientific, USA)

pH-meter pH 900 (Precisa, USA)

Pipette tips 10, 100 and 1000 µl (Axygen®Scientific, USA)

Power supply, Power PAC3000 (Bio-RAD Laboratories, USA)

Refrigerated incubator shaker (New Brunswick Scientific, USA)

Refrigerated microcentrifuge MIKRO 22R (Hettich Zentrifugen,Germany)

Sonicator (Bandelin Sonoplus, Germany)

SpectraMax M5 Multi-Mode Microplate Reader (Molecular Devices)

Touch mixer Model#232 (Fisher Scientific)

Trans-Blot SD Semi-Dry Transfer Cell (Bio-rad)

Water bath (Memmert)

96-well cell culture cluster, flat bottom with lid (Costar)

2.1.2 Chemicals and Reagents

100 mM dATP, dCTP, dGTP and dTTP (Promega)

5-bromo-4-chloro-3-indolyl phosphate (BCIP) (Fermentas)

2-Mercaptoethanol, C2H6OS (Fluka)

Absolute alcohol, C_2H_5OH (Hayman)

Acetic acid glacial, CH_3COOH (Merck)

Acrylamide, C_3H_5NO (Merck)

Agarose, low EEO, Molecular Biology Grade (Research Organics)

Agar powder, Bacteriological (Hi-media)

AP Substrate Kit (Bio-rad)

Aquacide II (Calbichem)

Alkaline phosphatase-conjugated goat anti-mouse IgG

(Jackson Immuno Research Laboratories, Inc.)

Alkaline phosphatase-conjugated goat anti-rabbit IgG

(Jackson Immuno Research Laboratories, Inc.)

Ammonium persulfate, $(NH_4)_2S_2O_8$ (Bio-Rad)

Anti-His antibody (Merck)

Azoalbumin(Sigma)

Bacto tryptone (Scharlau)

Bacto yeast extract (Scharlau)

Boric acid, BH_3O_3 (MERCK)

Blue Sepharose™ 6 Fast Flow (GE Healthcare)

Bovine serum albumin (Sigma)

Bromophenol blue (Merck, Germany)

Calcium chloride (MERCK)

Casein Enzyme Hydrolysate, Type-I, Tryptone Type-I (Hi-media)

Casein Peptone (Hi-media)

Chloroform, $CHCl_3$ (Merck)

Coomassie brilliant blue G-250 (Fluka)

Coomassie brilliant blue R-250 (Sigma)

D-Glucose anhydrous (Ajax)

Dithiothreitol (Pharmacia)

Diethyl pyrocarbonate (DEPC), $C_6H_{10}O_5$ (Sigma)

Di-Potassium hydrogen phosphate anhydrous (Sigma)

Ethylene diamine tetraacetic acid disodium salt, EDTA (Ajax)

Ethidium bromide (Sigma)

GeneRuler™ 100bp DNA ladder (Thermo Scientific)

GeneRuler™ 1kb DNA ladder (Thermo Scientific)

GENEzol™ Reagent (Geneaid)

Glycerol, $C_3H_8O_3$ (Ajax)

Glycine, USP Grade, NH_2CH_2COOH (Research organics)

Horseradish peroxidase (HRP)-conjugated rabbit anti-mouse IgG

(Jackson Immuno Research Laboratories, Inc.)

Hybond™-ECL membrane (GE Healthcare)

Hydrochloric acid (HCl) (Merck)

HiTrap phenyl HP column (GE Healthcare)

Imidazole (Fluka)

Isopropanol, C_3H_7OH (Merck)

Isopropyl-ß-D-thiogalactoside (IPTG), $C_9H_{18}O_5S$ (USBiological)

Marine broth(Difco)

Magnesium chloride, $MgCl_2$ (Merck)

Methanol, CH_3OH (Merck)

0.22μM and 0.45μM Millipore membrane filter (Millipore)

Nα-Benzoyl-DL-arginine 4-nitroanilide hydrochloride, BapNA (Sigma)

N, N, N´, N´-tetramethylethylenediamine (TEMED) (BDH)

N, N´-methylenebisacrylamide, $C_7H_{10}N_2O_2$ (USB)

Ni Sepharose 6 Fast Flow (GE Healthcare)

Nitroblue tetrazolium (NBT) (Thermo Scientific)

Page Ruler™ unstained protein Ladder (Thermo Scientific)

Page Ruler™ Prestained Protein Ladder (Thermo Scientific)

Paraformaldehyde (Sigma)

Peptone (Sigma)

Phosphoric acid (Labscan)

Potassium dihydrogen phosphate (Sigma)

Potassium chloride, KCl (Ajax)

PMSF (phenylmethanesulfonylfluoride) (Sigma)

RNase A (Sigma)

RQ1 RNase-free DNase (Promega)

Skim milk powder (Mission)

Silver nitrate (Merck)

Sodium chloride, NaCl (Ajax)

Sodium citrate, $Na_3C_6H_5O_7$ (Carlo Erba)

Sodium dodecyl sulfate, $C_{12}H_{25}O_4SNa$ (Vivantis)

Sodium dihydrogen orthophosphate, $NaH_2PO_4.H_2O$ (Ajax)

di-Sodium hydrogen orthophosphate anhydrous, NaH_2PO_4 (Ajax)

Sodium hydroxide, NaOH (Merck)

Triton® X-100 (Merck)

Tris (Vivantis)

Tryptic soy broth (Difco)

Tween™-20 (Fluka)

Urea (Affy Metrix USB)

Xylene cyanol FF, C25H27N2O6S2Na (Sigma)

Yeast extract (Sigma)

2.1.3 Kits

FavorPrep GEL/PCR Purification Kit (Favorgen)

FavorPrep™ Plasmid DNA Extraction Mini Kit (Favorgen)

FavorPrep™ Tissue Genomic DNA Extraction Kit (Favorgen)

RevertAID™ first strand cDNA synthesis kit (Thermo Scientific)

2.1.4 Enzymes

Advantage®2 Polymerase Mix (Clontech)

*Bam*HI (NEB)

*Nco*I(NEB)

*Not*I (NEB)

Phusion DNA Polymerases (Thermo Scientific)

Q5® High-Fidelity DNA Polymerase (NEB)

T4 DNA ligase (NEB)

Taq DNA polymerase (RBC Bioscience)

Trypsin,bovine pancreas (Sigma)

2.1.5 Antibiotics

Ampicillin (BioBasic)

Kanamycin (BioBasic)

Chloramphenicol (Sigma)

2.1.6 Microorganisms

Gram positive bacteria

Aerococcus viridans

Bacillus megaterium

Micrococcus luteus

Staphylococcus aureus

Staphylococcus haemolyticus

Gram negative bacteria

Enterobacter cloacae

Erwinia caratovora

Escherichia coli strain 363

Vibrio harveyi strain 639

Vibrio paraheamolyticus strain TM

Strains and Vectors Bacterial Expression

Escherichia coli strain XL-1-Blue

Escherichia coli strain XL-1-Gold

E. coli strain BL21-CodonPlus(DE3)-RIL

pET-22b(+) (Navogen)

pVR600 (pET-28b(+) derivative)

Software

BlastN and BlastX (http://www.ncbi.nlm.nih.gov/BLAST/)

Discovery studio 3.0 (http://accelrys.com/products)

ClustalW (http://www.ebi.ac.uk/Tools/msa/clustalw2/)

ExPASy ProtParam (http://au.expasy.org/tools/protparam.html)

EMBOSS Pairwise Alignment (http://www.ebi.ac.uk/Tools/emboss/align/)

GENETYX (Software Development Inc.)

PATCHDOCK(http://bioinfo3d.cs.tau.ac.il/PatchDock/)

PeptideCutter (http://web.expasy.org/peptide_cutter/)

PHYRE2 Protein Fold Recognition Server (http://www.sbg.bio.ic.ac.uk/phyre2)

PROSPER protease specificificity predictation

(https://prosper.erc.monash.edu.au/help.html)

SECentral (Scientific & Educational Software)

SignalP 4.1 Server (http://www.cbs.dtu.dk/services/SignalP/)

ZDOCK Server (http://zdock.umassmed.edu/)

2.2 General protocols

2.2.1 Quantitative method for DNA determination

The concentration of DNA fragment was determined by measuring the A_{260} and estimated in μg/ml using an equation: [DNA] (μg/ml) = A_{260} × dilution factor × 50 for one A_{260} corresponds to 50 μg/ml of DNA (Sambrook and Russell David 1989).

2.2.2 Primer design

All primer used in this studies were designed based on nucleotide sequences of the template DNA by SECentral program (Scientific & Educational Software). The melting temperature (Tm), self-priming, GC content and primer-dimer formation were carefully considered (Table 2.1)

Table 2.1 Nucleotide sequences of the primers and annealing temperature for PCR reaction.

Name	Purpose	Length (bp)	Sequence (5′-3′)	Annealing temperature(°C)
A2M_LV_forward	r*Lv*A2M	31	ACTGGGATCCACTG GTCGGAATCCTCCTCAG	74
A2M_LV_reverse	production	33	TATTATAGCGGCCGCGTCGCACCCTTCGACGTA	74
A2M_LV_QF2	r*Lv*A2M gene	20	CGAAGGAACAGCCAGGAGAG	64
A2M_LV_QR2	for sequencing	20	GAGGTTCTGCAGCGAGAGTG	64
PAP6_F_Full	full-length	30	GCACCATGGCA-CTTGAAGCAGAAGGCCCAG	76
PAP6_R	rPAP6 production	51	CGCGGATCCCTA**ATGGTGATGGTGATGGTG**-ATAGTCGTTACAGCTGCCTTC (include His-tag)	81
PAP6_F	patial-rPAP6	28	GCACCATGGCA-TCGCTTGTCCCTTTCGC	75
PAP6_R	production	51	CGCGGATCCCTA**ATGGTGATGGTGATGGTG**-ATAGTCGTTACAGCTGCCTTC (include His-tag)	81

* **Bold** character represent the nucleotide coding for His-tag

2.2.3 Competent cells preparation and transformation

There are two types of *Escherichia coli* competent cells used in this study, $CaCl_2$-treated cells and electrocompetent cells. A single colony of either E. coli strain XL-1-Blue, XL-1-Gold or BL21-CodonPlus(DE3)-RIL was inoculated into fresh Luria-Bertani media (1% (w/v) tryptone type-I, 0.5% (w/v) bacto yeast extract, and 1% (w/v)

NaCl) containing an appropriate antibiotic (50 μg/ml of chloramphenicol for BL21-CodonPlus(DE3)-RIL). The culture was grown overnight at 37 °C with 250 rpm shaking as a starter. The starter was diluted 1:100 in LB broth and incubated until OD_{600} reached 0.5-0.6.

2.2.3.1 Competent cells for electro-transformation

The cell suspension was cooled down by chilling on ice for 30 min, before harvested by centrifugation at 4,000 × g for 15 min at 4 °C. The cell pellet was washed twice using 1 and 0.5 volume, respectively, of sterile pre-cooled distilled water. Then, cell pellet was resuspended in an appropriate volume of iced-cooled 10% (v/v) glycerol. The cell suspension (50 μl) were aliquoted and immediately frozen at -80 °C until used.

2.2.3.2 Competent cells for $CaCl_2$-transformation

The 10 min pre-chilled culture was centrifuged at 4,000 × g for 5 min. Then, the cells were washed once with 0.5 volume of 10 mM $CaCl_2$ solution. The final cell pellet was resuspended in an appropriate volume of 100 mM $CaCl_2$ solution supplemented with 10% (v/v) glycerol and chilled on ice for about 30 min. The competent cells (50 μl) were taken into an aliquot and immediately frozen at -80 °C until used.

2.2.3.3 Transformation

For electro-transformation, plasmid solution at the maximum volume of 2 µl per 50 µl cells was transformed into electro-competent cells. The plasmid was incubated with competent cells on ice for 1 min, and then the mixture was transferred into cooled and cleaned 0.2 cm electrode gap cuvette for electroporation. The mixture was pulsed using Minipulser electroporation system (Bio-Rad) at constant 2.5 kV. The mixture was immediately transferred into 1 ml SOC media.

For $CaCl_2$ transformation, up to 20 µl plasmid was mixed with 100 µl of competent cells. The plasmid and competent cells were mixed and chilled on ice for at least 30 min. After that, the reaction was incubated at 42 °C for 1 min and optional on ice for 3 min. The SOC media (1 µl) was subsequently added to the mixture.

Afterward, 1 ml culture containing recombinant cell was incubated at 37 °C with shaking for 1 h. The cell suspension was spread onto LB agar plate supplemented with appropriate selective substances.

2.2.4 Plasmid DNA preparation using FavorPrep™ Plasmid DNA Extraction Mini Kit (Favorgen)

A recombinant bacterial clone was inoculated into 10 ml of Luria-Bertani (LB) medium containing appropriate antibiotic and grew overnight at 37 °C with shaking. The cells were collected by centrifugation for 10 min at 8,000 × g. The cell pellet was resuspended in 250 µl of FAPD1 buffer containing RNase A. The 250 µl of FAPD2 buffer

was added and mixed gently by inverting the tube 5 times to lyse the cells and incubate at room temperature for 2 min. The cell lysate was neutralized by adding 300 µl of FAPD3 buffer and mixed immediately and gently. After centrifugation at 15,000 × g for 3 min, the supernatant containing the plasmid was applied to a FAPD column in a Collection Tube by pipetting. The column was centrifuged at 15,000 × g for 1 min and the flow-through was discarded. The column was washed twice with 400 µl of W1 buffer and 750 µl of wash buffer containing ethanol, respectively, and then centrifuged for an additional 5 min to remove residual ethanol from wash buffer. Finally, the plasmid DNA was eluted by adding 50 µl of pre-heated elution buffer to the center of each column, incubating at room temperature for 2 min and centrifugation at 15,000 × g for 2 min. The eluent containing the plasmid was then stored at -20 °C until use.

2.2.5 Purification of PCR product by FavorPrep GEL/PCR Purification Kit (Favorgen).

2.2.5.1 Purification of PCR product from agarose gel

The PCR product was purified from agarose gel by FavorPrep GEL/PCR Purification Kit (Favorgen). The PCR band was excised from agarose gel with a clean sharp scalpel. Extra agarose was removed to minimize the size of the gel slice. The gel slice was weighted and transferred to a clean microcentrifuge tube. Up to 300 mg of of the gel slice into a microcentrifuge tube. The FADF buffer (500 µl) was added into the centrifuge and mix by vortexing. (For > 2% agarose gels, add 1000 µl of FADF

Buffer). The sample was incubated at 55 ℃ for about 10 min or until the gel slice dissolved completely. During incubation, interval vortex can accelerate the gel dissolved and make sure that the gel slice has been dissolved completely before proceed the next step. Cool down the sample mixture to room temperature and place a FADF column in a collection tube. The sample was loaded into the column and centrifuged at 11,000 × g for 1 min. If the sample mixture volumn is more than 800 µl, repeat this step for the rest sample mixture. The flow-through was discarded, and the column was washed with 750 µl of wash buffer (ethanol added) and centrifuged at 11,000 × g for 30 sec. After centrifugation, the silica membrane in column was dried by centrifugation at 11,000 × g for an additional 3 minutes. This step will avoid the residual liquid to inhibit subsequent enzymatic reactions. The FADF column was placed into a new 1.5 ml microcentrifuge tube. The DNA was eluted by adding 40 µl of elution buffer into the center of silica membrane and stand at room temperature for 2 min for effective elution, make sure that the elution solution is dispensed onto the membrane center and is absorbed completely. Centrifuge for 2 min to elute the DNA. The flow-through containing the DNA fragment was measured at A_{260} for its concentration and stored at -20 ℃ until used.

2.2.5.2 Purification of PCR product clean-up

The PCR product was transfer up to 100 µl of PCR product (If PCR product is more than 100 µl, separate it into multiple tubes) and add 5 volumes of FADF buffer

to a microcentrifuge and then mix by vortexing. The PCR product mixture was placed a FADF column into a collection tube and centrifuge for 30 sec. then discard the flow-through. Add 750 µl of Wash Buffer (ethanol added) to the FADF column and centrifuge for 30 sec. then discard the flow-through. Make sure that ethanol (96-100 %) has been added into Wash Buffer when first open. Centrifuge again for an additional 3 minutes to dry the column. This step will avoid the residual liquid to inhibit subsequent enzymatic reactions. The FADF column was placed into a new 1.5 ml microcentrifuge tube. Add 40 µl of Elution Buffer or deionized H_2O to the membrane center of the FADF column. Stand the FADF column for 2 min. Centrifuge for 2 min to elute the DNA. The flow-through containing the DNA fragment was measured at A_{260} for its concentration and Store the DNA at -20 ℃ until used.

2.2.6 Genomic DNA Extraction

The Genomic DNA was purified by FavorPrep™ Tissue Genomic DNA Extraction Mini Kit (Favorgen). The cell pellet was placed into a microcentrifuge tube. Use provided Micropestle to grind the cell pellet sample a few times. Or grind the cell pellet sample in liquid nitrogen. The FATG1 Buffer (200 µl) was added into the microcentrifuge tube and mix well by micropestle or pipette tip. The 10 mg/ml Proteinase K (20 µl) was added to the sample mixture. Mix thoroughly by vortexing. The sample was incubated at 60 ℃ until the pellet is lysed completely. Vortex every 10~15 min during incubation to break up the pellet sample. Briefly spin the tube to

remove drops from the inside of the lid. The genomic DNA is required RNA-free, add 4 µl of 100 mg/ml RNase A and incubate for 2 min at room temperature. 200 µl of FATG2 buffer was added to sample mixture, mix thoroughly by pulse-vortexing and incubate at 70 ℃ for 10 min. Briefly, spin and then 200 µl (96-100%) was added to the sample. Mix thoroughly by pulse-vortexing. The FATG Mini column was placed in a collection tube. The mixture (including any precipitate) was transferred carefully to FATG Mini column and centrifuge for 1 min then place FATG Mini column to a new collection tube. The FATG Mini column was washed twice with 500 µl and 750 µl of W1 buffer by centrifuge for 1 min then discard the flow-through. Centrifuge for an additional 3 min to dry the column. FATG Mini column was placed into elution tube and 50~200 µl of elution buffer (pH 7.5-9.0) was added to the membrane center of FATG Mini column. After 3 min, total DNA was eluted by centrifugation for 2 min. Total DNA was stored at -20℃ until used.

2.2.7 Agarose gel electrophoresis

The agarose gel was prepared by dissolving the agarose gel powder in 1× TBE buffer (89 mM Tris-HCl, 8.9 mM boric acid and 2.5 mM EDTA, pH 8.0). Then the agarose gel was melted and the solution was cooled down. The solution was poured into a tray equipped with comb for a well-forming. After the gel was polymerized, it was loaded into the chamber with 1× TBE running buffer. The DNA samples mixed with 1X loading dye (final concentration) (50 mM Tris-HCl, 2.5 mg/ml bromophenol blue, 2.5

mg/ml xylene cyanol, 60% glycerol at pH 7.6) were loaded into the wells. Next, the standard DNA markers (100 bp or 1 kb DNA ladders) were loaded into the well. The DNA was separated by electrophoresis at 100 volts for 25 min in 1× TBE buffer. The gel was stained with ethidium bromide solution for 30 sec. and de-stained in the water for 20 min. The DNA bands were visualized under the UV transilluminator.

2.2.8 Protein analysis

2.2.8.1 Analysis of recombinant protein by SDS-PAGE

The gel solutions for 12% separating gel, 2 ml of 30% acrylamide and 15% separating gel ,2.5 ml of 30% acrylamide 1.27 ml of 1.5 M Tris-HCl pH 8.8, 50 µl of 10% SDS, 50 µl of 10% APS, 2 µl of TEMED and 1.13 ml of distilled water) and 5% stacking gel (500 µl of 30% acrylamide, 380 µl of 1 M Tris-HCl pH 6.8, 30 µl of 10% SDS, 30 µl of 10% APS, 3 µl of TEMED and 2.06 ml of distilled water) were prepared. The separation gel solution was poured into the glass plates with 1 mm spacer and covered on top with distilled water. After 20 min, the gel was completely polymerized. Then, the stacking gel solution was poured on top of the separating gel and comb was immediately put between the glass plates. After the stacking gel was polymerized, the comb was removed and the wells were rinsed with distilled water to remove excess un-polymerized acrylamide. The protein samples were prepared by resuspending the proteins in 1× SDS loading buffer (12 mM Tris-HCl, pH 6.8, 5% glycerol, 0.4% SDS, 0.02% bromophenol blue, and 2.88 mM 2-mercaptoethanol). The samples were boiled for 5

min and spun down. The samples and protein standard marker were loaded into gel. Electrophoresis was run in 1× SDS running buffer (25 mM Tris-HCl, pH 8.3, 192 mM glycine, and 0.1% (w/v)) SDS with a constant current of 25 mA per gel until the dye front into the end of the gel. After electrophoresis, the gel was stained in the Coomassie brilliant blue-R250 staining solution (0.1% (w/v) (Coomassie brilliant blue R250, 10% (v/v) acetic acid, 45% (v/v) methanol) at room temperature with gentle shaking for 1 h. Next, the gel was destained using the destaining solution (10% (v/v) acetic acid, 10% (v/v) methanol) and shaken at room temperature until the gel background was clear.

2.2.8.2 Protein detection by Western blot analysis

To detect the expected protein, the Western blot analysis was performed using a specific antibody. After protein separation by SDS-PAGE, the gel was soaked in the transfer buffer (25 mM Tris base, 150 mM glycine and 20% methanol). The nitrocellulose membrane and six pieces of filter papers whose size is same as the gel size, were soaked in the transfer buffer for 10 min. Then, the first filter paper, nitrocellulose membrane, the gel, and the second filter paper, respectively were placed onto the platform of Trans-Blot SD Semi-Dry Transfer Cell (Bio-rad) and the air bubble was removed by rolling over the surface of filter paper by glass stirring rod. Then, the protein was transferred at constant 110 mA for 90 min. Then, the nitrocellulose membrane was blocked in a blocking solution 5% (w/v) skim milk in

PBS-Tween™-20 (1× PBS buffer and 0.05% (v/v) Tween™-20 at pH 7.4) at room temperature with gentle shaking for 1 h. Then, the membrane was washed for 3 times 10 min each with 1×PBS-Tween™-20. After that, the membrane was incubated with the primary antibody diluted at the a attentive concentration in 1×PBS-Tween™-20 containing 1% (w/v) skim milk for 3 h at 37 °C with gentle shaking. Afterwards, the membrane was washed for 3 times 10 min each with PBS-Tween™-20 again to remove the unbound protein. The secondary antibody conjugated with alkaline phosphatase or horseradish peroxidase (HRP) (Jackson Immuno Research Laboratories, Inc.) was diluted in 1×PBS-Tween™-20 containing 1% (w/v) skim milk at room temperature for 1 h. After washing, the substrate NBT and BCIP (Thermo Scientific) at the final concentration of 375 and 188 µg/ml, respectively, in 100 mM Tris- HCl, 100 mM NaCl and 50 mM $MgCl_2$, pH 9.5 was incubated with membrane for alkaline phosphatase detection. When the bands of protein were detected, the reaction was stopped by washing the membrane with distilled water.

2.2.8.3 Determination of protein concentration

The protein concentration was measured based on the method of Bradford (Bradford 1976) using bovine serum albumin (Sigma) as a standard protein. Preparation of Bradford working solution by diluting ratio 1:4 5X Bradford reagent (Bio-Rad) with deionized water respectively, as a standard solution. Preparation of five dilutions of a protein standard, which is representative of the protein solution to be tested. The

linear range of this microtiter plate assay is 0 mg/ml to approximately 8 mg/ml. Protein solutions are normally assayed in duplicate. The brown color of reaction was converted to the blue solution, and protein was detected by monitoring the absorption at 595 nm. A sample solution (1 µl) was mixed with 150 µl of Bradford working solution and incubated for 15 min at room temperature, A_{595} was subsequently measured.

2.3 Animal cultivation (shrimp)

The pacific white shrimp *(Litopenaeus vannamei)*, each size of about 3-5 g body weight use for cumulative mortality and about 10-15 g use for RNA extraction and protein purification. Shrimps were kindly provided from a local shrimp farm at Petchaburi province, Thailand. Shrimps were acclimatized in the laboratory aquaria at a temperature of 28±4 °C and at the salinity of about 15 ppt for at least 1 week before used in each experiment.

2.4 RNA preparation and first-stranded cDNA synthesis

2.4.1 Total RNA extraction

The hemocyte was withdrawn from the hemocoel of normal shrimp using a 24 G (0.55×25 mm) NIPRO hypodermic syringe needles sterile fitted onto a 1.0 ml syringe pre-loaded with 200 µl of anticoagulant [10% (w/v) sodium citrate]. The hemocytes were immediately separated from plasma by centrifugation at 800 × g for 10 min at 4 °C. The hemocyte samples were briefly homogenized by a pestle in 1 ml of ice-cold

GENEzol™ Reagent (Geneaid). The homogenate was stored at room temperature for 5 min to permit complete dissociation of nucleoprotein complexes. Then, 200 µl of chloroform was added. The sample were vigorously shaken for 10 second and incubated at room temperature for 2-5 min before centrifugation at 12,000 × g for 15 min at 4 °C. The RNA was in the colorless upper aqueous phase which is approximately 50% of the total volume. The colorless upper aqueous phase was transferred to a new 1.5 ml microcentrifuge tube (RNase-free). The total RNA was precipitated with 1 volumn of isopropanol to the aqueous phase then mix by inverting the tube several times. The mixture was incubated at room temperature for 10 min and centrifuged at 12,000 × g for 15 min at 4 °C to form a tight RNA pellet. The supernatant was carefully removed and discarded. The pellet of total RNA was washed in 1 ml of 70% ethanol and stored at -80 °C until used. The total RNA pellet in 70 % ethanol was centrifuged at 12,000 × g for 15 min at 4 °C. The supernatant was removed. The RNA pellet was briefly air-dried for 5-10 min. The total RNA was dissolved with 20-50 µl RNase-free water or an appropriate amount of diethyl pyrocarbonate (DEPC)-treated water and incubated on ice until it was completely dissolved.

2.4.2 Determination of the quantity and quality of RNA samples

The quantity and quality of total RNA was spectrophotometrically measured at 260 nm and analyzed by agarose gel electrophoresis,respectively.

The concentration of total RNA could be determined using the following formular: [RNA] = A_{260} × dilution factor × 40. One A_{260} corresponds to 40 µg/ml of RNA (Sambrook and Russell David 1989).

The relative purity of RNA samples was examined by measuring the ratio of $A_{260/280}$ and $A_{260/230}$. The maximum absorption of organic solvent, nucleic acid, and protein is at 230, 260, and 280 nm, respectively. The ratio of absorbance at 260 nm and 280 nm is used to assess the purity of RNA. An approximately ratio above 1.7 is generally accepted as pure RNA. If the ratio is appreciably lower, it may indicate the presence of protein, phenol or other contaminants that absorb strongly at or near 280 nm. The quality of the extracted RNA was analyzed an agarose gel electrophoresis. The total RNA was stained with EtBr and visualized bands under a UV transilluminator, respectively.

2.4.3 DNase treatment of total RNA samples

The obtained total RNA was further treated with RQ1 RNase-free DNase (Promega). The reaction contains 5 µg of total RNA in 1× RNase-free DNase buffer and 1 unit of RQ1 RNase-free DNase. The DNase treatment reactions were incubated at 37 ℃ for 30 min to remove the contaminating chromosomal DNA. Then, the RNA was purified by GENEzol™ Reagent and isopropanol precipitation. The reactions of DNase-treated RNA were adjusted the volume to 30 µl with DEPC-treated water and 200 µl of GENEzol™ Reagent were added. The reaction was vortexed for 15 sec. 40 µl of chloroform were added and vigorously shaken for 20 sec. The mixture was kept at room temperature for 10 min and centrifuged at 12,000 × g for 15 min at 4 ℃. After centrifugation, the aqueous upper phase was precipitated with 1 volume of isopropanol. The RNA pellet collected by centrifugation was washed with 1 ml of 70% ethanol. The RNA pellet was briefly air-dried and dissolved with an appropriate volume of DEPC-treated water. The quantity and quality of total RNA was examined as described in the section 2.4.2.

2.4.4 First-strand cDNA synthesis

The first strand cDNA was synthesized from 1 µg of the total RNA using the RevertAid™ First Strand cDNA Synthesis Kit (Thermo scientific). According to the kit's instruction, the reaction was performed in a final volume 12 µl containing 1 µg of the total RNA, 0.5 µg of the oligo(dT) primer and adjusted the volume by DEPC-treated

water. The mixture of RNA was incubated at 65 °C for 5 min and chilled on ice for 5 min to anneal the primer. After that, 4 µl of 5X reaction buffer, 1 µl of RiboLock™ RNase inhibitor (20U/µl), 2 µl of 10 mM dNTP mix and 1 µl (200U/µl) of RevertAid™ M-MuLV reverse transcriptase were added and gently mixed. The reaction mixture was incubated 42 °C for 1 h and finally heated at 70 °C for 15 min to terminate the reaction. The cDNA was stored at -20 °C until used.

2.5 Production of recombinant *Lv*A2M and anti-r*Lv*A2M polyclonal antibody

2.5.1 Construction of the expression plasmid

For the advantage of protein production, a modified expression vector pVR600 constructed from an expression vector pET-28b(+) by deleting the His-tag and T7-tag between *Nco*I and *Bam*HI sites (Figure 2.1), was used. The His-tag left at the C-terminal and at the 3' side of the reading frame was used for the protein purification as described below.

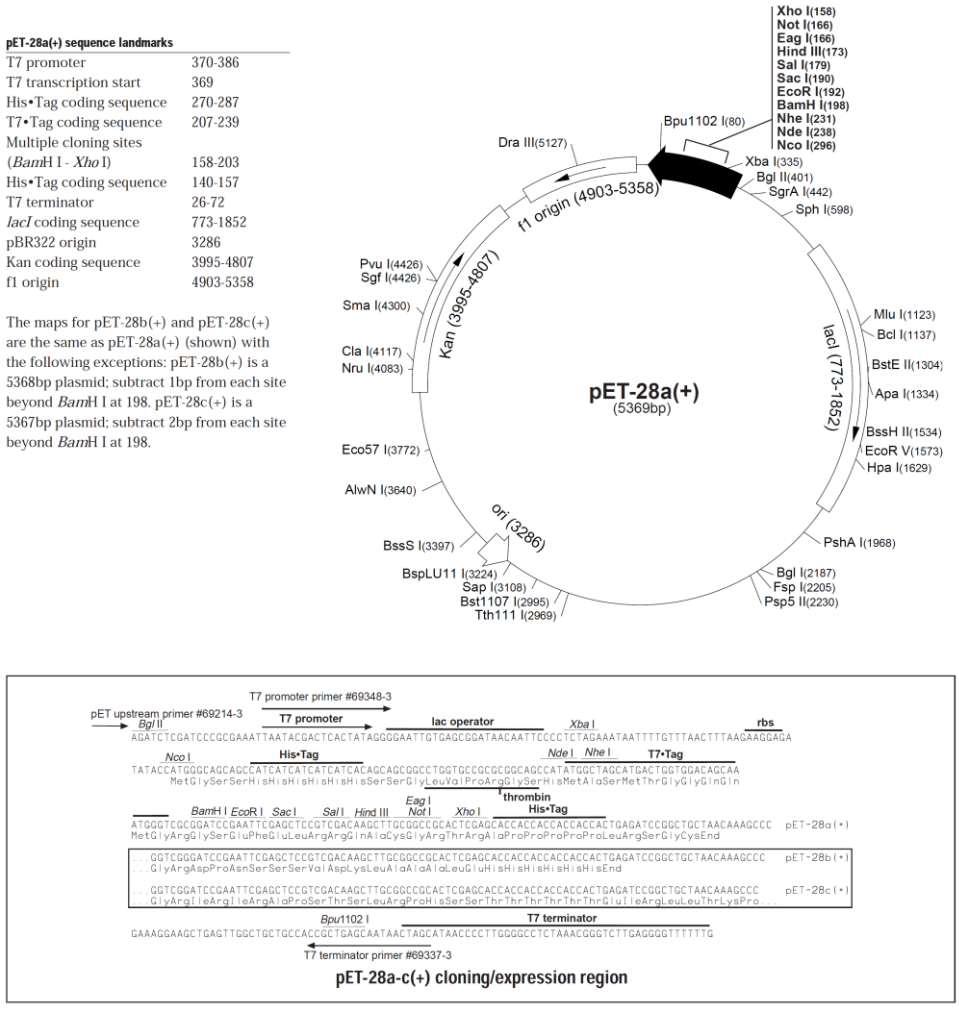

pVR600

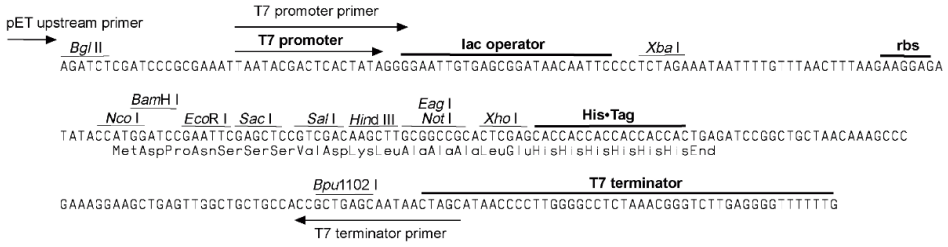

Figure 2.1 The pET-28b(+) vector map (Novagen®, Germany). The pVR600 was constructed by deleting the His-tag and T7-tag between *Nco*I and *Bam*HI sites.

2.5.2 Construction of expression plasmid for recombinant *Lv*A2M protein production

The nucleotide sequences of the full length *Lv*A2M (accession no. DQ988330) have been reported previously (Lin et al. 2007). In order to construct expression plasmid for the recombinant *Lv*A2M protein (r*Lv*A2M) production, the full length *Lv*A2M gene was amplified from cDNA using specific primers, A2M_LV_forward and A2M_LV_reverse (Table 2.1), respectively. The *Lv*A2M gene was amplified in a final reaction volume of 50 µl containing 0.02 µg of cDNA template, 0.5 µM of each primer, 25 µl of Q5 High-Fidelity 2X Master Mix and adjust volume to 50 µl by Nuclease-Free Water. The PCR amplification was carried out by Q5® High-Fidelity DNA Polymerase (NEB) with the PCR condition as following; the initial denaturation step at 98 °C for 30 sec, 30 cycles of 1) the denaturation step at 98 °C for 10 sec, 2) the annealing step at 72 °C for 30 sec and 3) the elongation step at 72 °C for 2 min 30 sec, and then a final extension at 72 °C for 2 min The PCR products (4,454 bp) was analyzed using 1% agarose gel electrophoresis, excised and purified FavorPrep GEL/PCR Purification Kit (Favorgen) and later digested with the *Not*I and *Bam*HI restriction enzymes at 37 °C overnight. The *Not*I and *Bam*HI digested product was cloned in-frame with clones sites of the expression vector pVR600 (pET-28b(+) derivative) cut with the same enzymes using T4 DNA ligase (NEB) by incubation at 16 °C overnight. The recombinant plasmid was (pVR600-*Lv*A2M) electroporated into *E. coli* strain XL-1 blue and XL-10 gold as described in the section 2.2.3.3 and the transformant was selected by LB agar medium

supplemented with 50 µg/ml kanamycin at 37 °C overnight. Afterwards, the plasmid was extracted from the positive clones and purified FavorPrep™ Plasmid DNA Extraction Mini Kit (Favorgen) according to the section 2.2.4. The recombinant clones were then selected and sequenced to confirm the correctness of the A2M sequences using T7 promoter, T7 terminator and specific primer (A2M_LV_QF2, A2M_LV_QR2) with an automated sequencer by a commercial service at Macrogen INC., South Korea

2.5.3 Expression of the recombinant *Lv*A2M protein

To produce the recombinant *Lv*A2M protein. The recombinant plasmid (pVR600-*Lv*A2M) was transformed into the *E. coli* strain BL21-CodonPlus® (DE3)-RIL, an expression host by heat-shock method and the transformant was selected by LB agar plate supplemented with 50 µg/ml kanamycin and 50 µg/ml of chloramphenicol at 37 °C overnight. The single colony of *E. coli* strain BL21-CodonPlus(DE3)-RIL containing pVR600-*Lv*A2M were cultured with shaking 250 rpm at 37 °C overnight in 5 ml of LB broth supplemented with 50 µg/ml kanamycin and 50 µg/ml of chloramphenicol was used for recombinant clone selection.

The starter was diluted 1:100 fold of LB-broth. The culture were grown at 37 °C with shaking at 250 rpm until the OD_{600} reached 0.4. The recombinant protein was induced by the addition of 1 M isopropyl-ß-D-1-thiogalactopyranoside (IPTG) to a final concentration of 1 mM. The bacterial cell was then collected at 0, 2, 4, and 6 h after IPTG induction by centrifugation at 8,000 x g for 10 min. The collected cells were

dispersed in SDS-PAGE sample buffer and the solution was incubated in heat box for 10 min. The over-expressed recombinant *Lv*A2M protein was later resolved by 10% (w/v) acrylamide SDS-PAGE and western blotting using monoclonal anti-His antibody (GE healthcare) as a primary antibody and goat anti-mouse IgG as a secondary antibody at the dilution of 1:5,000 and 1:10,000, respectively.

2.5.4 Purification of recombinant proteins and antibody production of the r*Lv*A2M

After harvesting, the cells were resuspended in 50 mM Tris-HCl buffer pH 8.0 and subjected to sonication. The crude protein in the inclusion bodies was dissolved by 50mM NaCl in 50 mM Tris-HCl pH 8.0 and run onto 10% SDS-PAGE.

The band corresponding to r*Lv*A2M, was cut and eluted by crushing and soaking the gel in 50mM Tris-HCl buffer pH 8.0. The purified r*Lv*A2M was concentrated by Amicon ultra-15 centrifugal filter MWCO 100 kDa and collected at -20 °C. Pior to use for further activity assays, it was checked for integrity by Coomessie stained 10% SDS-PAGE and quantified by Bradford assay

2.5.5 Antibody production and purification of anti-r*Lv*A2M polyclonal antibody

The mouse polyclonal antibodies against the r*Lv*A2M was commercially raised in experimantal animals at a commercial service of the Biomedical Technology Research Center, Faculty of Associated Medical Sciences, Chiang Mai University, Thailand.

The mouse polyclonal antiserum specific to *Lv*A2M protein was purified on protein A column by incubated with protein A bead (GE Healthcare) pre-equilibrated with binding buffer (100 mM Tris-HCl pH 8.0). After that, the bead was washed with 10 column volume of binding buffer and 10 mM Tris-HCl pH 8.0. The step of elution was carried out using 100 mM glycine pH 3.0 and 50 µl of 1M Tris pH 8.0 was added to each fraction.

2.6 Detection of *Lv*A2M protein in hemolymph of shrimp

*Lv*A2M protein in hemolymph of shrimp was analyzed using SDS-PAGE and western blotting techniques. First, the hemolymph from 3 shrimps was collected under equal volume of MAS buffer (27 mM sodium citrate, 336 mM NaCl, 115 mM glucose and 9 mM EDTA, pH 7.0) The protein content of hemolymph was measured by Bradford assay. BSA was used as a standard protein. Hemolymph (100 µg) was separated on a 10 % SDS-PAGE. The western blot analysis was performed using the purified. Anti-*Lv*A2M antibody as primary antibody at 1:10,000 dilution. Before incubation with secondary antibody at room temperature for an hour, the membrane was washed three times with PBS-Tween^{TM}-20. The secondary antibody, anti-mouse IgG conjugated with alkaline phosphatase ((Jackson Immuno Research Laboratories, Inc.) was diluted in 1% (w/v) skim milk in PBS-Tween^{TM}-20 for 1 h at 1:10,000 dilution. The membrane was washed three times with PBS-Tween^{TM}-20 before detection by adding NBT and BCIP (Fermentas) at the final concentration of 375 and 188 µg/ml, respectively.

2.7 A2M activity of alpha 2 macroglobulin with trypsin

2.7.1 A2M activity assay

A2M activity was assayed by determination the protease activity of the trapped target protease. A2M activity was measured by incubating (5, 10 and 20 µg) of purified native or recombinant *Lv*A2M in 50 ul of 50 mM Tris-HCl pH 8.0 with 10 µl of 1 mg/ml trypsin for 15 min at 37 °C. After incubation, 10 µl of 2 mg/ml soybean trypsin inhibitor were added and incubated for 10 min at 37 °C in order to inhibit the activity of free trypsin. Finally, 100 ml of trypsin substrate, 1 mg/ml BAPNA (Na-benzoyl-DL-arginine-p-nitroanilide) in 50 mM Tris-HCl pH 8.0, were added and incubated 2 h at 37 °C. The activity of trapped trypsin was determined by measuring A_{415}.

2.7.2 Bait region of *Lv*A2M binding to trypsin by molecular docking

The amino acid sequence of alpha 2 macroglobulin from *Litopenaeus vannamei* (*Lv*A2M) was retrieved from the sequence database of NCBI (ID: *Lv*A2M: ABI79454.2). Bait region of *Lv*A2M Analysis binding at the active site of trypsin for cleavage reaction was investigated by docking method using Trypsin/Brovine Pancreatic inhibitorII complex (PDB ID: 2PTC) as a model protease and the 6 possible peptides extracted from bait region of *Lv*A2M. Prediction of protease cleavage sites on bait region were identified using the PROSPER server (https://prosper.erc.monash.edu.au/) and PeptideCutter (http://web.expasy.org/ peptide_ cutter/) program. Structure preparation of the 6 peptides contacting the 10 residues from bait region was

constructed by homology modelling using trypsin inhibitor as a template using the Leap module in the Amber 12 software package. Each peptide was docked into the active site of Trypsin with 100 runs using the CDOCKER module of Accelrys Discovery Studio 3.0 (Accelrys, Inc.).

2.8 The purification of native A2M protein from pacific white shrimp

2.8.1 Hemolymph collection

Juvenile white shrimp (*Litopenaeus vannamei*) size of about 10-15 g body weight were obtained from a commercial farm (Junpa, Petchaburi, Thailand) and kept in aerated seawater (15 ppt) until used. The hemolymph was withdrawn from the ventral sinus located at the base of the first abdominal region, under an equal volumes of precooled MAS buffer (27 mM sodium citrate, 336 mM NaCl, 115 mM glucose and 9 mM EDTA, pH 7.0) supplemented with 1 mM PMSF. The hemocytes were immediately separated from plasma by centrifugation at 800 × g for 10 min at 4 °C and immediately placed in liquid nitrogen before being subjected to total RNA extraction and the plasma supernatant was immediately used for A2M purification.

2.8.2 Purification of native A2M protein

The purification method was modified from Gollas-Galvan et al. (2003). Cell-free plasma (20 ml) was filtered through 0.45μm membrane and applied to a Blue-Sepharose column (GE Healthcare) pre-equilibrated with 50 mM Tris-HCl pH 8.0. The

hemocyanin (the most abundant shrimp plasma protein) was separated from the column. The flow through fraction was collected and concentrated by Amicon ultra-15 centrifugal filter MWCO 100 kDa. The sodium chloride was added to the concentrated plasma to the final concentration of 3 M NaCl and then applied to a 1-ml HiTrap phenyl sepharose HP column (GE Healthcare) pre-equilibrated with 50 mM Tris-HCl buffer pH 8.0 containing 3M NaCl. The column was washed with 2 M NaCl in 50 mM Tris-HCl pH 8.0 to remove unbound proteins. The bound proteins were eluted by decreasing the ionic strength of the buffer (the NaCl concentration of 3 to 0 M). The eluted fractions were analyzed by 10% SDS-PAGE, and western blotting using polyclonal anti-r*Lv*A2M antibody. The fractions containing *Lv*A2M were pooled and collected at -20 ℃. The A2M activity was tested before used for further experiments.

2.9 A2M inhibitory activity assay against bacterial secreted proteases

2.9.1 Preparation of gram-positive and negative bacteria

A2M inhibitory activity was modified from Lin et al. (2007) on Gram positive bacteria: *Aerococcus viridans, Bacillus megaterium, Micrococcus luteus, Staphylococcus aureus, Staphylococcus haemolyticus and Gram negative bacteria : Enterobacter cloacae, Erwinia caratovora, Escherichia coli strain 363, Vibrio harveyi strain 639, Vibrio paraheamolyticus strain TM*. A single colony was then inoculated with shaking at 250 rpm for 12-16 h . For eachb bacterial condition, in LB-medium at 30 ℃ for *B. megaterium* and in TSB + 1.5% NaCl at 30 ℃ *S. haemolyticus, V. Harveyi,*

V. paraheamolyticus and in LB-medium 37 °C for *A. viridian, M. luteus, B. subtilis, S. aureus E. cloacae E. caratovora* and *E. coli*. The cells were harvested at 8,000 rpm for 15 min at 4 °C and the supernatant was collected and concentrated using lyophilization. The lyophilized crude protease was dialyzed with 50 mM Tris-HCl pH 8.0 before used as the crude protease.

2.9.2 The inhibitory activity of native LvA2M against protease secreted from bacterial secreted proteases

The inhibitory activity of native *Lv*A2M against protease secreted from bacterial secreted proteases was assayed using disc diffusion method. Various amount of A2M, 0.59 µM and 2.35 µM (5 and 20 µg in 50 µl) were mixed with 10 ul (10 µg) of crude bacterial proteases, then the final volumn was adjusted to 100 ul with 50 mM Tris-HCl buffer pH 8.0, and incubated 15 min before loading into a well of 1% gelatin agar plate. The plate was then incubated for 4 h at 37 °C. The crude crude bacterial proteases and 50 mM Tris-HCl pH 8.0 were used as positive and negative control, respectively.

2.9.3 Co-immunoprecipitation

Co-immunoprecipitation assays or Co-IPs was designed to isolate the antigen along with any proteins that are bound to it. In such instances the known antigen is termed the bait protein, and the protein it interacts with are called the prey protein. Briefly, the native A2M and crude *vibrio harveyi* proteases complex were incubated at

4 °C for 6 h by using the IP Lysis/Wash buffer. The protein complex was added to purified A2M antibody cross-linked protein A agarose column.The suggested amount of total protein per Co-IP reaction is 500-1,000 µg and Incubate for 1 hour to overnight at 4ºC to form the immune complex. 100 µl of cold IP Lysis/Wash buffer was added to column and discard the flow-through after each wash. The protein complex column was placed into a new collection tube and add 50 µl of elution buffer and incubated for 10 minutes at room temperature. And then protein complex column was Centrifuged and collected the flow-through. The protein complex was analyzed each eluted separately to ensure that the protein complex were completely by SDS-PAGE.

2.10 Production of recombinant of partial PAP6 (PAP6P) and full-length PAP6 (PAP6F) gene

2.10.1 Preparation of *V. harveyi* genomic DNA

Genomic DNA was prepared from the *V. harveyi* using FavorPrep ™ Tissue Genomic DNA Extraction Mini Kit (Favorgen) as described in section 2.2.6. The genomic DNA was washed with 70% ethanol in washing buffer, air-dried, and then dissolved in 50 µl of elution buffer (10 mM Tris-HCl pH 8.0 and 1 mM EDTA pH 8.0). Store total DNA at -20°C until used.

2.10.2 Quality of genomic DNA

The quality of genomic DNA was checked by 1% agarose gel electrophoresis. One µl of experimental genomic DNA (0.1 µg/µl) and 1 µl of control genomic DNA (0.1 µg/µl) were loaded and run on 1 % agarose gel in 1× TBE buffer.

2.10.3 Preparation of the pET-22b expression vector

Stock solution of pET-22b vector (Novagen) (Figure. 2.2) was transformed into *E. coli* strain XL-1-Blue. The positive clones were selected by plating the transformants onto LB plate containing 100 µg/ml ampicillin. The vectors were extracted and purified from an overnight culture of a single colony of transformant in LB broth containing ampicillin using FavorPrep™ Plasmid DNA Extraction Mini Kit (Favorgen) as described in section 2.2.4. The vector was determined for quality and concentration by spectrophotometric method.

The vector was digested with restriction enzymes *Nco*I and *BamH*I by incubating at 37 °C overnight. The linear vector was purified by agarose gel elution using FavorPrep GEL/PCR Purification Kit (Favorgen) as described in section 2.2.5.1, determined the concentration by spectrophotometric method and stored at -20 °C until used.

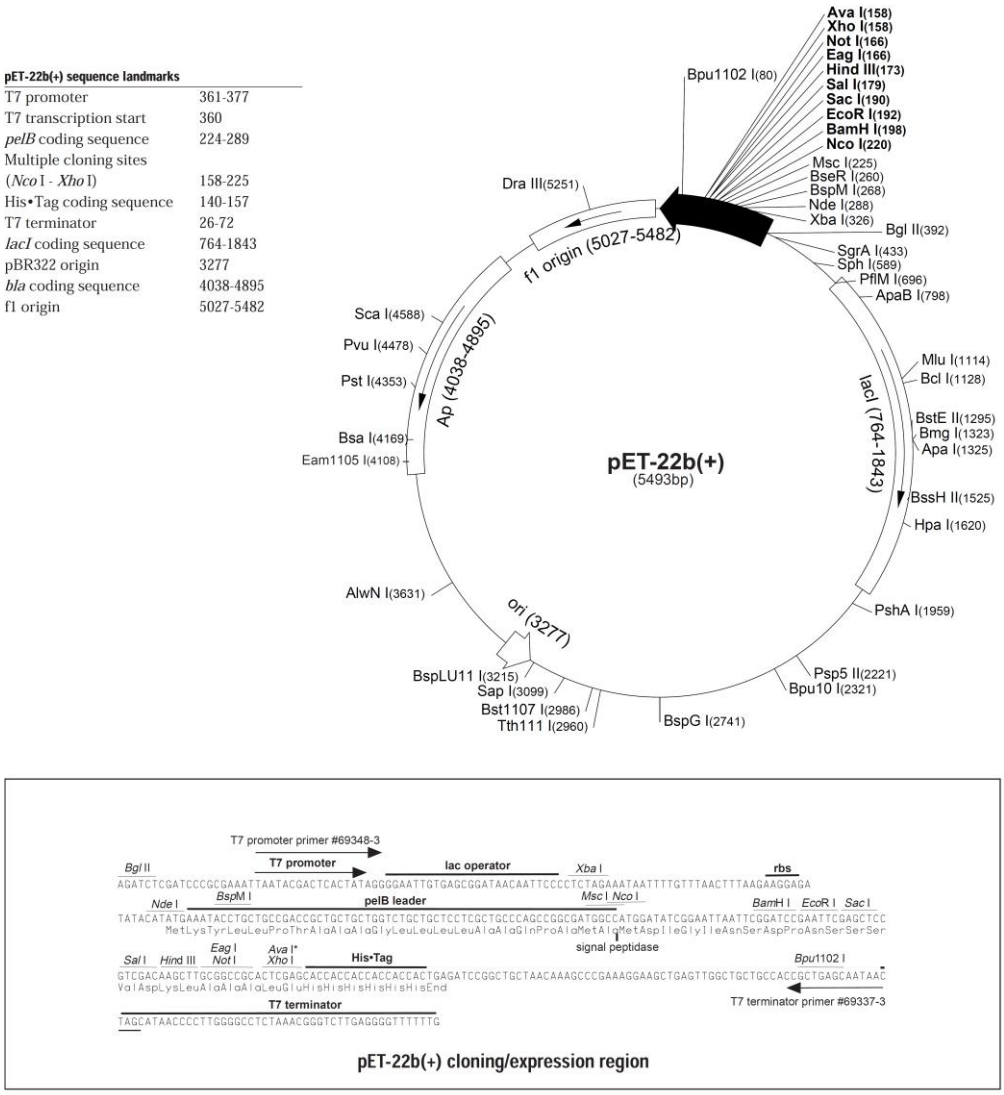

Figure 2.2 The pET-22b(+) vector map (Novagen®, Germany)

2.10.4 Amplification of partial PAP6 and full-length PAP6 gene

In this study we selected partial PAP6 that N-terminal sequences was cleaved (Figure 2.3) and full-length PAP gene for further study. Therefore, to express the recombinant *V. harveyi* protease, two primer pairs, PAP6_F : GCACCATGGCA-TCGCTTGT CCCTTTCGC and PAP6_R: CGCGGATCCCTA**ATGGTGATGGTGATGGTG**-ATAGTCGTTA CAGCTGCCTTC (include His-tag) for partial PAP6 , PAP6_F_Full : GCACCATGGCA-CTTGAAGCAGAAGGCCCAG and PAP_R_Full : CGCGGATCCCTA**ATGGTGATGGTGATGGTG** -ATAGTCGTTACAGCTGCCTTC (include His-tag) for PAP6F (Teo et al. 2003), were designed as described in table 2.1. The primers were designed for the amplification of gene fragment encoding PAP6P and PAP6F ORF with extension of *Nco*I restriction site at 5'-end of forward primer (underlined) and hexa-histidine taq (bolded) and *BamH*I restriction site (underlined) at 5'-end of reverse primer. The plasmid containing PAP6P and PAP6F ORF were used as PCR template and amplified in a final reaction volume of 50 µl containing 10 µl of 5× Phusion HF buffer, 1 µl of 10 mM each dNTP mix, 2.5 µl of 10 µM primer each, 2 µl of 5 fold diluted DNA template, 31.5 µl of ultrapure water, and 0.5 µl of 2U/µl of Phusion DNA polymerase (Thermo). The PCR amplification was carried out by predenaturation at 98℃ for 30 sec following with 30 cycles of denaturation at 98 ℃ for 10 sec, annealing 60 ℃ for 30 sec, and extension at 72 ℃ for 30 sec, before final extension at 72 ℃ for 10 min. The PCR products were analyzed using 1.5 % agarose gel electrophoresis, excised and purified using FavorPrep GEL/PCR Purification Kit (Favorgen) as described in section 2.2.5.2 The PCR product of PAP6P

and PAP6F of about 1540 bp and 2034 bp, respectively. The concentration of the purified PCR products were examined as described in section 2.2.7

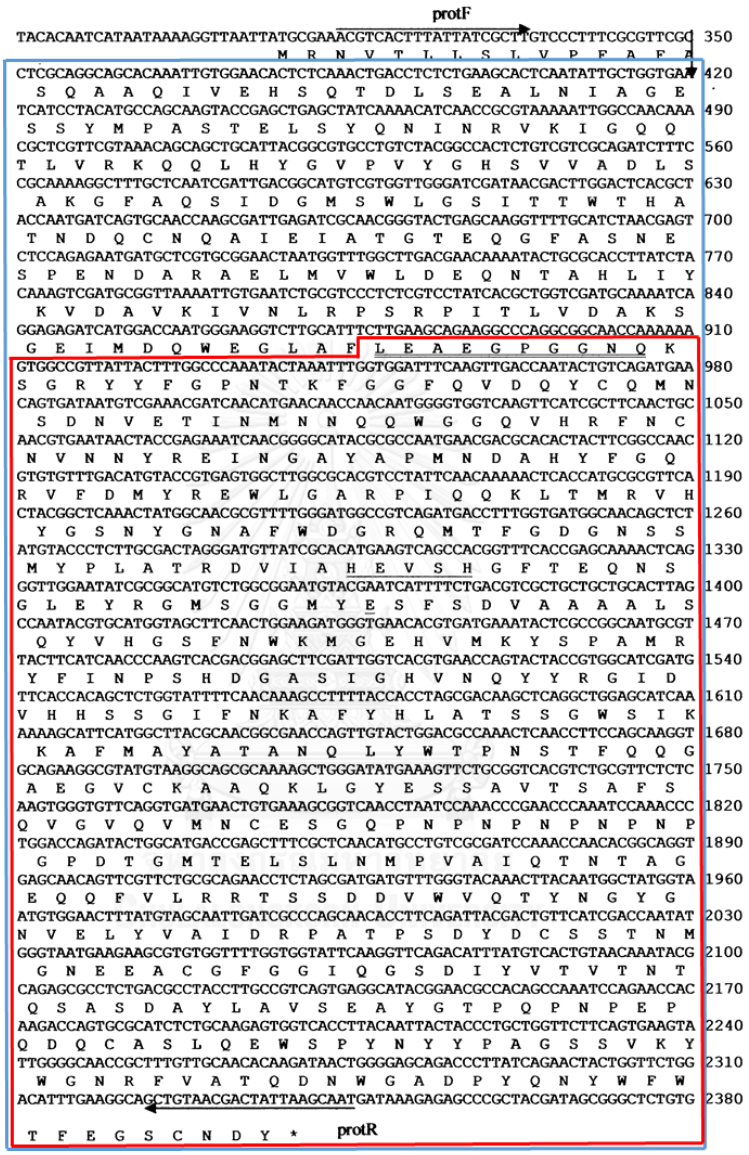

Figure 2.3 Nucleotide and peptide sequences of Pap6P and PAP6F . The vertical arrow pointing downwards indicates a possible signal peptide cleavage site. The conserved zinc motif HEXXH, metalloproteases of the thermolysin family is underlined. The ORF PAP6F gene are blue box and partial of Pap6 are red box .

2.10.5 DNA sequencing

To confirm the correctness of inserted gene sequence, the purified pET-22b(+)/PAP6P and pET-22b(+)/PAP6F plasmid was sequenced in both direction using T7 promotor and T7 terminator primers with an automated sequencer by a commercial service (Macrogen Inc., Korea). The obtained sequences were analyzed using several bioinformatics programs such as ClastalW and SECentral.

2.10.6 Transformation of pET-22b(+)/PAP6P or PAP6F into *E. coli* strain BL21-CodonPlus(DE3)-RIL

The pET-22b(+)/PAP6P and pET-22b(+)/PAP6F plasmid was transformed into expressionhost, *E. coli* strain BL21-CodonPlus(DE3)-RIL by heat shock method. The positive clones were then screened on LB agar plate with 100 µg/ml ampicillin.

2.10.7 Small scale over-expression of recombinant PAP6P and PAP6F

The single positive clone of *E. coli* strain BL21-CodonPlus(DE3)-RIL carrying pET-22b(+)/PAP6P and pET-22b(+)/PAP6F plasmid was inoculated into LB media supplemented with 100 µg/ml ampicillin and incubated at 37 ^{o}C with 250 rpm shaking. The overnight cultured was inoculated at the dilution of 1:100 into fresh LB-ampicillin media. The density of culture was monitored by spectrophotometric assay at 600 nm until the OD600 reached 0.4. An inducer, IPTG, was added to a final concentration of 1 mM. One milliliter of cell culture was collected every hour during 6 h of induction.

The culture was centrifuged to collect the cells. The pellets were lysed in 100 µl of 1X SDS-loading dye and analyzed by SDS-PAGE and Western blotting using monoclonal anti-His antibody (GE healthcare) as a primary antibody and goat anti-mouse IgG as a secondary antibody conjugate AP at the dilution of 1:5,000 and 1:10,000 respectively. The small scale expression was performed again, and the cell pellet was collected at 6 h after induction by centrifugation at 8,000 x g for 10 min. The cell pellet was completely broken using sonicator. After centrifugation at 8,000 x g for 15 min, the pellet and supernatant were analyzed for recombinant protein expression by SDS-PAGE and Western blotting as above to determine whether the PAP6P and PAP6F protein was expressed in soluble or inclusion bodies forms.

2.10.8 Large scale over-expression of PAP6P and PAP6F

The recombinant PAP6P and PAP6F protein was produced in an *Escherichia coli* expression system. The recombinant PAP6P and PAP6F producing clone was cultured in LB broth contain ampicillin antibiotic at 100 µg/ml was used for recombinant clone selection. The culture was induced for the expression by adding isopropyl ß-D-1-thiogalactopyranoside (IPTG) to a final concentration of 1 mM. After induction, the cells were harvested at appropriate times and resuspended in 1x Phosphate buffer saline pH 7.4. The cell suspension was freeze-thawed three times before the cells were completely lysed by sonication. The cell lysate and inclusion bodies were separated by centrifugation. The PAP6P and PAP6F production was verified by separating either whole cells or fractions of cell lysate and inclusion bodies on 12% SDS-PAGE.

2.10.9 Purification of recombinant PAP6P and PAP6F proteins

After sonication, the inclusion bodies of PAP6P and PAP6F proteins were collected. They were tested for solubilizing conditions with either 1xPBS supplement with 8M urea, pH 7.4 for denaturing condition. The recombinant proteins were subjected to SDS-PAGE analysis. Both of them were completely soluble in denaturing condition. For PAP6P and PAP6F protein, it was purified under denaturing condition using nickel affinity chromatography (GE Healthcare). The Ni Sepharose 6 Fast Flow bead was packed into the PD-10 column and washed with 10 column volumns of distilled water and equilibrated with 5-10 column volumes of binding buffer (1xPBS with 6M urea, pH 7.4 containing 0.5 M NaCl, and 20 mM imidazole). The soluble protein fraction was applied to the column and incubated at room temperature for 2 h. Then, the column was washed with 5-10 column volumes of binding buffer to remove unbound proteins. The elution was performed using 5 column volumes of 1xPBS supplement with 6M urea, 0.5 M NaCl, pH 7.4 buffer containing 50 mM imidazole, 100 mM imidazole, 150 mM imidazole, and 500 mM imidazole, respectively. The elution fractions were run on 12% SDS-PAGE. The fractions containing expected recombinant protein were pooled and refolded protein by dialysis for overnight at 4 ℃ against 1× PBS, pH 7.4.

2.11 Protease activity of recombinant PAP6P and PAP6F

2.11.1 Proteolytic activity

Protease assay was determined using azocasein (Sigma.) as the substrate (Teo et al. 2003). Briefly, 10 µl of 1 mg/ml PAP6P and PAP6F solution was added to 100 ml of azocasein (5 mg/ml) in 50 mM Tris–HCl buffer pH 8.0. The mixture was incubated at 37 C for 2 h. The reaction was terminated by adding 500 ml of 10% trichloroacetic acid (TCA) and keeping on ice for 30 min. The mixture was centrifuged at 12,000 rpm for 10 min and 500 ml of the supernatant were added to 500 ml of 1 M NaOH. After mixing, the absorbance was measured at 442 nm. . For the positive control, 10 µl of 1mg/ml trypsin was added instead of PAP6P or PAP6F and 10 ul of 50 mM Tris–HCl buffer pH 8.0 for negative control.

2.11.2 Zymography

Zymography is an electrophoretic technique for the detection of proteolytic enzymes according to Sambrook et al. (1989) using 5% stacking gel and 10% resolving gel. Gelatin-gel zymography analysis was used to characterize protease activity in the protein samples. Ten mg/ml of gelatin was co-polymerized in 12% SDS-PAGE gels. The purified PAP6 and PAP6 protein were run under non-reducing conditions and were not boiled prior to loading. After electrophoresis, gels were washed in 50 mM Tris–HCl pH 8.0 and 2.5% Triton X-100 for 1 h and incubated overnight at 37 ^{o}C in 50 mM Tris–HCl

pH 8.0 buffer containing 2 mM $CaCl_2$ and 2 mM $MgCl_2$. Protein bands with gelatinase activity in the gels were visualized by Coomassie blue staining

2.12 Protein-protein interaction assay between recombinant PAP6P or PAP6F and native *Lv*A2M from *L. vannamei* by *indirect* enzyme-linked immunosorbent assay (iELISA)

All of the assay parameters were optimized and standardized. The coating *Lv*A2M was excessed concentration. Add 100 uL of the antigen solution (*Lv*A2M) to the wells. Seal the plate and incubate for overnight at 4°C. And then washing three times with100 µL/well of 1xPBST (8.0 g NaCl, 0.2 g KH_2PO_4, 2.13 gNa_2HPO_4, 0.2 g KCl), 0.05% Tween-20, pH 7.4), the plate was blocked overnight at 4 °C by adding 200 µL per well of PBST containing 5 % BSA. The plate was washed three times again and then wash the plate three times with 1xPBST. Next 100 µL of PAP6P or PAP6F was diluted twofold from 5 µM to 0.126 µM added to the wells. One hundred microliters of recombinant PAP6P or PAP6F in 1x PBS were incubated overnight.

After washing the plate three times, 50 µL rabbit anti-PAP6 was diluted 1:5,000 in 1xPBST containing 1 % BSA and added to each well. The plates were incubated for 2 h at 37°C and then washed three times. And then, 50 µL goat anti-rabbit conjugate AP was diluted 1:10,000 n 1xPBST containing 1 % BSA and added to each well Finally, 100 µL of AP substrate solution (Bio-rad) 1 pNPP tablets diluted in 5x diethanolamine buffer was added to each well and incubated in the dark at RT for 10 min. The color

reaction was stopped by adding 50 µL of 1 M NaOH to each well. The absorbance of each well at 450 nm was determined by an microplate reader SpectraMaxM5 (Molecular Devices). Positive and negative serum controls were included in each plate.

2.13 Neutralization of crude Pir toxin from *V. parahaemolyticus* by *Lv*A2M

2.13.1 Determination of the optimum concentration crude Pir toxin used for cumulative mortality assay

In this research, the crude Pir toxin were produced from *V. parahaemolyticus* pathogen of EMS strain and purified by Center of Excellence for Shrimp Molecular Biology and Biotechnology (CENTEX SHRIMP), Mahidol University. To investigated the appropriate concentration of Pir toxin for cumulative mortality assay. Ten shrimps (3-5 grams body weight) were cultured individually in the box (30 cm×50 cm×30 cm) and acclimated for a 2 day period, in the 15 ppt salinity water (seawater; Marine Environment), and fed daily with commercial feed. Each box connected to a circulation system with sponge filter pump and air supply.

The crude Pir toxin was varied amount of protein in 1xPBS buffer to 0.3, 0.2 and 0.1 µg. Equal volume (50 µl) of each amount of protein was incubated for 10 min at room temperature. Shrimp were injected at second abdominal segment with various concentrations of crude toxin prepared. The shrimp cumulative mortality was observed and recorded every 1 h for the first day and every 6 h of 2 days. 1xPBS buffer and 10 ug of *Lv*A2M was used as a control. The experiment was performed in triplicate. The

amount of crude toxin protein was 0.2 ug protein which caused 100% death of shrimp in 2 days was selected for cumulative mortality assay.

2.13.2 The survival rate assay

In this experiment, 10 shrimps of 3-5 g body weight was used for each group. For the crude Pir toxin was positive control group, 10 µl of 0.2 µg of crude Pir toxin adjusted volume to 50 µl with the 1xPBS buffer was injected into the second abdominal segment of the shrimp. For the injection control group, 50 µl of 1xPBS buffer only was injected into the shrimp. The group showing toxin neutralizing activity of *Lv*A2M was shrimp injected with 50 µl mixture of crude Pir toxin pre-incubated with 20 µg of *Lv*A2M in the 1xPBS for 15 min at room temperature. The 10 ug of *Lv*A2M protein was used as a control protein as of the test groups. The percentage of survival of shrimp was observed every 2 h post injection for the duration of 5 days. The experiment was performed in triplicate.

2.14 Protein-protein interaction assay between the recombinant Pir toxin from *V. parahaemolyticus* and *Lv*A2M from *L. vannamei*

2.14.1 Preparation of the purified recombinant PirA and PirB toxin proteins

The recombinant proteins of Pir A and PirB as well as specific antibodies were expressed, purified by Center for Shrimp Disease Control and Genetic Improvement,

National Cheng Kung University. The *Lv*A2M proteins was purified from shrimp hemolymph system as described previously.

2.14.2 *In vitro* pull-down assay

The interaction between Pir toxin protein and *Lv*A2M protein was confirmed by *in vitro* pull-down assay. The purified recombinant protein of Pir toxin and *Lv*A2M were used for the investigation. The Ni Sepharose (GE healthcare) was used to trap a bait protein, 6X His-Pir toxin protein then the interaction between *Lv*A2M and Pir-toxin was tested, the interaction between 6xHis-PirA or PirB and *Lv*A2M was examined by incubating 6xHis-rPir toxin fusion protein with a nickel chelate resin (100 µl of 50% bed slurry) for 2 h at 4 °C with gentle rocking. Then, the beads were washed 12 times with 400 µl of Wash Solution (1× PBS pH 7.4). the Ni bead was washed with excess volume of the wash solution until the all the unbound protein was removed. In this step, the last fraction of wash solution was kept for checking on 12% SDS-PAGE. The purified *Lv*A2M protein was added, and incubation was continued for another 12 h at 4 °C with gentle rocking. After incubation, the unbound *Lv*A2M protein designated as the prey flow-through fraction was removed from the column by centrifugation. Then, the column was washed 12 times with 400 µl of wash solution until the unbound *Lv*A2M protein was completely removed. The last fraction of wash solution was kept for checking on 12% SDS-PAGE. The protein complex of Pir toxin and *Lv*A2M was eluted by adding 100 µl of the elution buffer (1xPBS containing 250 mM imidazole) and

incubated with gentle rocking motion at 4 °C for 30 minutes. The protein complexs were resolved on 12% SDS-PAGE and detected with comassie staining.

For control, the PirA or PirB was used as a bait control and the *Lv*A2M was used as prey control. They were incubated with a Ni sepharose. After incubation, the bait and prey protein was then washed 12 times with Wash Solution and eluted at the same concentration as above.

2.14.3 Protein-protein interaction assay between the recombinant Pir toxin and LvA2M by indirect enzyme-linked immunosorbent assay (iELISA)

To investigate of protein-protein interaction assay between the recombinant Pir A or Pir B toxin and purified *Lv*A2M protein by indirect enzyme-linked immune sorbent assay (iELISA) was described in the section 2.12

2.15 Confirmation of the protein-protein interaction between Pir toxin and *Lv*A2M by Molecular docking

The amino acid sequences of *Lv*A2M and Pir toxin from *V. parahaemolyticus* were retrieved from the sequence database of NCBI (ID: *Lv*A2M: ABI79454, PirA: AIL49948.1 and PirB: AIL49949.1). Experimentally solved structure of the *Lv*A2M/Pir complex was not available in the Protein Data Bank (PDB), therefore the present study focuses on developing this 3D model. (Kelley & Sternberg, 2009). BLASTP search was performed to find suitable template for PirA and PirB proteins. The template was

selected based on the maximum identity and score between the focused protein and available crystal structure. Then the homology modeling of PirA and PirB toxin proteins were carried out using the Phyre^2 **P**rotein **H**omology/analog**Y** **R**ecognition **E**ngine V 2.0 (http://www.sbg.bio.ic.ac.uk/phyre2/html/page.cgi?id=index) with the normal modelling mode. Mode of binding interaction between these two Pir toxin proteins *in silico*, was studied by the Patch Dock (http://bioinfo3d.cs.tau.ac.il/Patch-Dock) with 100 docking runs. Alpha-2-macroglobulin structure from Human, *Homo sapien* (PDB ID: 4ACQ) was used to build the *Lv*A2M template. Unfortunately, the bait region and receptor binding domain was lacking in the human A2M crystal structure. The missing bait region was constructed using the Modeller module in Discovery studio 3.0 program. Finally, the protein-protein binding between *Lv*A2M and Pir complex was performed by the Patch Dock (http://bioinfo3d.cs.tau.ac.il/Patch-Dock).

CHAPTER III
RESULTS

3.1 Recombinant expression of *Litopenaeus vannamei* alpha 2 macroglobulin protein (r*Lv*A2M)

3.1.1 *L. vannamei* alpha 2 macroglobulin gene and primer design

As reported previously, *L. vannamei* alpha 2 macroglobulin (*Lv*A2M) is a large proteinase inhibitor found in hemocyte and hemolymph of shrimp. The *Lv*A2M cDNA contained an open reading frame of 4,454 bp coding for amino acid protein of 1489 residues. Three common putative functional domains including the bait region (amino acid 692–791), thioester motif (amino acid 985–991), and the receptor-binding domain (amino acid 1225–1484) are found (Fig. 3.1) (Lin et al, 2008). According to nucleotide sequences of *Lv*A2M gene (Lin et al, 2008) (GenBank accession no DQ988330), the gene specific primers for amplification of nucleotide sequences coding for mature *Lv*A2M protein such as A2M_LV_forward (ACTGGGATCCACTGGTCGGAATCCTCCTCAG) and A2M_LV_reverse (TATTATAGCGGCCGCGTCG CACCCTTCGACGTA), were designed (Figure 3.1).


```
1       ATGGATCCATACGTCGTCACGACTCCGAGGCAATGGATTCCCGGAGAAGACAGTCAGCTC      60
         M  D  P  Y  V  V  T  T  P  R  Q  W  I  P  G  E  D  S  Q  L
61      TGCATAAACCTCCAGAACTCGCACTCTGCCGGGGGAGACCTTAGACTCAGCATGATCACA      120
         C  I  N  L  Q  N  S  H  S  A  G  G  D  L  R  L  S  M  I  T
121     CCGCAGGGCAGGTCGTATAAGGAAGAAGCTAACATTACGATCCTGCCCACGCAAACACTG      180
         P  Q  G  R  S  Y  K  E  E  A  N  I  T  I  L  P  T  Q  T  L
181     ACGATCGCTGCAGGGCAATCCCACCAGTGCTACGACTTCCGGCTTCCTGAGGGCGAATTC      240
         T  I  A  A  G  Q  S  H  Q  C  Y  D  F  R  L  P  E  G  E  F
241     TACCGAGGCTACCTGGCCCTGAGCGGAAGGCTGGGCGGCGCCAGTGTCGAGGAGACGGTG      300
         Y  R  G  Y  L  A  L  S  G  R  L  G  G  A  S  V  E  E  T  V
301     GAGGTCTCCCTCAGGAGGAGCAGGAACCTGACCTTCATTCAGACGAACAAGTACCTGTAT      360
         E  V  S  L  R  R  S  R  N  L  T  F  I  Q  T  N  K  Y  L  Y
361     CAGCCAGGACAGGAGGTCAAGTTCAGGATACTTACCGTTTACGGATGGAAGGCATTCGTG      420
         Q  P  G  Q  E  V  K  F  R  I  L  T  V  Y  G  W  K  A  F  V
421     TCCAGGGAAGAGTACCCCGAAGTATGGGTGACGTCGCCGTCGCAGACTCGCATCGCGCAG      480
         S  R  E  E  Y  P  E  V  W  V  T  S  P  S  Q  T  R  I  A  Q
481     TGGAAACGCGTCGACAACTCGGCCGGCCTCGTCCACCTGGCTTTCCAGCTGGCTGACGAG      540
         W  K  R  V  D  N  S  A  G  L  V  H  L  A  F  Q  L  A  D  E
541     CCCGAGGAGGGCACTTACACCATCAACGTGCGCAGCGCCGACAAGATGCTCAACACCAGG      600
         P  E  E  G  T  Y  T  I  N  V  R  S  A  D  K  M  L  N  T  R
601     ACCTTCAAGGTCAGGGAGTACGTCCTGCCCCGCTTCGAGGTCGAGGTCACACCGCCCAAG      660
         T  F  K  V  R  E  Y  V  L  P  R  F  E  V  E  V  T  P  P  K
661     TACATGTTAGGAACTGACGATCGATTCAACTTCAGAGCCTGCGCCAACTATACCTATGGG      720
         Y  M  L  G  T  D  D  R  F  N  F  R  A  C  A  N  Y  T  Y  G
720     CAGCCAGTCAAGGGCAAGATGACACTCGAAGTCTCCAACAATGAGCGAAGACGATGCCTA      780
         Q  P  V  K  G  K  M  T  L  E  V  S  N  N  E  R  R  R  C  L
781     TCCAAATACAAGAGAACTGTACTGGTCACAGGCTGCCATGACTTCGAAGTGACGGCCGAG      840
         S  K  Y  K  R  T  V  L  V  T  G  C  H  D  F  E  V  T  A  E
841     GAGCTGCGCCTCATGGACTGTTCCGTTTACAGCGTGCGCGCGACGGCCACCATGGAGGAA      900
         E  L  R  L  M  D  C  S  V  Y  S  V  R  A  T  A  T  M  E  E
901     GAGGGCACAGGGATCACCTTCAATGCCACCGCCAGGGAGAGAGTCCGCCGTACCGCCGTG      960
         E  G  T  G  I  T  F  N  A  T  A  R  E  R  V  R  R  T  A  V
961     ACACTGAGGGCGGTGCGTGAGGACGCCTACAAAAAGCCAAATCTACCCTACGTCCTTCGA     1020
         T  L  R  A  V  R  E  D  A  Y  K  K  P  N  L  P  Y  V  L  R
1021    GTGCAGGCCTCTTTACCTGATAATACCCCGGCTCCTGGTTTGCCCATAGAGGTATGCTAC     1080
         V  Q  A  S  L  P  D  N  T  P  A  P  G  L  P  I  E  V  C  Y
1081    GCTGGCCGCTGTAGGAACAGGACCTCGGACGCCGAGGGGAAGATCATAGCTGTCGTCCTG     1140
         A  G  R  C  R  N  R  T  S  D  A  E  G  K  I  I  A  V  V  L
1141    TCGGGAAATTTCCACAGAATCATAATGTCGACCTTGAACTGCCGCGCCGAGATGAGGGCG     1200
         S  G  N  F  H  R  I  I  M  S  T  L  N  C  R  A  E  M  R  A
1201    AGTGTTTTCTCGAAGAACCTGGAACATTACTTCTCGCCCTCGAATTCAGCGCTGCAGATC     1260
         S  V  F  S  K  N  L  E  H  Y  F  S  P  S  N  S  A  L  Q  I
1261    CAAGTGCCTGAGGAGTCGATATCCTGCACTTCAGGAAAGCACAAGAGATACCTCATCGAT     1320
         Q  V  P  E  E  S  I  S  C  T  S  G  K  H  K  R  Y  L  I  D
1321    ATCATGTACTCGGCCAATAACACGGCGTCTACGCGTCTAAACTGTCAGATCATAGCCCGC     1380
         I  M  Y  S  A  N  N  T  A  S  T  R  L  N  C  Q  I  I  A  R
1381    GGTAAGGTCCAAAAGTGGTGGAGCGTTCCCGTAGAATTCAAACCTGCTCAGCTCCCCTAC     1440
         G  K  V  Q  K  W  W  S  V  P  V  E  F  K  P  A  Q  L  P  Y
1441    GACACACAACAGTTAGTGGAGGACCCTTACACACCTGCCCACCCCATTGTCACGGGCGTC     1500
         D  T  Q  Q  L  V  E  D  P  Y  T  P  A  H  P  I  V  T  G  V
1501    GTCAGAGTCCCCATCACCATTACGCCCACTAGCGCACCCTCAGTGCAGGTTCTAGTGTGG     1560
         V  R  V  P  I  T  I  T  P  T  S  A  P  S  V  Q  V  L  V  W
1561    TACACCCGCGACGACGGCGAGGTGGTGTCTGACGCAGCGGAGTTGAAGGTGGACTCGTGT     1620
         Y  T  R  D  D  G  E  V  V  S  D  A  A  E  L  K  V  D  S  C
1621    CTGCTCCACGAAACGCGCCTCACGTGGGAGACCCCGAAGGAACAGCCAGGAGAGAAAACC     1680
         L  L  H  E  T  R  L  T  W  E  T  P  K  E  Q  P  G  E  K  T
1681    ACGCTGTCACTGCAGGCTCGGGGTGATGCTCTCTGCTCTGTGGGCGTCGTGGACAAGAGC     1740
         T  L  S  L  Q  A  R  G  D  A  L  C  S  V  G  V  V  D  K  S
1741    GCCGAGCTCCTTAACCCCGACCCGGACCCCATTAGGCTGGAGAGGGTCATCGACTACCTG     1800
         A  E  L  L  N  P  D  P  D  P  I  R  L  E  R  V  I  D  Y  L
1801    GGTGACTACAAAATCTACCCGTGGATTAATTCACAGATCGATGACACCAAGTACTGCGAG     1860
         G  D  Y  K  I  Y  P  W  I  N  S  Q  I  D  D  T  K  Y  C  E
1861    AGGAAGATTTTCAGACAAGGTGGCGTTCAGCAGGATTCCGGACCTGGAACAGAAGACATA     1920
         R  K  I  F  R  Q  G  G  V  Q  Q  D  S  G  P  G  T  E  D  I
1921    CTTCCTCCAAATCGTCGACGATACTATAGCGAGTACGTTGACTCCCTCAGGATGTTCAGT     1980
         L  P  P  N  R  R  R  Y  Y  S  E  Y  V  D  S  L  R  M  F  S
1981    GATTCTGGTCTCTACGTCTTCTCAGACCTCACTCTTGAGACGAAACCTTGCGAGGAAGAT     2040
```

```
          D  S  G  L  Y  V  F  S  D  L  T  L  E  T  K  P  C  E  E  D
2041 GTGTGGGACTTCTACGACCGACCCTACGACGGTGGGCCGGTCTACGCCAATATCCCTACA 2100
          V  W  D  F  Y  D  R  P  Y  D  G  G  P  V  Y  A  N  I  P  T
2101 TCCGCTATGGGACCCGACCGTGAATTCGACGAACCCGACCTATCCGACAGCGGGGCGAAG 2160
          S  A  M  G  P  D  R  E  F  D  E  P  D  L  S  D  S  G  A  K
2161 GAGAACCGTCCGAGAACCCGCTTCCCAGAGACATGGCTGTGGGACATCGTTGTCGTGCCG 2220
          E  N  R  P  R  T  R  F  P  E  T  W  L  W  D  I  V  V  V  P
2221 TCAAGTGGCGTCTTGAGCCAGAGCGTGACCCTTCCCGACACAATAACGGAGTGGGTTGGC 2280
          S  S  G  V  L  S  Q  S  V  T  L  P  D  T  I  T  E  W  V  G
2281 AAGGCCGTGTGTGCCCATCCGGAAGTGGGTGTCGGGCTGTCGGAGAAGGTTTCCATCACC 2340
          K  A  V  C  A  H  P  E  V  G  V  G  L  S  E  K  V  S  I  T
2341 GCCTTCACGCCCTTCTTCACGGACCTTACCATCCCGCCCTCCGTCAAGCGCGGCGAGATC 2400
          A  F  T  P  F  F  T  D  L  T  I  P  P  S  V  K  R  G  E  I
2401 CTTCCCGTCAAGATATCGGTCTTCAACTACCTCGAGCAGCATTTGAAGGTGACGGTCCAC 2460
          L  P  V  K  I  S  V  F  N  Y  L  E  Q  H  L  K  V  T  V  H
2461 CTTCTGGAGAGCCCCGAGTACGAGTTGGTGGAGGACCCGTCGCCGCGAGGAGTCGGGAAG 2520
          L  L  E  S  P  E  Y  E  L  V  E  D  P  S  P  R  G  V  G  K
2521 CGTAAGTCGGCCTGTGTGGCACCGCAGGATAAGGTCGTGCACGTAATCAAGATCCGGCCC 2580
          R  K  S  A  C  V  A  P  Q  D  K  V  V  H  V  I  K  I  R  P
2581 CTGGCACTGGGCAACGTCAATCTCACCGTGTCGGCTTTCACGGACACGAGCGGCGTCTCT 2640
          L  A  L  G  N  V  N  L  T  V  S  A  F  T  D  T  S  G  V  S
2641 TCGTGTGGCGTCGGTCGTCCGGTTCAGAGGAGAGACACCCTTATTAAGCCAATCAAAGTA 2700
          S  C  G  V  G  R  P  V  Q  R  R  D  T  L  I  K  P  I  K  V
2701 GAAGCTGAGGGCTTTTTAAGAGAAAAGACGTTTACCAAATACGTTTGTGCTAATGAGATG 2760
          E  A  E  G  F  L  R  E  K  T  F  T  K  Y  V  C  A  N  E  M
2761 GGTAGCGAGCCGGACTCTGCCGTCCTGTGGGAGTTGTCGCCGCCCGCGGACATCGTCCCG 2820
          G  S  E  P  D  S  A  V  L  W  E  L  S  P  P  A  D  I  V  P
2821 GACTCGGCGCGCGGTTGGGTCACGGTTGTCGGAGACCTGCTCGCACTCTCGCTGCAGAAC 2880
          D  S  A  R  G  W  V  T  V  V  G  D  L  L  A  L  S  L  Q  N
2881 CTCGGCTTCCTGATCCGCATGCCCTCCGGCTGTGGTGAGCAGAACATGATCAACTTCGCC 2940
          L  G  F  L  I  R  M  P  S  G  C  G  E  Q  N  M  I  N  F  A
2941 CCAAACGTCTACATGATGCAGTACCTGACGGCGACGAAGCAGAATACCCCCGAGAGCACA 3000
          P  N  V  Y  M  M  Q  Y  L  T  A  T  K  Q  N  T  P  E  S  T
3001 GAGAAGCTCCTCAGGTTTATGAAGCTGGGATACCAAAGGGAACTGCTTTATCTCCGCAGC 3060
          E  K  L  L  R  F  M  K  L  G  Y  Q  R  E  L  L  Y  L  R  S
3061 AATGGTTCCTACAGCGCCTTCGGGAACGCTGATGATTCTGGCTCAACTTGGCTCACGGCC 3120
          N  G  S  Y  S  A  F  G  N  A  D  D  S  G  S  T  W  L  T  A
3121 TTCGTCCTTAAGTCCTTTGTTCAAGCAAAGGCATTCATCTACATCGATGACTCCAGCCTG 3180
          F  V  L  K  S  F  V  Q  A  K  A  F  I  Y  I  D  D  S  S  L
3181 AACCGAACCCGAGTTTGGCTAATGGATTCTGAGCTGGACCGCAGCGGGTGTGTCATCCAA 3240
          N  R  T  R  V  W  L  M  D  S  E  L  D  R  S  G  C  V  I  Q
3241 GTGGGGAAGGTCTTCAGCAAAGGCCTCAAGGGAGGTCTGCAGGGCAAGGGATCGCCCGTG 3300
          V  G  K  V  F  S  K  G  L  K  G  G  L  Q  G  K  G  S  P  V
3301 CCGCTGACTGCCTATGTGCTCATCGCCCTACTTGAGGCAGGCGCGCCCGCCGACGCCCCG 3360
          P  L  T  A  Y  V  L  I  A  L  L  E  A  G  A  P  A  D  A  P
3361 ATCGTTCTCCAAACGACGCGCTGCGTGCTGGGCGATATGACCAGGGACCCCTACACCATC 3420
          I  V  L  Q  T  T  R  C  V  L  G  D  M  T  R  D  P  Y  T  I
3421 GCCCTCAAGGCCTACGCTCTCGCCCTGGCTGGGCATCCCCGGTATACGGCCGTCCTGCTG 3480
          A  L  K  A  Y  A  L  A  L  A  G  H  P  R  Y  T  A  V  L  L
3481 CAGCTGCTCGAGTTAGCCGTCGAGGACGACGAGGGAATGTACTGGGAGGTGCAGCGAATG 3540
          Q  L  L  E  L  A  V  E  D  D  E  G  M  Y  W  E  V  Q  R  M
3541 TTCTACAGGAGCAACTCCCTCGCTGTGGAGACGGCGGGCTACGCAATCATGGCCATGATG 3600
          F  Y  R  S  N  S  L  A  V  E  T  A  G  Y  A  I  M  A  M  M
3601 GCCAATCCCGAGAGATACTTATTGGACGCGAGGAAGATCGTCAAGTGGATCACCACCAAG 3660
          A  N  P  E  R  Y  L  L  D  A  R  K  I  V  K  W  I  T  T  K
3661 AGGAACGGATACGGAGGTTTCTACTCTACACAGGACACAATAGTGGCCCTGCAAGCCCTG 3720
          R  N  G  Y  G  G  F  Y  S  T  Q  D  T  I  V  A  L  Q  A  L
3721 GCCAGCTACGAGACCAATACGTACGAAGGGAAGCTTGATGTTGTGGCCACAGTCACATCT 3780
          A  S  Y  E  T  N  T  Y  E  G  K  L  D  V  V  A  T  V  T  S
3781 TTCAGCTTCCGCGAATCGGAGAAGGTCCAGCAGTCGCAGCAATTCCAACAATCACAAAAG 3840
          F  S  F  R  E  S  E  K  V  Q  Q  S  Q  Q  F  Q  Q  S  Q  K
3841 TTGCAGTATAAGCGGTCCGTACCCACTGTCGGTAACCTCGTGCACGAATTCATTATCAAT 3900
          L  Q  Y  K  R  S  V  P  T  V  G  N  L  V  H  E  F  I  I  N
3901 GAGGACAGCAAGCTTTTGCAGCAGCAAGTGAGTCTTCCGGACTTCCCCACCTACGTGAAG 3960
          E  D  S  K  L  L  Q  Q  Q  V  S  L  P  D  F  P  T  Y  V  K
3961 ATTAGCATGGAGGGGCAGGGATGCGCCGTGATGCAGGCGGTCCTTCGCTACAACGTTCCC 4020
          I  S  M  E  G  Q  G  C  A  V  M  Q  A  V  L  R  Y  N  V  P
4021 GTCGCCGAACCGAGCGATGCCTTCAGCCTCAAAGTCGACGGCGACAACGCACCTGGGAGG 4080
          V  A  E  P  S  D  A  F  S  L  K  V  D  G  D  N  A  P  G  R
4081 GACTGCGCCCGCAAGCGAATCCGCGCCTGCTCCGCCTACATCCTGCCGGACGGCGAGTCC 4140
          D  C  A  R  K  R  I  R  A  C  S  A  Y  I  L  P  D  G  E  S
4141 AACATGGCCGTCATCGAAGTGAACCTCATTTCCGGCTTCATCCCCGTGAAGGACGACCTC 4200
          N  M  A  V  I  E  V  N  L  I  S  G  F  I  P  V  K  D  D  L
```

```
4201      AAGGCGGTCGTGAGGCGAAACCCTAAGGTCATAAAGCGCTACGAGGTGGACGGCAGCAAA      4260
           K  A  V  V  R  R  N  P  K  V  I  K  R  Y  E  V  D  G  S  K
4261      GTGTCCTTCTACATCGAGGAGTTCACGGCCGAGGAGGTGTGCGTCGCCTTCAACATCTTG      4320
           V  S  F  Y  I  E  E  F  T  A  E  E  V  C  V  A  F  N  I  L
4321      CGCGAGGTTGAGGTCGAGAACACCAAGCCGGGAACCGTGGTTGTTTACGACTACTACGAG      4380
           R  E  V  E  V  E  N  T  K  P  G  T  V  V  V  Y  D  Y  Y  E
4381      CCCGACTTCGCCGTCAGCACGACATACGCCTTCCCGTACGTCGAAGGGTGCGACGCGGCC      4440
           P  D  F  A  V  S  T  T  Y  A  F  P  Y  V  E  G  C  D  A  A
4441      GCACTCGAGCACCACCACCACCACCACTGA                                   4470
           A  L  E  H  H  H  H  H  H  -
```

Figure 3.1 The *Litopenaeus vannamei* alpha 2 macroglobulin (LvA2M) nucleotide sequence and deduced amino acid sequences. (A) The domain structure of *Lv*A2M showing positions of the bait region (692–791), thioester motif (985–991), and the receptor-binding domain (1225–1484) (B) Nucleotide (above) and deduced amino acid (below) sequences of the recombinant *Lv*A2M.

3.1.2 Construction of expression vector

The total RNA isolated from the hemocytes of the white shrimp *P. vannamei* using TRI reagent was analyzed for the intrigrity by 2.0 % agarose gel electrophoresis. (Figure 3.2). The first-strand cDNA was synthesized and the nucleotide sequences encoding for mature peptide of r*Lv*A2M (4,454 bp) was amplified (Figure 3.3A), cut with *Not*I and *BamH*I and cloned in-frame into the *Not*I and *BamH*I digested expression vector pVR600 (pET-28b(+) derivative). The recombinant plasmid was then transformed into *E. coli* strain XL-1blue. The recombinant plasmid was checked for the presence of insert by restriction enzyme digestion (Figure 3.3B). The recombinant plasmid was checked for the correctness of the sequences by DNA sequencing. The predicted molecular mass and pI of r*Lv*A2M (1,489 amino acid) was 166.9 kDa and 5.77 respectively.

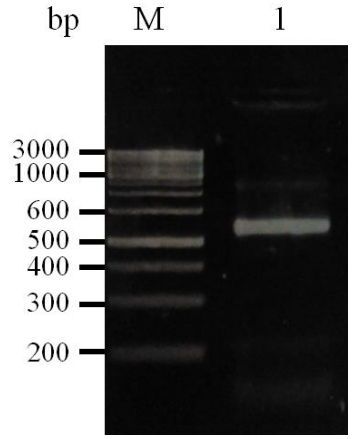

Figure 3.2 Analysis of total RNA isolated from normal shrimp *L. vannamei* hemocytes on 2.0 % agarose gel electrophoresis**.** Lane M: 100 bp DNA ladder markers. Lane 1: total RNA from normal shrimp.

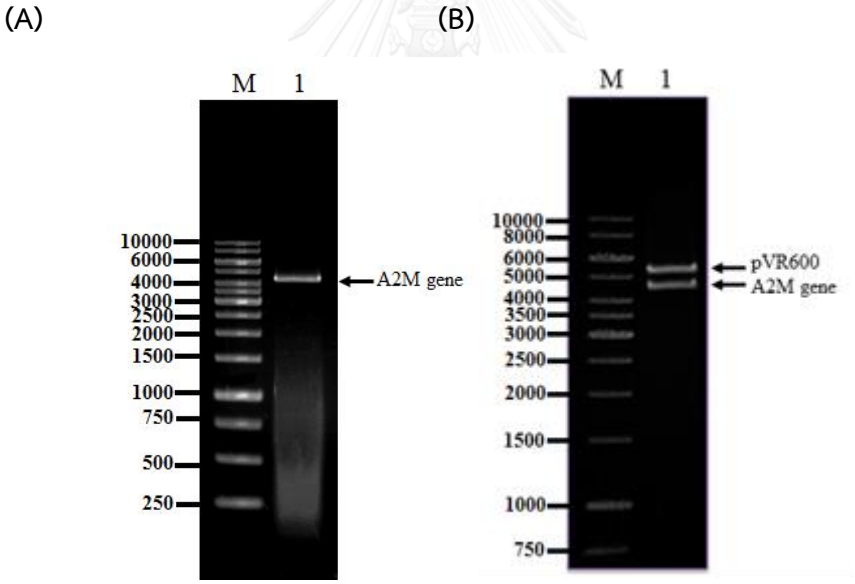

Figure 3.3 Construction of expression vector for the r*Lv*A2M production (A) The cDNA sequences coding for mature *Lv*A2M protein containing 6X-His tag at the C-terminus was amplified from hemocyte cDNA of *L. vannamei* using specific primers and run on 1% agarose gel electrophoresis. After cloning in-frame into pVR600 plasmid, (B) the

recombinant plasmid was analyzed for the insertion by *BamH*I and *Not*I double-digestioin. Lane M: 1 kb DNA markers.

3.1.3 Expression of the r*Lv*A2m protein

The recombinant plasmid, pVR-A2M was transformed into the expression host *E. coli* BL21-CodonPlus(DE3)-RIL. The recombinant clone was selected and then cultured. The expression of the r*Lv*A2M protein was induced by 1 mM IPTG for 0-6 h. The r*Lv*A2M production was analyzed by SDS-PAGE and western blot analysis using anti-His antibody. The r*Lv*A2M with expected MW 170 kDa was successfully produced in *E. coli* BL21-CodonPlus(DE3)-RIL**.** The expression of the r*Lv*A2M was highest at 4 h post-IPTG induction (Figure 3.4).

(A) **(B)**

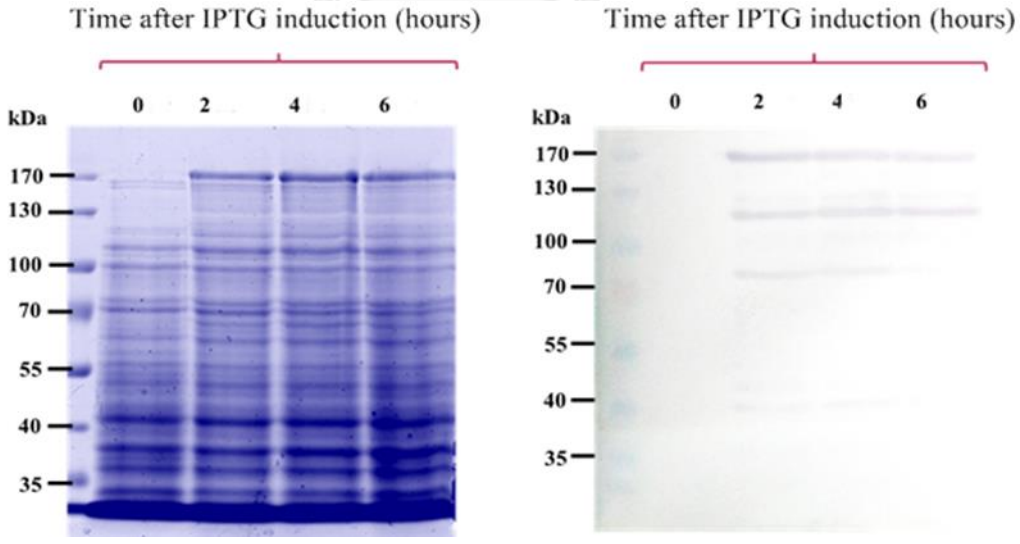

Figure 3.4 10% SDS-PAGE and western blot analysis of r*Lv*A2M expressed in *E. coli* strain BL21-CodonPlus(DE3)-RIL after 0, 2, 4 and 6 h of IPTG induction.

3.1.4 Purification of the r*Lv*A2m protein

After harvesting, the cells were resuspended in 50 mM Tris-HCl buffer pH 8.0 and subjected to sonication. The crude r*Lv*A2M protein was detected in the inclusion bodies. After SDS-PAGE analysis, the band corresponding to r*Lv*A2M protein, was cut and eluted from the 10% SDS-PAGE (Crush and soak method) using 50 mM Tris-HCl buffer pH 8.0. This purified r*Lv*A2M was concentrated and analyzed by 10% SDS-PAGE and Western blotting (Figure 3.5A). The purified r*Lv*A2M was used for antibody production and activity assay.

The specificity of the mouse anti-r*Lv*A2M polyclonal antiserum was verified by SDS-PAGE and western blotting techniques to detect the native A2M protein in hemolymph of shrimp, *P. monodon* and *L. vannamei* were performed using 5% gel SDS-PAGE and western blotting techniques. The result showed the cross-reactivity of detecting A2M from *P. monodon* and *L. vannamei* by anti-r*Lv*A2M antiserum (Figure 3.5B).

(A)

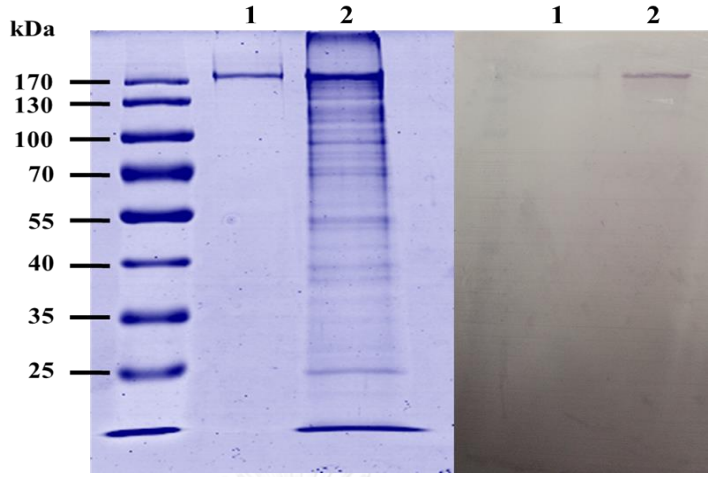

(B)

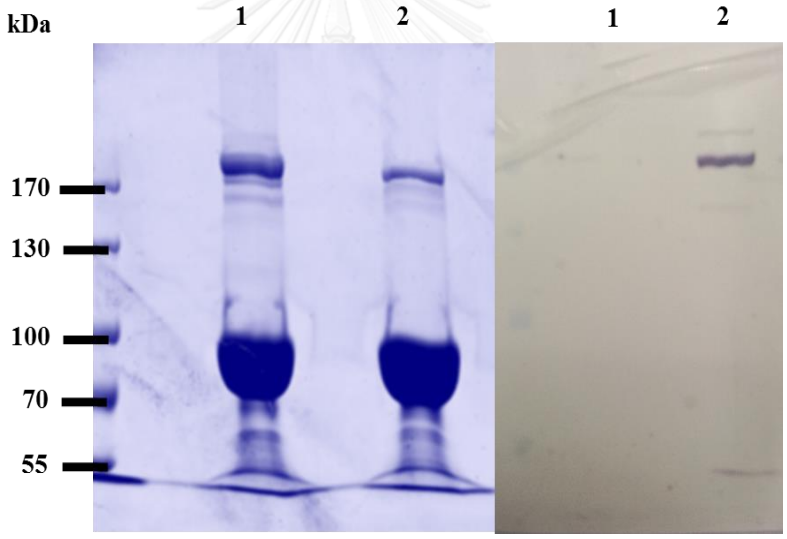

Figure 3.5 Analysis of the purified r*Lv*A2M protein and anti-r*Lv*A2M antibody specificity. (A) The r*Lv*A2M with the expected size was over-produced and the band corresponding to rLvA2M was purified by cutting, crushing and soaking the gel with buffer. The purified and crude r*Lv*A2M proteins were detected by 10 % SDS-PAGE and western blot analysis using anti-HIS antibody as primary antibody Lane 1: The purified r*Lv*A2M protein Lane 2: Inclusion bodies in 50 mM Tris-HCl buffer pH 8.0 (B) *Lv*A2M protein in hemolymph

of shrimp was analyzed using SDS-PAGE and western blotting using anti-r*Lv*A2M antibody. Lane 1 : Hemolymph from *P. monodon* Lane 2 : Hemolymph from *L. vannamei*

3.1.5 Activity of r*Lv*A2M

The activity of the purified r*Lv*A2M was determined by incubating various concentration (30, 60 and 120 µM) of the purified r*Lv*A2M with excess amount of trypsin and the activity of the trapped trypsin was determined by measuring A_{415} after adding trypsin substrate, BAPNA. The result showed that the activity of bound trypsin is quite low indicating that the r*Lv*A2M protein has very low activity (Figure 3.6).

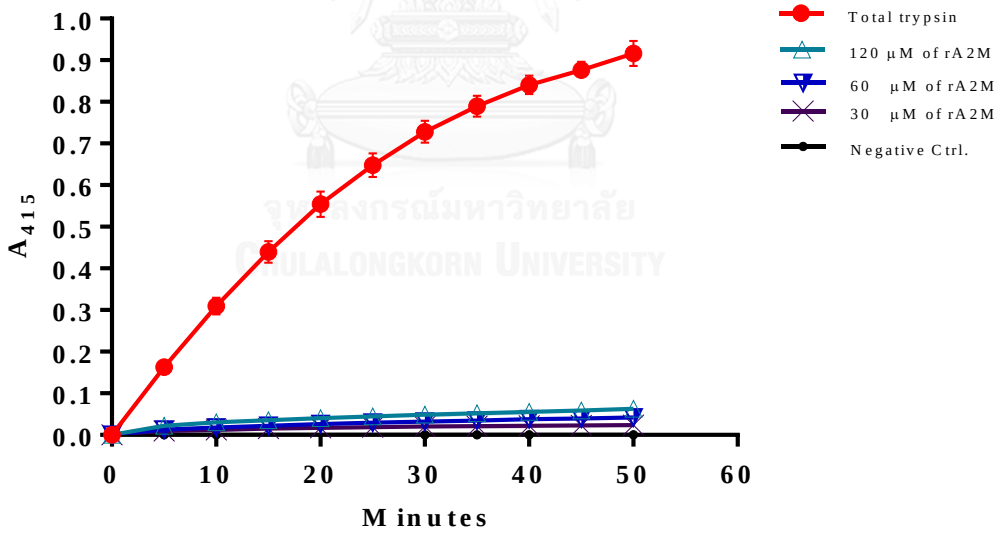

Figure 3.6 Activity of the r*Lv*A2M protein assayed by determination of the protease activity of the trapped target protease. This activity was measured by incubating 5, 10 and 20 µg of recombinant *Lv*A2M and by measuring A_{415}. Line 1: Total trypsin (10 µl of 1 mg/ml trypsin), Line 2: 120 pmol of rLvA2M (20 ug), Line 3: 60 pmol of r*Lv*A2M

(10ug), Line 4: 30 pmol of rLvA2M (5 ug) and Line 5: Negative control (50 mM Tris-HCl pH 8.0).

3.2 Purification of native A2M from *L. vannamei* hemolymph

3.2.1 Purification of native A2M

The native *Lv*A2M was partially purified from the plasma of *L. vannamei*. The hemocyte-free plasma was applied to the Blue-Sepharose column where hemocyanin, the major hemolymph protein, was trapped. Therefore, The flow through fraction was collected and subjected to ultrafiltration on 100 kDa cutoff membrane to exchange the buffer to 50 mM Tris-HCl pH 8.0 3 M NaCl and concentrate the protein before further purification through a Phenyl-Sepharose column. *Lv*A2M interacted strongly with the matrix. It was eluted at 0 M NaCl as a unique protein band of around 170 kDa observed in SDS-PAGE (Figure 3.7).

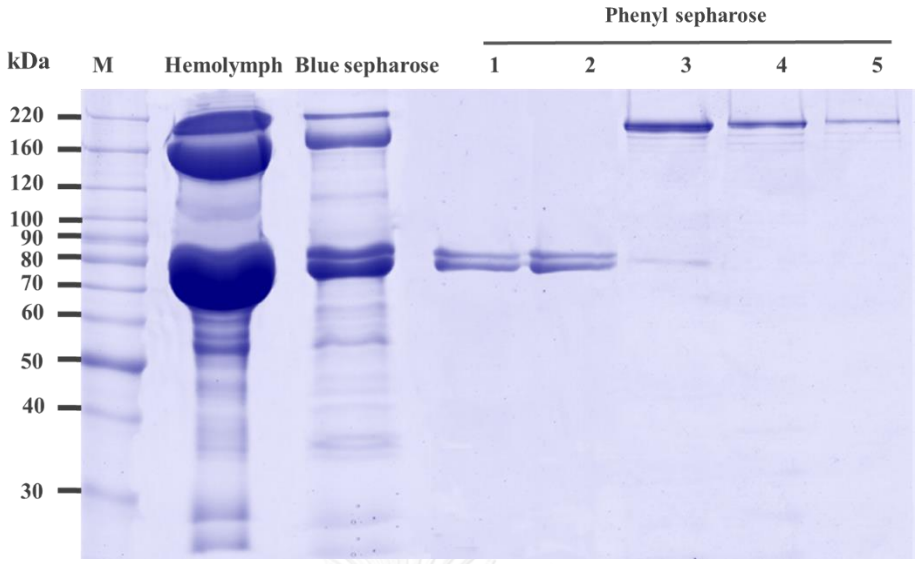

Figure 3.7 Purification of an alpha-2-macroglobulin from the *L. vannamei* hemolymph. Lane Hemolymph : Cell-free shrimp hemolymph, Lane Blue-sepharose : flow-through fraction after applied to the Blue-Sepharose column. The partial purified hemolymp in proteins 50 mM Tris-HCl pH 8.0, 3 M NaCl (Lane 1) was loaded onto a pre-equilibrated phenyl-sepharose column, and subsequently eluted by stepwise with buffer containing different NaCl concentrations: 2 M, 1 M, 0.5 M and 0 M NaCl (Lanes 2-5).

3.2.2 Activity of A2M native and recombinant *Lv*A2M protein

The obtained purified native *Lv*A2M was assayed for activity as bottom. As compared to the activity of total trypsin added to the reaction (positive control), the amount of trypsin trapped by native *Lv*A2M increased dependently on the *Lv*A2M concentration. From our investigation, native *Lv*A2M at 120, 60 and 30 μM could trap 60.5, 39.6 and 24.8% of trypsin, respectively. The recombinant A2M displayed significantly low activity where it could trapped 6.9, 4.6 and 2.3 % of trypsin,

respectively. The result indicated that the activity of native *Lv*A2M was higher than r*Lv*A2M (Figure 3.8).

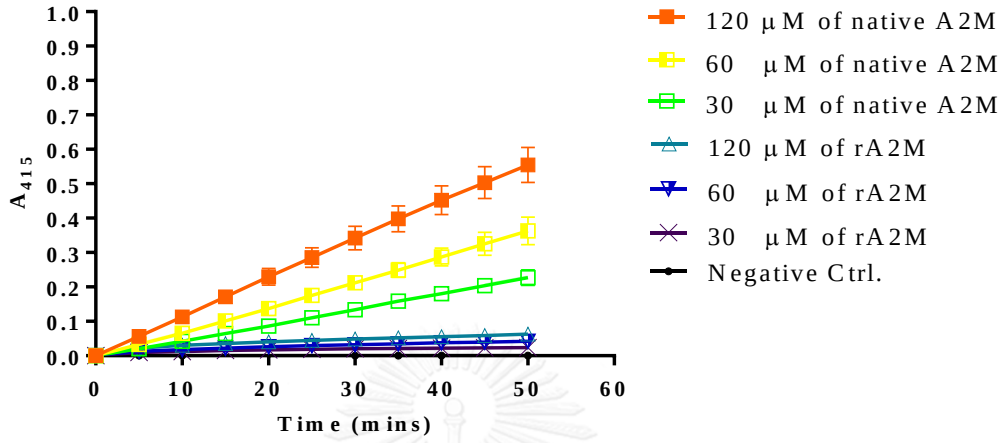

Figure 3.8 Activity of the native and recombinant *Lv*A2M protein assayed by determination the protease activity of the trapped target protease. This activity was measured by incubating (5, 10 and 20 µg) of native and recombinant *Lv*A2M and by measuring A_{415}. Line 1: Total trypsin (10 µl of 1 mg/ml trypsin), Line 2: 120 µM of A2M (20 ug), Line 3: 60 µM of A2M (10ug), Line 4: 30 µM of A2M (5 ug), Line 5: 120 µM of rA2M (20 ug), Line 6: 60 µM of rA2M (10ug), Line 7: 30 µM of rA2M (5 ug), Line 8: Negative control (50 mM Tris-HCl pH 8.0).

3.2.3 Analysis of bait region of *Lv*A2M binding to trypsin by molecular docking

From the sequence of *Lv*A2M *Lv*A2M bait region in Figure 3.9A, the Peptide Cutter and PROSPER programs suggested that the cleavage residues involved in inhibitor binding were the P1-P1' residues of 31-32, 44-45, 49-50, 51-52, 85-86 and 100-101 for the peptides 1-6 in Figure 3.9B. Based on the 100 separate docking runs, the lowest interaction energy between the 10 residues of the 6 peptides from the bait region and Trypsin was chosen and the docking results were shown in Figure 3.9C. Interaction energy of the 6 peptide/Trypsin complexes on bait region were of -110.6, -99.0, -95.2, -88.2, -91.3 and -90.6 kcal/mol, respectively. Interestingly, the binding strength of these 6 *Lv*A2M peptides was significantly lower than the Bovine Pancreatic trypsin inhibitor II (Peptide 0 < -86.1 kcal/mol resulted from re-docking) with a formation of hydrogen bond interactions in particular at the cleavage reaction center (P1 residue). Thus, the results indicate that all candidate peptides from bait region might be able to be cleaved by Trypsin.

(A)

```
          10         20         30         40         50
CEEDVWDFYD RPYDGGPVYA NIPTSAMGPD REFDEPDLSD SGAKENRPRT

          60         70         80         90        100
RFPETWLWDI VVVPSSGVLS QSVTLPDTIT EWVGKAVCAH PEVGVGLSEK
```

* Bold character represent cleavage site of bait region was cleaved by trypsin

(B)

Peptide	P5	P4	P3	P2	P1	P1’	P2’	P3’	P4’	P5’
0	THR	GLY	PRO	CYS	LYS	ALA	ARG	ILE	ILE	ARG
1	MET	GLY	PRO	ASP	ARG	GLU	PHE	ASP	GLU	PRO
2	ASP	SER	GLY	ALA	LYS	GLU	ASN	ARG	PRO	ARG
3	GLU	ASN	ARG	THR	ARG	THR	ARG	PHE	PRO	GLU
4	ARG	PRO	ARG	THR	ARG	PHE	PRO	GLU	THR	TRP
5	GLU	TRP	VAL	GLY	LYS	ALA	VAL	CYS	ALA	HIS
6	GLY	LEU	SER	GLU	LYS	VAL	SER	ILE	THR	ALA

(C)

Protein complex	Residues of bait region (P5 - P5')	Interaction energy (kcal/mol)	Hydrogen bond (H-bond)
0	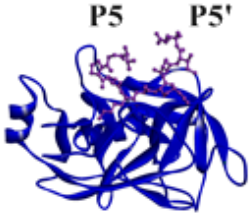 T-G-P-C-/-A-R-I-I-R	-86.1	PRO3:O – GLY216:HE LYS5:O – GLY193:HN CYS4:O – GLN192:HE LYS5:O – SER195:HN ALA6:O – SER195:HN
1	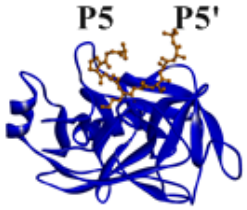 M-G-P-D-R-/-E-F-D-E-P	-110.6	PRO3:O – GLY216:HN ARG5:O – GLY193:HN ARG5:O – SER195:HN ASP8:OD1–LYS60:HZ3 ASP8:OD2–LYS60:HZ3 GLU9:OE1–TYR39:HH
2	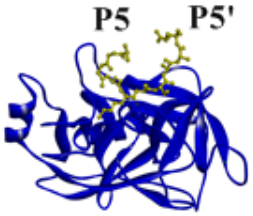 D-S-G-A-K-/-E-N-R-P-R	-99.0	ASP1:OD2–GLY219:HN ASP1:OD1–GLN192:HE22 ALA4:O – GLN192:HE21 LYS5:O – SER195:HN LYS5:O – GLY193:HN ASN7:OD1 – TYR151:HH PRO9:O – TYR39:HH
3	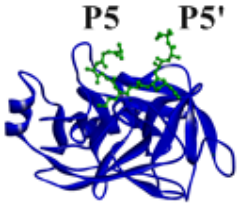 E-N-R-P-R-/-T-R-F-P-E	-95.2	GLU1:OE1 – LYS60:HZ3 GLU1:OE2 – LYS60:HZ3 ASN2:O – TYR39:HH ARG5:O – GLY193:HN

4	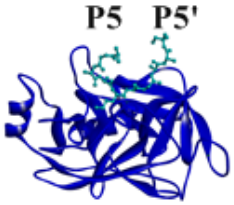 R-P-R-T-R-/-F-P-E-T-W	-88.2	ARG3:O – GLY216:HN THR4:O – GLN192:HE ARG5:O – GLY193:HN ARG5:O – SER195:HN
5	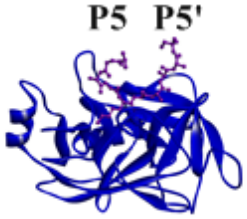 E-W-G-V-K-/-A-V-C-A-H	-91.3	GLU1:OE1–GLN192:HE21 GLU1:OE1–GLN192:HE22 GLY193:HN–ALA6:O LYS5:O – SER195:HN LYS5:O – SER195:HG LYS5:HN – E:SER214:O
6	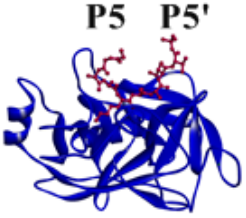 G-L-S-E-K-/-V-S-I-T-A	-90.6	SER3:O – GLY216:HN GLU4:O – GLN192:HE21 LYS5:O – SER195:HN LYS5:O – GLY193:HN SER7:OG – TYR151:HH

Figure 3.9 (A) The amino acid sequence of LvA2M bait region. Bold alphabet indicates the possible cleavage sites by Trypsin. (B) The 10 residues of the polypeptides and respective binding of bait region towards Trypsin. (C) The 3D-model, interaction energy (kcal/mol) and hydrogen bonding of the *LvA2M* peptide/trypsin complex

(A)

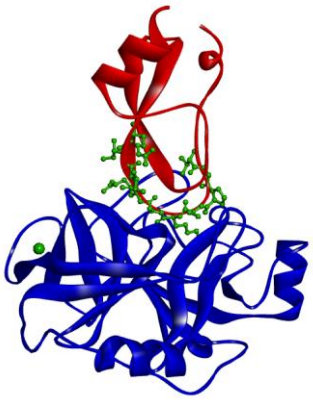

(B)

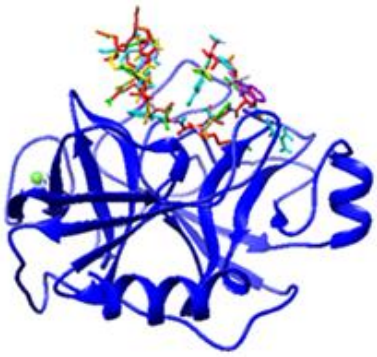

Figure 3.10 (A) Comparison between the re-docked structure of the 10 residues of Bovine Pancreatic trypsin inhibitor II (green bond and stick model) and the whole crystal structure of this inhibitor (red ribbon, PDB ID: 2PTC) in complex with trypsin (blue ribbon). (B) Superimposed structures of the 6 possible peptides extracted from the bait region of *Lv*A2M binding with trypsin. This 6 peptides were differentiate colors: inhibitor of trypsin(red), Peptide 1 (orange), Peptide 2 (yellow), Peptide 3 (green), Peptide 4 (cyan), Peptide 5 (violet) and Peptide 6 (pink).

3.3 A2M inhibitory activity assay against *Vibrio harveyi* secreted protease

The inhibitory activity of r*Lv*A2M and native *Lv*A2M against protease secreted by *V. harveyi* was assayed by agar diffusion method. The clear zone observed indicated the protease activity of the crude protease secreted by *V. harveyi*. In the presence of either r*Lv*A2M or native *Lv*A2M, the percentage of clear zone inhibition was determined. The native *Lv*A2M not the r*Lv*A2M, significantly inhibits protease activity when compared to the control (crude *V. harveyi* proteases (CVPs) only (Figure 3.11A). The percentage of remaining activity of native A2M was 83, 66.7 and 41.6 % at 30, 60 and 120 μM, respectively (Figure 3.11B).

(A)

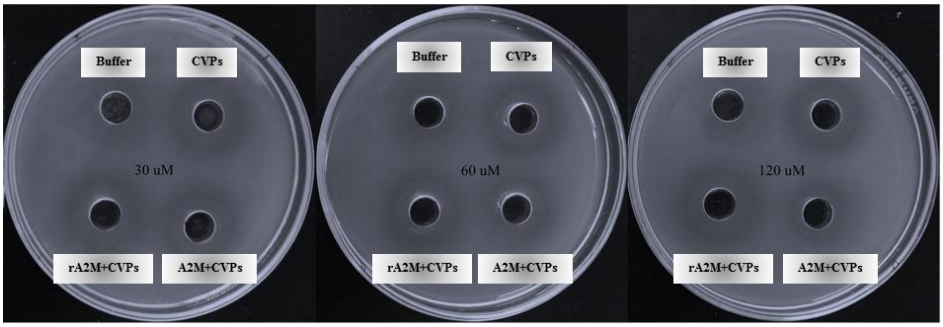

(B)

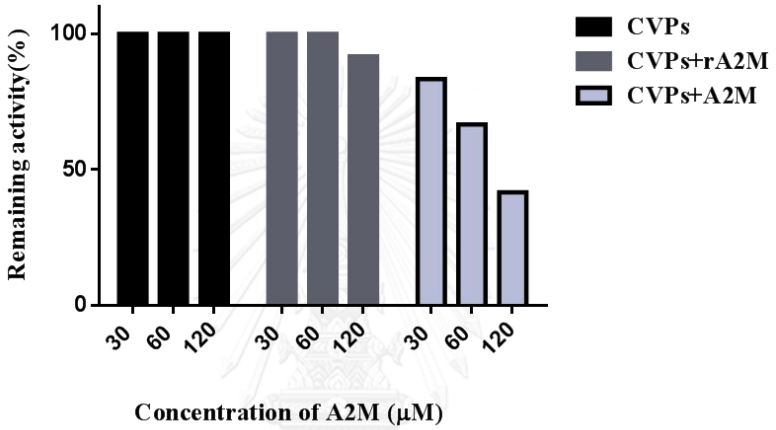

Figure 3.11 A2M inhibitory activity assay against *Vibrio harveyi* secreted protease by agar diffusion method. (A) The recombinant and native *Lv*A2M protein at various concentrations was incubated with the crude *V. harveyi* proteases (CVPs) on the gelatin agar plates. The reduction of clear zone indicated the protease inhibitory activity of native *Lv*A2M. (B) The percentage of remaining activity of CVPs was plotted against various concentration of A2M.

Next, the native *Lv*A2M inhibitory activity against the bacterial secreted proteases was further determined. The crude secreted proteases from 9 bacterial strains, including Gram positive bacteria: *Aerococcus viridans, Bacillus megaterium,*

Micrococcus luteus, Staphylococcus aureus, Staphylococcus haemolyticus and Gram negative bacteria : *Enterobacter cloacae, Erwinia caratovora, Escherichia coli* strain 363, *Vibrio harveyi* strain 639, *Vibrio paraheamolyticus* strain TM, were prepared and tested for protease activity using disc method. Of those, only bacterial secreted proteases from 4 bacteria (*S. aurues, M. luteus, E. coli* and *V. parahaemolyticus*) exhibited protease activity appeared as the clear zone on gelatin agar plate (Figure 3.12A). The inhibitory activity of native *Lv*A2M against protease secreted from bacterial secreted proteases was assayed using disc diffusion method. The native A2M (120 µM) were mixed with 10 µg of crude bacterial proteases and incubated into a well of 1% gelatin agar plate**.** 10 ug of trypsin and 50 mM Tris-HCl pH 8.0 were used as positive and negative control, (Figure 3.12B) respectively**.** The protease secreted from Gram-positive bacteria, *S. aureus and M. luteus,* and Gram-negative bacteria, *E. coli* and *V. parahaemolyticus* were significantly inhibited by the native A2M when compared to the control (Figure 3.12B)

(A)

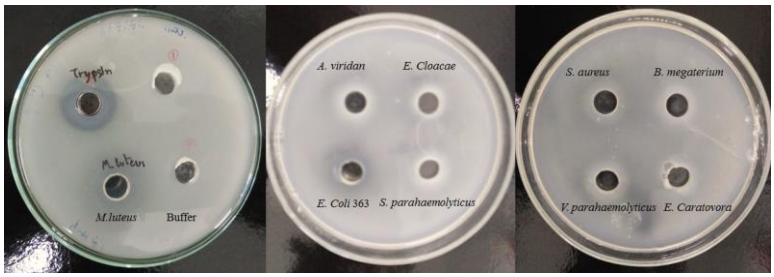

(B)

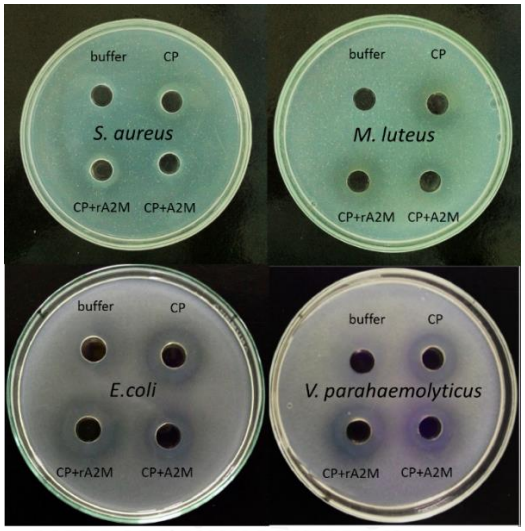

Figure 3.12 A2M inhibitory activity assay against bacterial secreted protease by agar diffusion method. (A) The bacterial secreted protease activity on Gram positive bacteria : *Aerococcus viridans, Bacillus megaterium, Micrococcus luteus, Staphylococcus aureus, Staphylococcus haemolyticus* and Gram negative bacteria : *Enterobacter cloacae, Erwinia caratovora, Escherichia coli strain 363, Vibrio harveyi strain 639, Vibrio paraheamolyticus* on gelatin agar plate. (B) The recombinant and native *Lv*A2M protein at 120 μM incubated with the crude bacterial protease proteases (CVPs) *S. aureus, M. luteus, E. coli and V. parahaemolyticus* on the gelatin agar plates.

3.4 Identification of target protease from *Vibrio harveyi* with *L. vannamei* alpha 2 macroglobulin

3.4.1 Identification of target protease by co-immunoprecipitation

From the above section, the inhibitory activity of native *Lv*A2M against protease from *V. harveyi* was revealed. In order to identify the specific target protease, co-immunoprecipiation was performed. The A2M-protease complexes were incubated with anti-r*Lv*A2M antibody -coupled resin then the bound complexes were analyzed by SDS-PAGE. In the control reaction (*Lv*A2M only), a 170 kDa protein, which is *Lv*A2M, and a 60 kDa protein of *Lv*A2M autocleaved product, were detected. None of A2M-protease complex was detected (Figure 3.13).

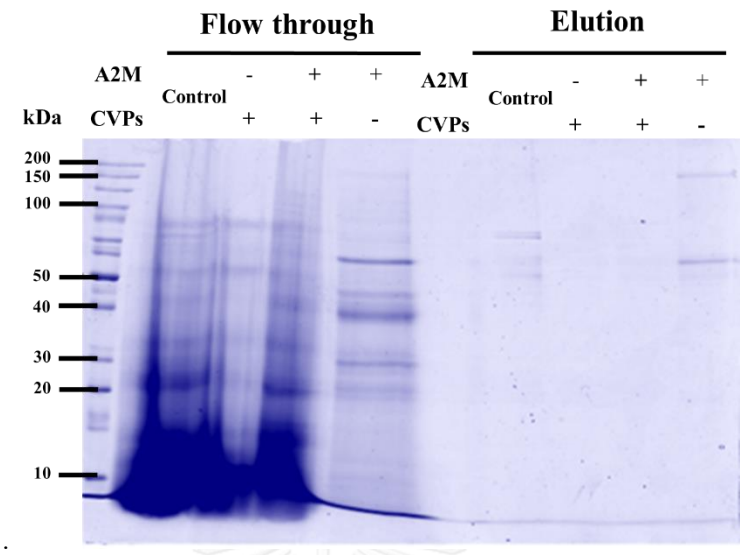

Figure 3.13 Co-immunoprecipitation of the native *Lv*A2M and crude protease *from V. harveyi* protein (CVPs) complexes. The native A2M was immobilized on mouse anti-*Lv*A2M conjugated agarose bead. After extensive washing, the CVPs protein was added and incubated for 15 min. The excess protein was extensively washed and the bound proteins were eluted. The elution fraction was then analyzed for the presence of the protein complex by 15% SDS-PAGE. Group flow through and Group elution as described, Lane control: *Lv*A2M-CVPs complex was incubate with agarose bead, Lane prey control : CVPs protein only was incubated with anti-*Lv*A2m conjugated agarose bead, Lane protein complex : *Lv*A2M-CVPs protein complex was incubated with anti-*Lv*A2m conjugated agarose bead, Lane bait control : *Lv*A2M only was incubated with anti-*Lv*A2m conjugated agarose bead.

3.4.2 Identification of target protease by zymogram method

Zymogram method was used for identification the target protease. Various amount of native *Lv*A2M (0, 5, 10 and 20 µg) was incubated with 5 µg of crude protease from *V. harveyi* for 15 min, 37 °C. The mixture of protease-*Lv*A2M was separated by 1 % gelatin SDS–PAGE under nonreducing conditions and then renatured in 50mM Tris–HCl pH 8.0 containing 2.5% (v/v) Triton X-100. The renatured gels were incubated at 37 °C for 18 h. The crude protease were observed as light bands against a dark blue background, due to the digestion of the gelatin present in the gel by the protease, except at the site where the inhibitor is present (Figure 3.14). We expected that the intensity of protease band should be decreased when the concentration of *Lv*A2M increased. This result indicated that the target protease of *Lv*A2M could not be identified because the decrease intensity of band on zymogram was not observed.

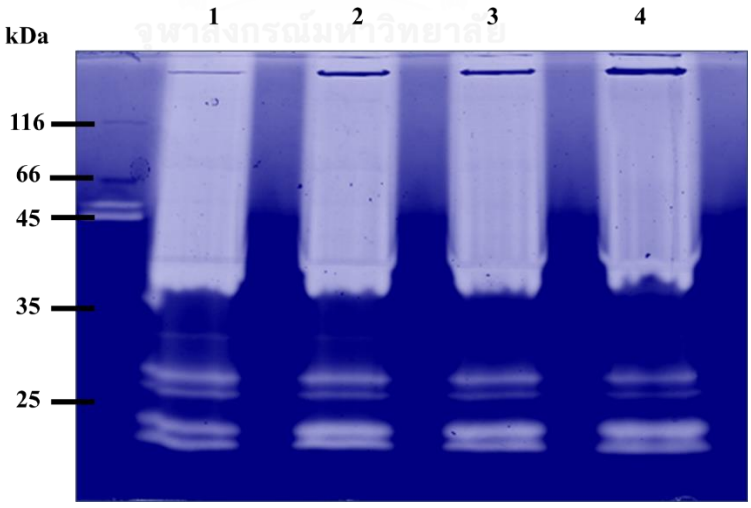

Figure 3.14 *Lv*A2M target protease analysis by zymography. Inhibition reactions of crude *V. harveyi* protease (CVPs) (5 µg) by various concentration of native *Lv*A2M were

separated on 1% gelatin-SDS-PAGE. Lane 1: Positive control (Only crude *V. harveyi* protease), Lane 2: 5 µg of the native LvA2M Lane 3: 10 µg of the native *Lv*A2M Lane 4: 20 µg of the native *Lv*A2M

3.5 Expression of metalloprotease gene (PAP6)

From previous study, PmA2M could inhibit metalloprotease and the serine protease families (Chaikeeratisak et al., 2014). Moreover, a novel PAP6 from *V.harveyi* strain AP6 was reported as metallprotease (Teo et al, 2003). Thus, we expected that PAP6 might be a target protease of *Lv*A2M. Therefore, PAP6 gene was cloned and expressed in order to investigate this speculation.

3.5.1 Cloning of full-length and partial pap6 gene

Genomic DNA from *V. harveyi* strain 639 was purified using FavorPrep™ Tissue Genomic DNA Extraction Kit (Favorgen). The quality of genomic DNA was checked by 1% agarose gel electrophoresis (Figure 3.15). From previous study, the recombinant metalooprotease from *V. harveyi* strain AP6 it likely that Pap6 protein is processed into its mature protein by cleavage of the signal peptide and the N-terminal propeptide (Teo et al., 2003). In this study, the full-length PAP6 (PAP6F) and partial PAP6 (PAP6P) genes were cloned and expressed in *E. coli* system. The PAP6F gene consists of an open reading frame of 2034 base pairs coding for a protein of 677 amino acids and the PAP6P nucleotide sequences consisted of partial sequences of 1542 base pairs coding for a protein of 514 amino acids (Figure 3.16). The PAP6P and PAP6F sequences was

amplified (Figure 3.17A), cloned into expression vector pET-22(b) and transformed into *E. coli* strain XL-1blue. The recombinant clones were first selected with LB/amp. agar plates and further selected by colony PCR (Figure 3.17B) and restriction enzyme digestion (Figure 3.17C). A positive clone was selected and its recombinant plasmid was sequenced to confirm the correction of the junction between vector and inserted DNA. The recombinant proteins obtained from pET-22(b) -PAP6F or PAP6P contained pelB gene at N-terminus. At C-terminus, 14 extra amino acids and six histidines were obtained from the pET-22(b). This clone was used for metalloprotease PAP6 recombinant protein expression.

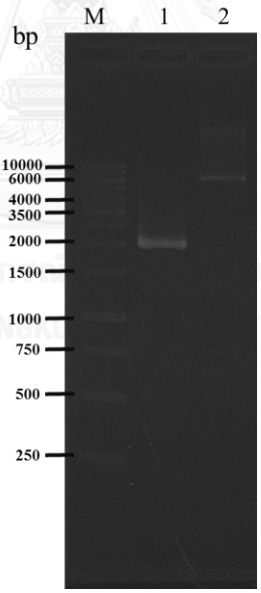

Figure 3.15 Analysis of genomic DNA of *V. harveyi* strain 639. Genomic DNA of *V. harveyi* strain 639 was purified using Tissue Genomic DNA Extraction Kit (Favogen). Lane M: DNA marker Lane 1: amplified PAP6 gene Lane 2: the *V. harveyi* strain 639 genomic DNA

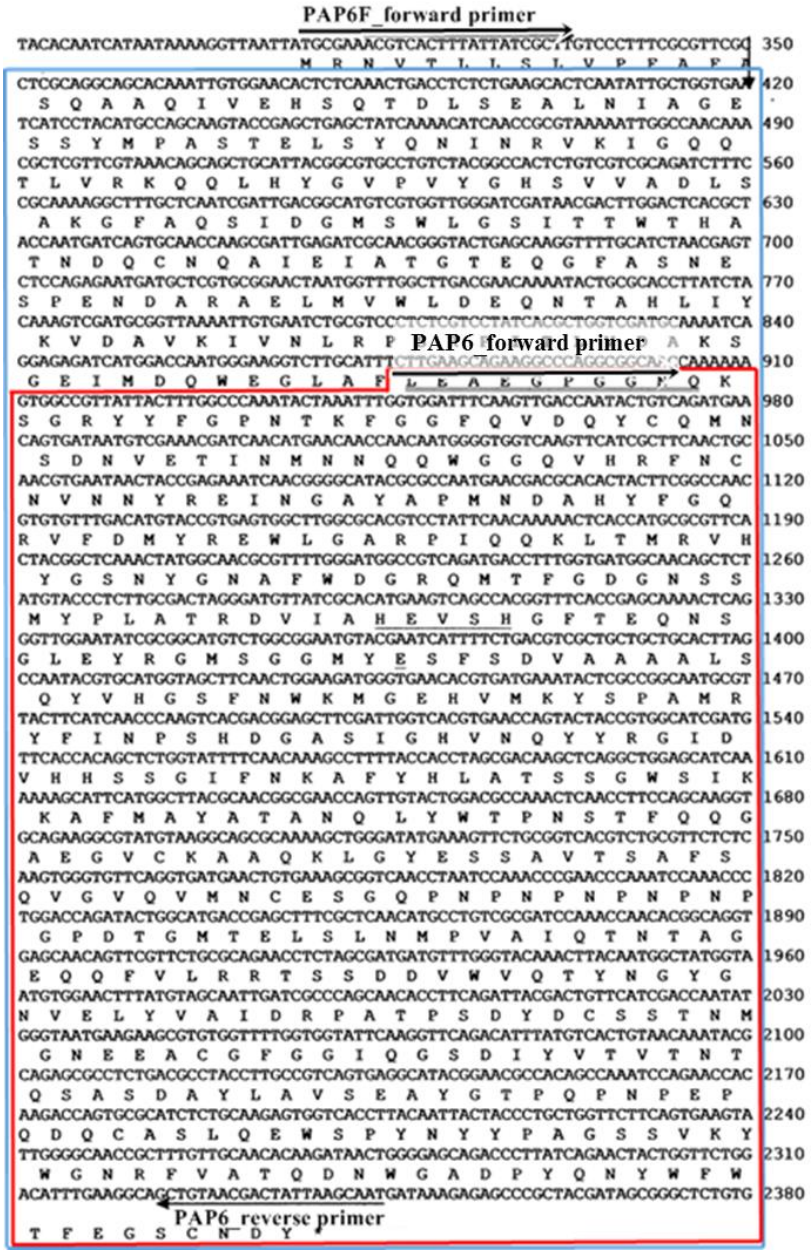

Figure 3.16 Nucleotide and deduced amino acid sequences of PAP6 gene *from V. harveyi.* The nucleotide sequences (above) and amino acid sequences (below) of PAP6 gene are shown with the indicated primer positions (arrows) for full-length (PAP6F) and partial PAP6 (PAP6P) gene amplification. Amino acids are shown as single letter abbreviation (Teo et al., 2003).

(A)

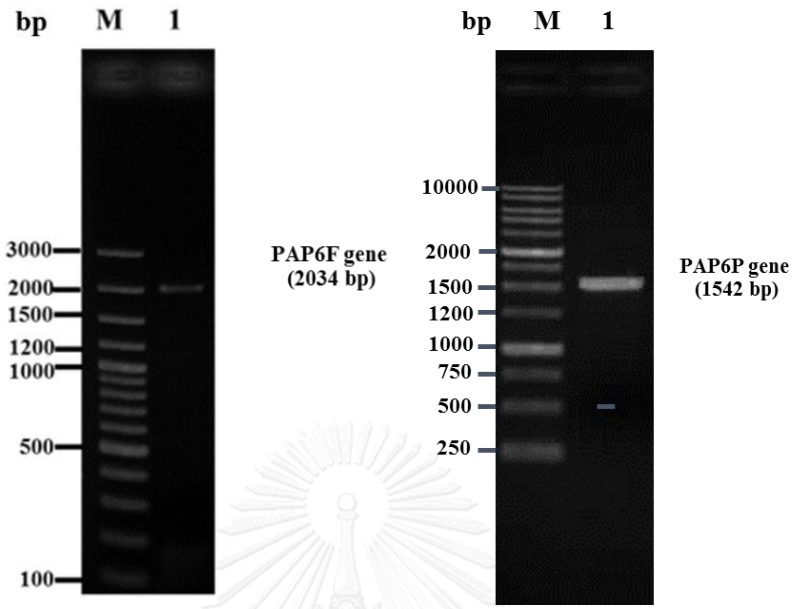
bp
M
1
3000
2000
1500
1200
1000
500
100
PAP6F gene
(2034 bp)
bp
M
1
10000
2000
1500
1200
1000
750
500
250
PAP6P gene
(1542 bp)

(B)

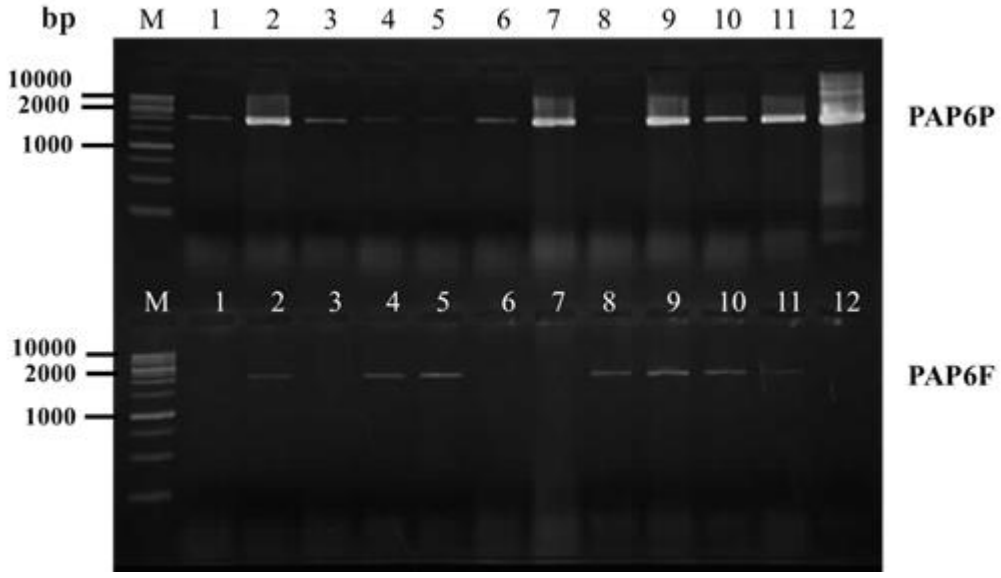
bp
M 1 2 3 4 5 6 7 8 9 10 11 12
10000
2000
1000
PAP6P
M 1 2 3 4 5 6 7 8 9 10 11 12
10000
2000
1000
PAP6F

(C)

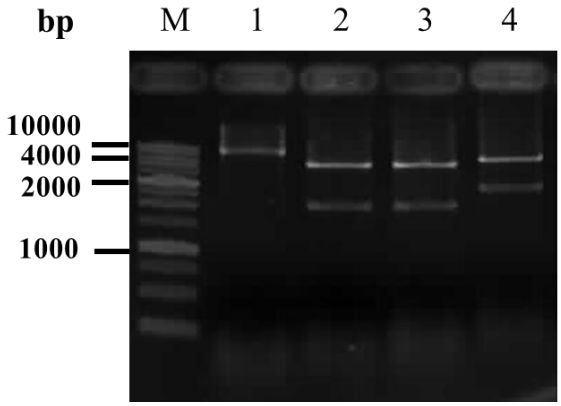

Figure 3.17 Construction of PAP6F and PAP6P expression plasmids. (A) The nucleotide sequences coding for PAP6P and PAPF gene were amplified from genomic DNA of *V. harveyi* Lane M: 100 bp DNA ladder markers. Lane 1: The purified PCR product of PAP6F and PAP6P gene fragments. (B) The recombinant plasmid for PAP6F and PAP6P expression were screened by colony PCR. The expected size of PAP6F and PAP6P fragment was 2034 bp and 1543 bp, respectively. Lane M: 1 kb DNA ladder markers. Lanes 1-12: PCR product from colony PCR analysis. (C) The recombinant plasmids of positive clones were extracted and digested with *Nco*I and *BamH*I. The expected size of PAP6F and PAP6P fragments was 2034 bp and 1542 bp, respectively. Lane M: 1 kb DNA ladder markers. Lanes 1-2: Digestion products from recombinant plasmids PAP6P in pET22b(+). Lane 4 : Digestion products from recombinant plasmids PAP6F in pET22b(+).

3.5.2 Expression of recombinant PAP6F and PAP6P

The clone containing recombinant PAP6F and PAP6P was inoculated and grown in LB medium containing 50 µg/ml amplicillin. Expression of the metalloprotease PAP6F and PAP6P in the transformants was induced with 1 mM IPTG, 0 to 6 hour for PAP6F and 0 to 4 for PAP6P. After induction step, the cells were collected and lysed. Both groups of cell lysate, PAP6F and PAP6, were electrophoresed on 10 % SDS-PAGE in Figure 3.18

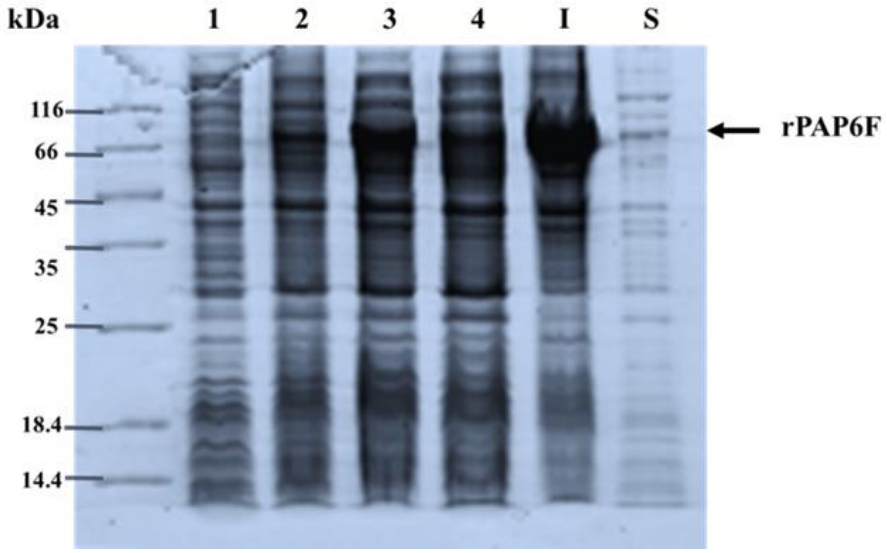

Figure 3.18 Expression of rPAP6F in *E. coli* strain BL21(DE3) CodonPlus(DE3)-RIL. The recombinant clone was cultured and induced for rPAP6F expression by 1 mM IPTG at 0, 2,4 and 6 h, respectively. The cells were collected and checked for protein expression by coomassie stained 10% SDS-PAGE. The expected size of rPAP6F was 75 kDa. The soluble and inclusion bodies fractions obtained after sonication were analyzed by Coomassie stained 10% SDS-PAGE. Lane 1: The whole cell at 0 h without

IPTG induction Lane 2: The whole cell at 2 h with IPTG induction Lane 3: The whole cell at 4 h with IPTG induction Lane 4: The whole cell at 6 h with IPTG induction Lane I: The inclusion fraction Lane S: The soluble fraction and Lane M: Unstained protein markers.

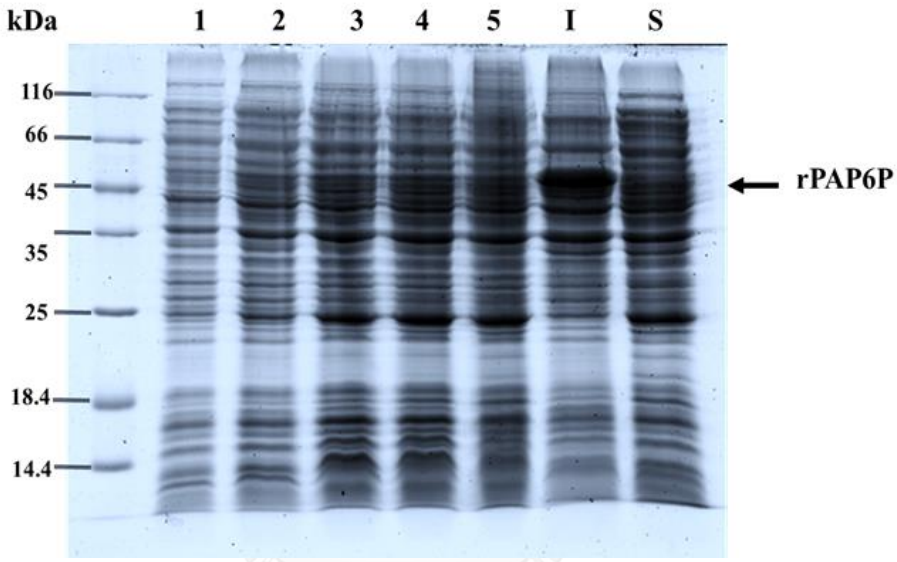

Figure 3.19 Expression of rPAP6P in E. coli strain BL21(DE3) CodonPlus(DE3)-RIL. The recombinant clone was cultured and induced for rPAP6 expression by 1 mM IPTG at 0, 1, 2, 3 and 4 h, respectively. The cells were collected and checked for protein expression by coomassie stained 10% SDS-PAGE. The expected size of rPAP6P was 59 kDa. The soluble and inclusion bodies fractions obtained after sonication were analyzed by Coomassie stained 10% SDS-PAGE. Lane 1: The whole cell at 0 h without IPTG induction Lane 2: The whole cell at 1 h with IPTG induction Lane 3: The whole cell at 2 h with IPTG induction Lane 4: The whole cell at 3 h with IPTG induction. Lane

4: The whole cell at 4 h with IPTG induction Lane I: The inclusion fraction after 4 h of IPTG induction Lane S: The soluble fraction and Lane M: Unstained protein markers.

3.5.3 Purification of the recombinant PAP6F and PAP6P proteins

Previously, the recombinant PAP6F and PAP6**P** proteins containing the His6-tag were expressed as the inclusion bodies after 4 h of IPTG induction. Denaturing buffer (1xPBS, pH 7.4 and 8M urea) were used for solubilizing the proteins from the inclusion bodies. The rPAP6F and rPAP6P proteins were further purified by Ni Sepharose 6 Fast Flow bead. For rPAP6F and rPAP6P protein purification, the elution buffers; 20 mM Tris-HCl, 0.3 M NaCl, pH 7.4 buffer supplement with 6 M urea and 50, 100, 150, and 500 mM imidazole, respectively, were used (Figure. 3.20 and 3.21). Next, the purified proteins of rPAP6F and rPAP6P were analyzed by 10% SDS-PAGE and Western blot analysis (Figure. 3.22). The expected bands of rPAP6F protein (75 kDa) and rPAP6 protein (59 kDa) were observed.

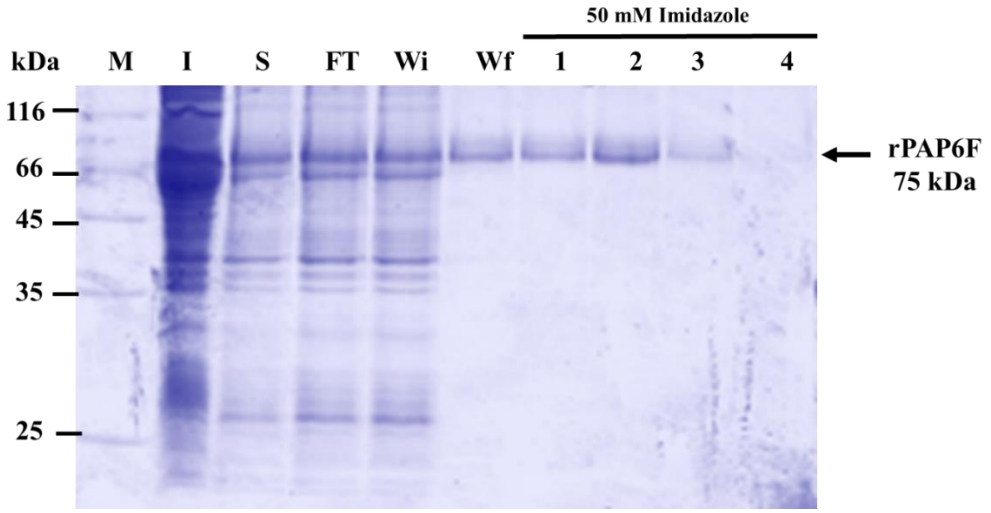

Figure 3.20 Purification of the rPAP6F protein by Ni affinity chromatography. The crude soluble fractions of rPAP6F were passed through Ni Sepharose 6 Fast Flow column under the denaturing condition. After washing, the bound protein was eluted with 1xPBS pH 7.4 buffer supplement with 8 M urea and 50, 100, 150, and 500 mM imidazole, respectively. The fractions were then run on 10% SDS-PAGE. Lane M: the unstained protein Ladder. Lane I: The inclusion fraction. Lane S: The soluble fraction. Lane FT: flowthrough fraction. Lane Wi: The initial of wash fraction. Lane Wf: The final of wash fraction. Lanes 1-4 : elute fractions with elution buffer containing 50 mM imidazole. The arrow indicates the expected band of the purified rPAP6F protein.

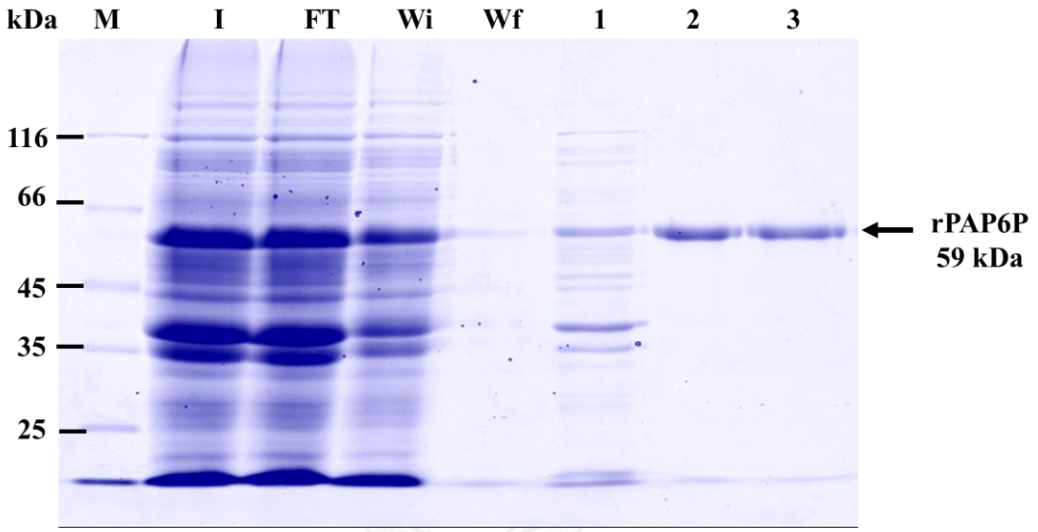

Figure 3.21 Purification of the rPAP6P protein by Ni affinity chromatography. The crude soluble fractions of rPAP6P were passed through Ni Sepharose 6 Fast Flow column under the denaturing condition. After washing, the bound protein was eluted with 1xPBS pH 7.4 buffer supplement with 8 M urea and 50, 100, 150, and 500 mM imidazole, respectively. The fractions were then run on 10% SDS-PAGE. Lane M: the unstained protein Ladder. Lane I: The inclusion fraction. Lane FT: flowthrough fraction. Lane Wi: The initial of wash fraction. Lane Wf: The final of wash fraction. Lanes 1-3 : elute fractions with elution buffer containing 50 mM imidazole. The arrow indicates the expected band of the purified rPAP6P protein

(A)

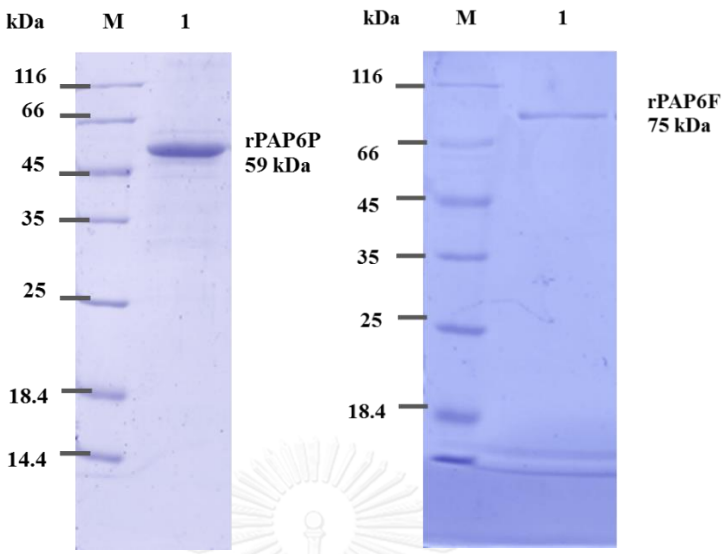

(B)

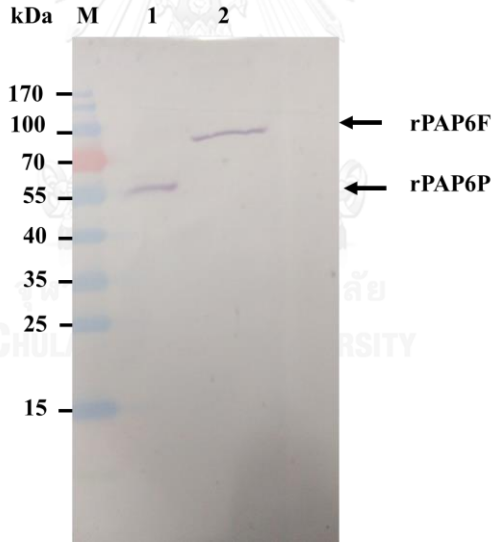

Figure3. 22 Analysis of the purified rPAP6F and PAP6 protein. (A) The purified of rPAP6F and PAP6P protein protein was analyzed by 10 % SDS-PAGE (B) Western blot analysis using the mouse anti-his as a primary antibody and the alkaline phosphatase conjugated goat anti-mouse IgG as a secondary antibody. Lane M is unstained protein marker. The arrow indicates the expected band of the purified rPAPF and PAP6P protein

3.5.4 Protease activity of the recombinant PAP6F and PAP6P protein

The rPAP6F and rPAP6P was assayed for protease acitivity. The purified rPAP6F and rPAP6P were tested with azocasein as the common protease substrate, by measured absorbance at 442 nm. The assay revealed that the rPAP6F and PAP6P could digest azocasein substrate, it lower than 30% when compare with trypsin (Figure 3.23A) The detection of proteolytic enzymes using zymography technique. Sonicated cell lysates or supernatants made from *E. coli* showed no proteolytic activity (Figure 3.23B). Gelatin zymograms obtained using the culture supernatant of BL-21 CodonPlus(DE3)-RIL containing PAP6 gene revealed that the proteolytic band was absence band in soluble and inclusion body.

(A)

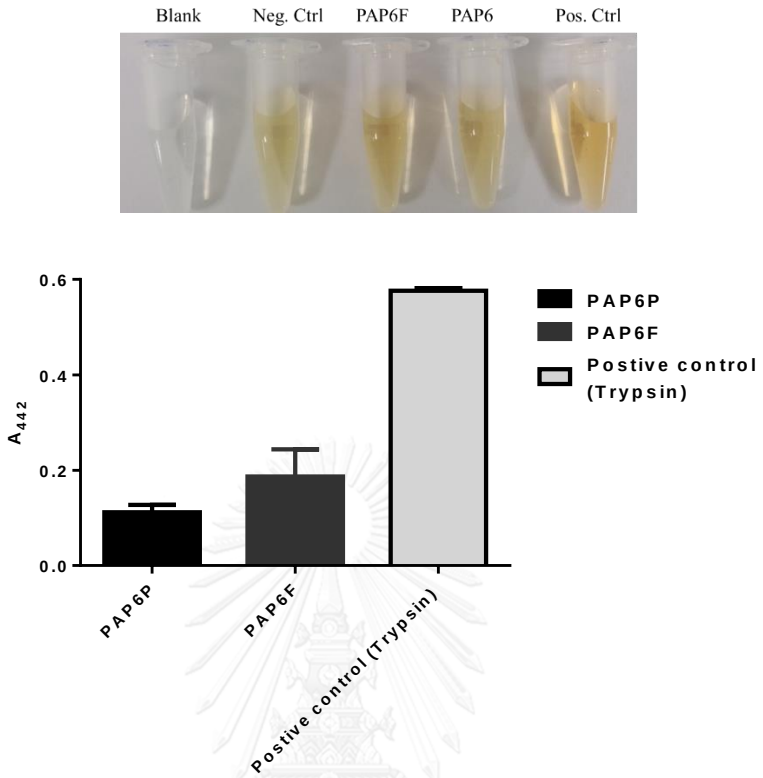

(B)

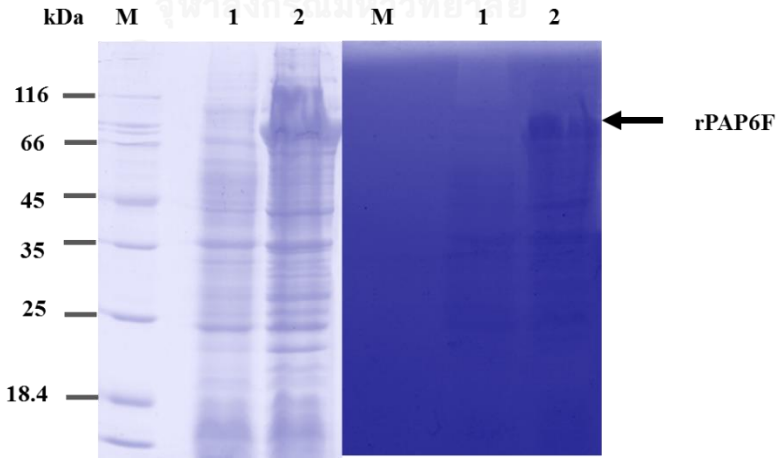

Figure 3.23 Protease activity of the recombinant PAP6P and PAPF. (A) Protease assay was determined using azocasein as the substrate. After 2 hours of incubation, the protease activity was determined at 442 nm. The results are means of three replicates

± SD. (B) Protease activity was detected using a 10% SDS-PAGE gel co-polymerized with 10 mg/ml of gelatin. Lane M: Unstained protein marker. Lane 1: Soluble fraction of *E. coli* BL-21 CodonPlus(DE3)-RIL; lane 2, Inclusion body fraction.

3.5.5 Protein-protein interaction assay between PAP6F or PAP6P and *Lv*A2M by *indirect* enzyme-linked immunosorbent *assay* (*iELISA*)

To determine whether *Lv*A2M could bind to the recombinant protease PAP6, the binding activity of purified native *Lv*A2M protein with two different proteinases, full-length PAP6 and partial PAP6 was performed by ELISA. As shown in Figure 3.24, the PAP6F and PAP6P bound to native *Lv*A2M protein directly in a concentration-dependent manner with a saturable process. The apparent dissociation constant (Kd) of the PAP6F to *Lv*A2M and PAP6P to *Lv*A2M, calculated from the saturation curve fitting according to the one-site model, was 8.064×10^{-7}M and 1.141×10^{-6}M, respectively.

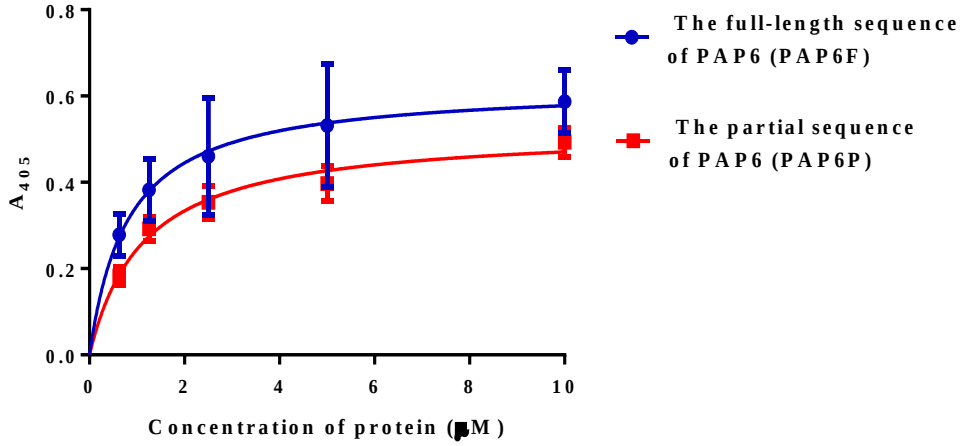

Figure 3.24 The binding activity of *Lv*A2M assay between recombinant PAP6P or PAP6F by indirect enzyme-linked immunosorbent assay. The result showed the quantitative binding of rPAP6F and rPAP6P (0 to 10 μM) to immobilized *Lv*A2M as verified by ELISA. The result was curve-fitted using a single-site binding model with *Lv*A2M (Kd = 8.064×10^{-7}M and 1.141×10^{-6}M).

3.6 Inhibitory activity of *Lv*A2M on *Vibrio parahaemolyticus* toxin

From previous study, A2M binds ligands of related biological functions through the toxin binding mechanism, A2M binds proteinases primarily through ß-cystenyl-γ-glutamyl thiol ester bonds and binds cell function modifying factors, including some cytokines and toxins, through disulfide bonds (Borth, 1992; Armstrong, 2010) and cysteinyl residue of A2M can bind bacterial toxin (Liu et al., 2001; FitzGerald et al., 1993). Therefore, functional role of *Lv*A2M in neutralizing toxin from pathogen was characterized.

3.6.1 Shrimp mortality assay of *V. parahaemolyticus* toxin – injected shrimp

The crude Pir toxin was produced from *V. parahaemolyticus* pathogen of EMS strain and purified by Center of Excellence for Shrimp Molecular Biology and Biotechnology (CENTEX SHRIMP), Mahidol University for investigated of Pir toxin for cumulative mortality assay. The recombinant proteins of Pir A and PirB as well as specific antibodies were expressed and purified by Center for Shrimp Disease Control and Genetic Improvement, National Cheng Kung University for examined protein-protein interaction assay (Figure 3.25).

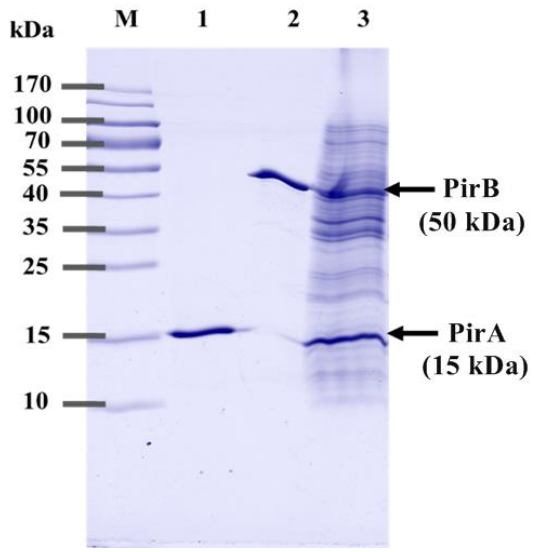

Figure 3.25 Analysis of the Pir toxin protein. The crude Pir toxin protein was analyzed by the 12% SDS-PAGE staining with Coomassie brilliant blue. Lane M: prestained protein marker. Lane 1: the purified recombinant PirA protein. Lane 2: the purified recombinant PirB protein, Lane 3: the crude Pir toxin protein. The arrow indicates the expected band of PirA and PirB protein

To investigate the appropriate dosage of the crude toxin from *V. parahaemolyticus* for survival rate of shrimp, the amount of crude toxin was varied from 0 to 0.3 µg of crude toxin and injected into shrimp. The survival rate of shrimp reached 100% within 24 hours for 0.3 µg of crude toxin, 48 hours for 0.2 µg of crude toxin.

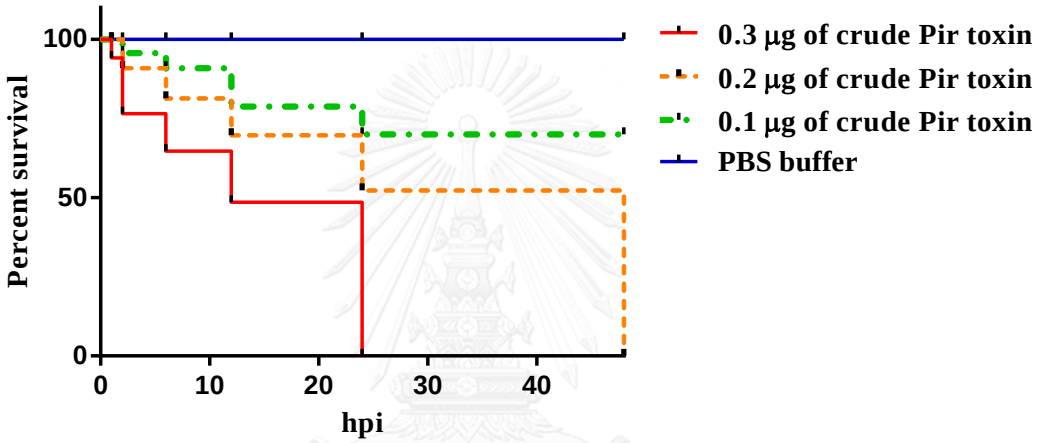

Figure 3.26 The verify dosage of the crude toxin from *V. parahaemolyticus* for survival rate of shrimp. Shrimp were challenged with 1xPBS buffer, 0.3 µg of Pir toxin, 0.2 µg of Pir toxin, 0.1 µg of Pir toxin. The percentage of survival rate of shrimp was observed for 2 days. The experiment was performed in triplicate.

In order to find an appropriate amount of native *Lv*A2M that are effectively neutralized Pir toxin for the neutralizing activity. The amount of the purified native *Lv*A2M protein was incubated with toxin for 15 min then injected into shrimp. The survival rate was observed. The result showed that significant difference of toxin-neutralizing activity of the *Lv*A2M was observed (Figure 3.27). To ensure that the *Lv*A2M

proteins of interest can effectively bind to Pir toxin protein and the toxin-neutralizing activity. The excess amount of the A2M protein (20 µg) was chosen for testing the effect of toxin protein binding on *Lv*A2M-neutralizing activity.

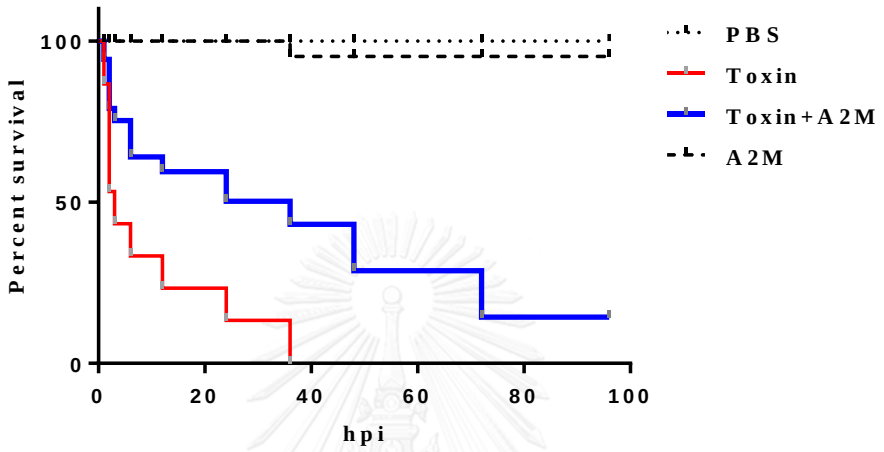

Figure 3.27 Toxin-neutralizing activity of the *Lv*A2M protein. Shrimp were challenged with 1xPBS buffer, 0.2 µg of Pir toxin+*Lv*A2M The percentage of survival rate of toxin-infected shrimp was observed for 3 days. The experiment was performed in triplicate. The values shown here in the graph are means of % survival rate

3.6.2 A2M-toxin protein binding assay

The *Lv*A2M-interacting proteins identified with PirA and PirB were confirmed the interaction between toxin from *V. parahaemolyticus* and *Lv*A2M by *in vitro* pull-down assay. In this experiment, the recombinant PirA and PirB protein containing the 6× His-tag was used as a bait. It was incubated with a nickel chelating resin and the resin was washed to remove the excess protein. The final wash fraction was collected

and checked on SDS-PAGE to ensure that there was no excess rPirA or rPirB protein left in the column. Then, the prey protein *Lv*A2M was added and allowed to bind to the rPirA or rPirB protein. The resin was again washed to remove excess *Lv*A2M protein. The wash fraction was collected and checked on SDS-PAGE to ensure that there was no excess the rPirA or rPirB protein and *Lv*A2M protein left in the column. Then, the protein complex was eluted and resolved by SDS-PAGE. As shown in Figure 3.28, the nickel chelating bead effectively pulled-down the protein complex of rPirA (~15 kDa), PirB (~50 kDa) and *Lv*A2M (~170 kDa). The results indicated that the PirA and PirB toxin protein could specifically bind to *Lv*A2M *in vitro*.

(A)

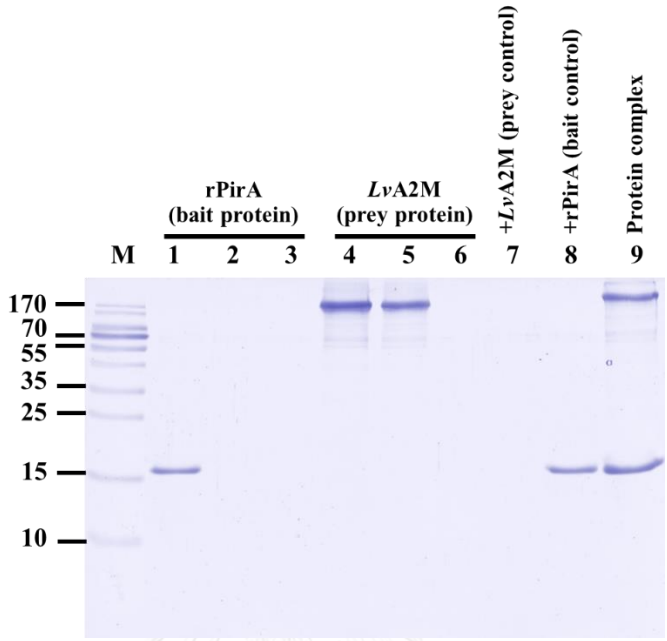

(B)

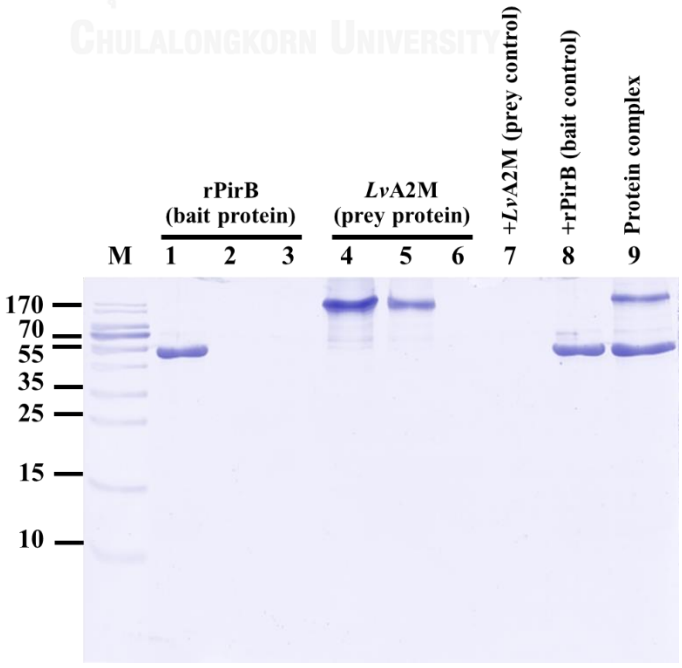

Figure 3.28 *In vitro* pull-down assay between rPirA or rPirB and *Lv*A2M proteins. rPirA or PirB was immobilized on the nickel chelate resin. After extensive washing, the *Lv*A2M was added and incubated for 12 h, 4 ^{o}C. The excess protein was extensively washed and the bound proteins were eluted. The elution fraction was then analyzed for the presence of the protein complex by 10% coomassie stained SDS-PAGE. Lane M: prestained protein marker. Lane 1: purified rPirA or PirB protein in 1xPBS buffer, pH 7.4 (bait protein); Lane 2: flow through fraction of rPirA or PirB after binding to nickel agarose column for 2 h at 4 ℃. Lane 3: the wash fraction of rPirA or PirB. Lane 4: *Lv*A2M protein (prey protein); Lane5: flow through fraction of *Lv*A2M after incubation with immobilized bait for 12 h at 4 ℃; Lane 6: the wash fraction of *Lv*A2M; Lane 7: prey control (*Lv*A2M only). Prey treated as described in lanes 1-6 and subsequently eluted. No prey added-just binding buffer. Lane 8: bait control (PirA or PirB only). bait treated as described in lanes 1-6 and subsequently eluted. No bait added-just binding buffer and Lane 9: elution of bait:prey complex (prepared in lanes 1-6) from the agarose beads with 250 mM imidazole.

The recombinant PirA and PirB proteins were used to check the binding activity by using Enzyme linked immunosorbent assay (ELISA) technique to observe whether protein can bind with *Lv*A2M. The serial dilution concentration of rPirA and rPirB were incubated each well triplicate in microtiter plate, were coated with *Lv*A2M. The rPirA and rPirB protein was incubated with mouse anti-Pir antibody as a primary antibody.

The colorimetric detection used secondary antibodies for linked to enzymes-substrate (ρ-nitrophenylphosphate) reaction that were detect the absorbance at 405 nm The results showed the dissociation constant (Kd) of rPirA and rPirB be able to bind with *Lv*A2M were 13.561×10^{-7}M and 5.814×10^{-7}M, respectively. The graph and constants were created by using graphad prism 6.0 that calculated the non-linear single-site specific binding parameter

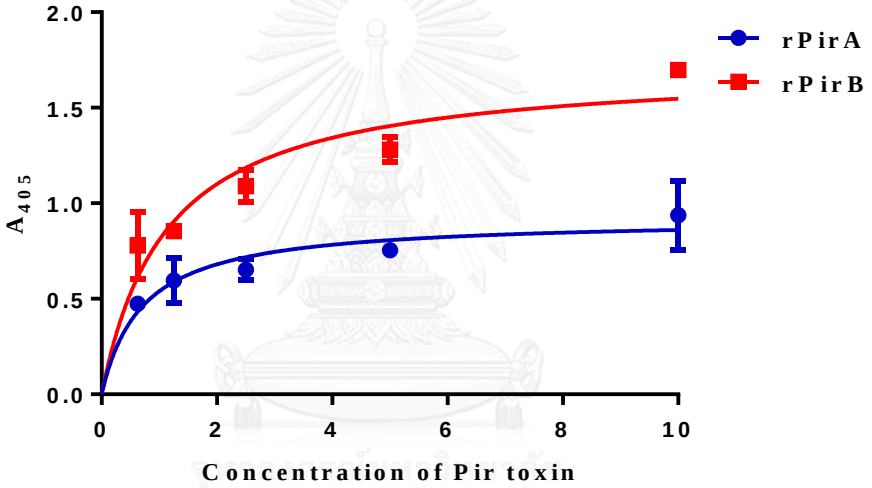

Figure 3.29 The binding activity of PirA and PirB assay between native A2M by indirect enzyme-linked immunosorbent assay. The result showed the quantitative binding of PirA and PirB (0 to 5 μM) to immobilized *Lv*A2M as determined by ELISA. The result was curve-fitted using a single-site binding model with *Lv*A2M (Kd= 3.561×10^{-7}M and 5.814×10^{-7}M respectively).

3.6.3 Analysis of PirA PirB toxin with A2M by molecular docking

The amino acid sequences of *Lv*A2M and Pir toxin from *V. parahaemolyticus* were obtained from the sequence database of NCBI (ID: *Lv*A2M: ABI79454, PirA: AIL49948.1 and PirB: AIL49949.1). The PirA model was built from beta-glucosidase, bgl1 from *hypocrea jecorina* (21% Identity and 71.2% confidence), while PirB model was constructed from insecticidal delta-endotoxin (Cry8 protein, only 382 residues available) from *bacillus thuringiensis* (87% Identity and 100% confidence). The best three ranked structures (B1-B3) in according to the docking score, area and hydrogen bond for protein-protein binding were illustrated in Figure 3.30B. The hydrogen bond pairs of protein-protein interaction for the best complex structure (B1) were only shown. Figure 3.30C (left) presents the *Lv*A2M model constructed based on the Alpha-2-macroglobulin from Human, *Homo sapiens* (29.4% Identity and 52.9% similarity). Using the same criteria above for the docked results of Pir complex and *Lv*A2M model, the most possible binding of Pir complex was found at the receptor binding region of *Lv*A2M (C1, yellow in Figure 3.30C) with a formation of the 14 hydrogen bonds. Taken altogether, the homology modelling suggested that the *Lv*A2M might be able to interact and neutralize to Pir toxin from *V. parahaemolyticus* (Figure 3.30C).

(A)

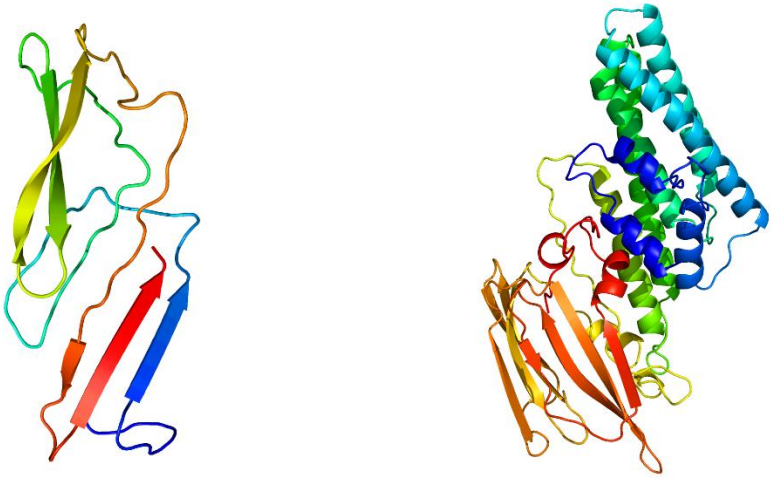

PirA PirB

(B)

3D Model	Pir toxin complex	Area	Score	H-bond
B1	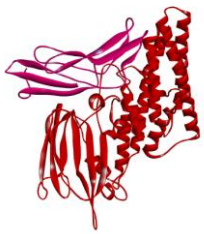	2891	16170	10
B2	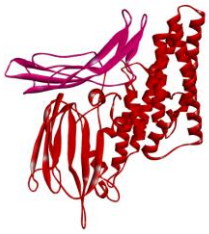	2650	16124	9

B3	2315	15912	4

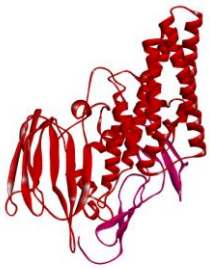

3D Model	Hydrogen bond (H-bond)			
B1	PirA	PirB	PirA	PirB
	SER12:OG.....OH:TYR35		ARG76:NH1.....OE2:GLU182	
	ARG39:NH1.....OD1:ASP412		ARG76:NH2.....OE1:GLU182	
	ARG39:NH2.....OD1:ASP412		ARG76:NH2.....OE2:GLU182	
	ARG39:NH1.....OD2:ASP412		ASP77:O.....OH:TYR179	
	ARG76:NH1.....OE1:GLU182		TYR110:OH.....O:TYR350	

(C)

3D Model	Pir/LvA2M complex	Area	Score	H-bond
C1	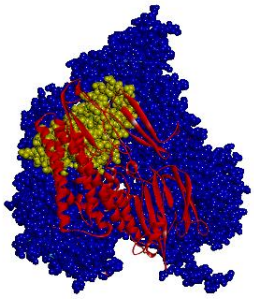	4480	24728	14
C2	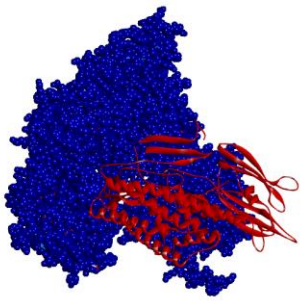	4006	21548	8
C3	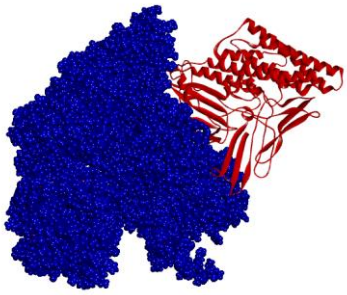	3358	21542	4

Structure	H-bond pair			
C1	**A2M**	**Pir toxin**	**A2M**	**Pir toxin**
	ARG253:NE	O:ASP383	SER1181:OG	OD2:ASP290
	ARG254:NE	O:THR385	ASN1182:OD21	OE2:GLU333
	CYS968:N	O:VAL325	ASN1182:OD22	OE2:GLU333
	PHE1082:N	O:PRO295	LYS1217:N	OE1:GLU336
	SER1083:N	O:PRO295	ASN1219:ND21	OE2:GLU318
	ARG1176:NE	OE1:GLU333	TYR1225:OH	O:GLY335
	SER1181:OG	O:THR286	SER1226:N	OG1:THR331

Figure 3.30 (A) Homology models of PirA and PirB. The three best ranked complexes and interactions of (B) PirA/PirB (pink/red) and (C) Pir toxin/A2M (red/blue) from docking study.

CHAPTER IV
DISCUSSIONS

The A2M protein is a fairly non-specific protease inhibitor that exists in vertebrates and invertebrates. The inhibitory mechanism of A2M differs from other protease inhibitors. The inhibition of A2M is achieved by physical entrapment of the proteases in its ‘‘Venus flytrap’’ like structure, resulting from a conformational change triggered by cleavage within the bait region (Sottrup-Jensen 1989; Lin et al. 2012; Meyer et al. 2012). The enclosure forms by A2M for entrapment of proteinases is a unique molecular structure (Marrero et al. 2012). The entrapment in the A2M cage prevents the entrapped enzyme from accessing external proteins as substrates for proteolytic attack and protects the entrapped enzyme molecule from inactivation by macromolecular active site protease inhibitors (Armstrong 2010). A2M has probably evolved as proteins of a primitive defense system or perhaps a pre immune system to protect primitive species from invading pathogens, thereby increasing the survival rate of the host. A2M has been implicated in attenuating infection and parasite growth in various species by counteracting contentious proteinases from bacteria (Chaikeeratisak et al. 2014; Craig-Barnes et al. 2010; Sjobring et al. 1989). In some species, A2M is a major plasma factor that offers protection from virus infection (Chen et al. 2011; Ma et al. 2010). In invertebrates, A2M is a broad range proteinase inhibitor and a highly abundant plasma protein that is crucially involved in many immune responses, such

as phagocytosis in the hard tick, *Ixodes ricinus* (Buresova et al. 2009), and in the mosquito, *Anopheles gambiae* (Levashina et al. 2001) the prophenoloxidase activating system in the crayfish, *Pacifastacus leniusculus* (Soderhall et al. 1990), and the blood clotting system in *P. leniusculus* (Hall and Söderhäll 1994) and the horseshoe crab, *Limulus polyphemus* (Armstrong et al. 1984).

In penaied shrimp, A2Ms have been cloned and characterized from white shrimp, *L. vannamei* (Gollas-Galvan et al. 2003), the kuruma shrimp, *Marsupenaeus japonicus* (Rattanachai et al. 2004), the black tiger shrimp, *P. monodon* (Lin et al. 2007), the chinese white shrimp, *Fenneropenaeus chinesis* (Ma et al. 2010) and the Atlantic shrimp, *Farfantepenaeus paulensis* (Perazzolo et al. 2011). The different A2Ms have different orders of multimerization but in case of shrimp, they are homodimers. Immunogold labeling of A2M in the hemocytes of *F. paulensis* indicated that it was stored in the vesicles of the shrimp granular hemocytes (Perazzolo et al. 2011). Remarkably, the shrimp A2M expression level was responsed upon bacterial, viral and fungal infections at either the transcriptional or the translational levels (Ma et al. 2010; Perazzolo et al. 2011; Somboonwiwat et al. 2010). The A2M from *P. monodon* can bind to syntenin, a cytosolic protein with diverse biological functions (Tonganunt et al. 2005). They also may facilitate the entry of the phagocytosis activating protein (PAP) into phagocytic cells and increase the survival rate of the shrimp after being infected by WSSV (Chotigeat et al. 2007). The expression profile of A2M protein in the major

immune tissues of *V. harveyi* infected *P. monodon* indicated that it was the most strongly altered protein in hemocytes (Somboonwiwat et al. 2010) and lymphoid organ (Chaikeeratisak et al. 2012) following *V. harveyi* infection. *Pm*A2M was located on the shrimp clot and functioned as inhibitor of clot fibrinolysis. Recently, it has been shown that the secreted proteases from *V. harveyi*, required for clot fibrinolysis were catergorized in the metalloprotease and the serine protease families (Chaikeeratisak et al. 2012; Chaikeeratisak et al. 2014).

In the present study, the recombinant *Lv*A2M could be produced in *E. coli* system but protein was unable to purify by Ni-NTA purification system. rA2M was purified by cutting band and eluting from gel. The activity of r*Lv*A2M was not significant observed when compared with the native A2M from shrimp plasma. Although the r*Lv*A2M can be successfully purified but the purified r*Lv*A2M did not exhibit protease inhibitory activity. The *Lv*A2M is a large homodimeric glycoprotein and consists of 9 *N*-linked glycosylation and 11 disulfide bonds (Lin et al. 2008). While, 8 *N*-linked glycosylation sites were observed in the A2M sequence of *P. monodon* (Lin et al. 2007) and *M. japonicus* (Rattanachai et al. 2004). Considering structure of *Lv*A2M, it is a high molecular weight protein. Therefore, the loss of r*Lv*A2M activity could result from misfolding of molecule as well as lacking of glycosylation in *E. coli* system. Also, the activity of A2M depends on the presence of a reactive internal ß-cystenyl-γ-glutamyl

thiol ester. In *E. coli*, this thiol ester bond would be difficult to produce causing impair of A2M activity.

Among the 6 possible peptides extracted from bait region of *Lv*A2M binding at the active site of target protein, trypsin, the peptide 1 (M-G-P-D-R-/-E-F-D-E-P) showed the strongest binding to trypsin (interaction energy of -110.6 kcal/mol) which was much better than the Bovine Pancreatic inhibitor II from the X-ray complex structure (-86.1 kcal/mol). At the cleavage reaction center of P1 residue, the carbonyl oxygen of Arg5 was well stabilized by the catalytic residue Ser195 and the residue Gly193. The latter one is a component of oxyanion hole. This finding was in good agreement with the common substrate or inhibitor binding with serine proteases (Decha et al. 2008; Yotmanee et al. 2015). The salt bridge interaction was formed between the Asp8 of bait region (P3' residue) and Lys60 of trypsin. The P3 and P4' residues of *Lv*A2M bait region interacted with Gly216 and Try39, respectively.

The inhibitory activity of A2M against bacterial protease has been reported. ***A****eromonas salmonicida* protease was inhibited by A2M of rainbow trout serum (Ellis 1987) A2M in cobia, *Rachycentron canadum* exhibited protease inhibitory activity against extracellular products (ECP) of *Vibrio alginolytius* (Chuang et al. 2014). Herein, the native A2M inhibitory activity against crude secreted proteases from 10 bacterial proteases including *Aerococcus viridans, Bacillus megaterium, Micrococcus luteus, Staphylococcus aureus, Staphylococcus haemolyticus*, *Enterobacter cloacae, Erwinia*

caratovora, Escherichia coli strain 363, *Vibrio harveyi* strain 639, *Vibrio paraheamolyticus* strain TM was tested. We found that only 5 bacteria including *V. harveyi, S.aurues, M. luteus, E. coli* and *V. parahaemolyticus* presented protease activity implying that A2M could inhibit these bacterial proteases.

Immunoprecipitation was performed to identify protease-inhibitor complex such as in American Horseshoe Crab, *Limulus polyphemus* (Melchior et al. 1995), A2M-plasmin complex (Harpel 1973), and A2M-HSV (herpes virus) protease complex in human (Alonso et al. 2001). The identification of target protease for *Lv*A2M from *V.harveyi* was performed by co-immunoprecipitation but the target protease could not be identified. We assumed that protease from *V. harveyi* might identified digest antibody which cross link to beads. From previous study, zymography targets protease of humanA2M as a 33-kDa protein prostate-specific antigen (PSA) (Birkenmeier et al. 1998). The novel A2M from human epidermis could inhibit chymotrypsin in casein zymogram (Galliano et al. 2006) The inhibitory activity of MMP-2, MMP-9 and serine proteinases of A2M in human was evaluated by gelatin zymography (Bísaro de Lorenc et al. 2005) Unfortunately, we could not identify target protease from *V.harveyi*.

Vibriosis is one of the most serious diseases in cultured marine farming (Austin and Zhang 2006; Egidius 1987). Pathogenic vibrios produce various pathogenic factor, and protease that play pathogenic roles after infection (Shinoda and Miyoshi 2011). These pathogenic vibrios produce various pathogenic factors including enterotoxins,

hemolysin, cytotoxin, adhesive factor, hemagglutinin and protease (MIYOSHI 2006) such as cysteine protease from *V. peneacida* (Aguirre-Guzman et al. 2005), serine proteases and metalloproteases from *V. parahaemolyticus* (Ishihara et al. 2002; Kim et al. 2002; Yu and Lee 1999), zinc metalloprotease (Teo et al., 2003). From previous study, A2M inhibited secreted proteases from *V. harveyi* that were characterized as serine proteases and metalloproteases. (Chaikeeratisak et al., 2014). Several extracellular proteases belonging to *V. harveyi* have been identified: a 22-kDa cysteine protease, which is an important exotoxin (Liu et al., 1997; Liu and Lee, 1999), and three alkaline metal-chelator-sensitive proteases (Fukasawa et al. 1988). Other species of *Vibrio* have been found to secrete serine protease (Park et al., 2009) and metalloprotease (Chang et al., 2005; Kwon et al., 2007). Moreover, a novel PAP6 from *V. harveyi* strain AP6 was reported as zinc metallprotease (Teo et al, 2003). We expected that PAP6 might be a target protease of *Lv*A2M. Therefore, the recombinant protein of the full-length and partial PAP6 gene were produced in *E. coli* system. Following purification by Ni affinity chromatography, protease acitivity assay using azoalbumin substrate and zymogram showed that both PAP6P and PAPF did not exhibit protease activity. It was evidence that activity of PAP6 depends on structure of protein and co-factor. (Teo et al., 2003; Hasegawa and Häse, 2009). Lacking of protease activity of the recombinant PAP6 protein is probably due to protein misfolding. To determine whether PAP6 is possibly the *Lv*A2M target protease, binding of *Lv*A2M recombinant protease PAP6, was performed by indirect ELISA. The result showed that the binding ability of the PAP6F

(Kd = 8.064×10^{-7}M) to *Lv*A2M is stronger than that of partial PAP6 protein. (Kd = 1.141×10^{-6}M)

A2M binds ligands of related biological functions through the same mechanism, A2M binds proteinases primarily through ß-cystenyl-γ-glutamyl thiol ester bonds and binds cell function modifying factors, including some cytokines and toxins, through disulfide bonds (Borth, 1992; Armstrong, 2010). *Vibrio parahaemolyticus* can cause acute hepatopancreatic necrosis disease (AHPND). This disease is responsible for mass mortalities in farmed penaeid shrimp and is referred to as early mortality syndrome (EMS) **(**Sirikharin et al 2015**)**. Virulence-associated proteins similar to *Photorhabdus* insect-related (Pir) toxins encoded by 2 genes (PirA and PirB) for 15 and 50 kDa proteins, respectively (Han et al., 2015). In this study, the ability of *Lv*A2M to neutralize Pir toxins from *V. parahaemolyticus* were revealed. The rPirA and rPirB proteins could specifically bind to *Lv*A2M *in vitro* with the Kd of 3.561×10^{-7}M and 5.814×10^{-7}M, respectively. The binding of PirA/PirB toxin complex with *Lv*A2M was studied by molecular docking. The results suggested that the *Lv*A2M might be able to interact and neutralize to Pir toxin from *V. parahaemolyticus* through the protein-protein interaction at the receptor binding region of A2M. The functional role of *Lv*A2M in neutralizing toxin from pathogen is of great interests which would be further elucidated.

However, further investigations are yet needed to confirm its target protein of *Lv*A2M. This will be fulfill and extend knowledge based on the shrimp immune defense, especially defense against pathogenic *Vibrio* spp. infections.

CHAPTER V
CONCLUSIONS

The alpha-2-macroglobulin (A2M) played an important role in *L. vannamei* immunity against pathogenic infection. Identification of *Lv*A2M target protease could provide better understanding on its immune function against bacterial infection in shrimp. The *Lv*A2M gene contained an open reading frame of 4,454 bp. The predicted molecular mass of r*Lv*A2M (1,489 amino acid) is 166.9 kDa and pI is 5.77. The recombinant *Lv*A2M protein with expected size was successfully produced in *E. coli* but was unable to purify by Ni-NTA purification system. Therefore, r*Lv*A2M was directly purified from SDS-PAGE. The functional shrimp A2M was partially purified from the plasma of *L. vannamei*. The inhibitory activity against *V. harveyi* proteases of native *Lv*A2M was higher than r*Lv*A2M. The inhibitory activity of native *Lv*A2M inhibited all bacterial secreted proteases (*S. aurues, M. luteus, E. coli* and *V. parahaemolyticus*). However, target protease of *Lv*A2M could not be identified by co-immunoprecipitation and zymogram techniques.

From previous report, metalloprotease from *V. harveyi* has been shown to be inhibit by *Lv*A2M. Consequently, the metalloprotease (PAP6) from *V. harveyi* was selected for analysis. The full length PAP6F protein (75 kDa) and the partial PAP6P protein (53 kDa) were successfully produced but did not exhibit protease activity. Anyway, both PAP6F and PAP6P could interact with *Lv*A2M as determined by indirect

ELISA. Moreover, the neutralizing activity of *Lv*A2M on the toxins from a shrimp pathogenic bacterium was studied. The *Lv*A2M could neutralize toxicity of the crude Pir toxin in shrimp. Protein-protein interaction of *Lv*A2M and Pir toxin were confirmed by *in vitro* pull down assay, ELISA and molecular docking. The results suggested that *Lv*A2M might participate in many immune responses to inhibit different target proteases and toxins of invading bacteria as well as controlling the host immune reactions.

REFERENCES

Aguirre-Guzman G, Ascencio F, Saulnier D (2005) Pathogenicity of Vibrio penaeicida for white shrimp Litopenaeus vannamei: a cysteine protease-like exotoxin as a virulence factor. Dis Aquat Organ 67 (3):201-207. doi:10.3354/dao067201

Ahantarig A, Chantawat N, Waterfield NR, Kittayapong P (2009) PirAB toxin from Photorhabdus asymbiotica as a larvicide against dengue vectors. Applied and environmental microbiology 75 (13):4627-4629

Ahyong ST, Lowry JK, Alonso M, Bamber RN, Boxshall GA, Castro P, Gerken S, Karaman GS, Goy JW, Jones DS (2011) Subphylum Crustacea Brünnich, 1772. Zootaxa 3148:165-191

Ai HS, Liao JX, Huang XD, Yin ZX, Weng SP, Zhao ZY, Li SD, Yu XQ, He JG (2009) A novel prophenoloxidase 2 exists in shrimp hemocytes. Dev Comp Immunol 33 (1):59-68. doi:10.1016/j.dci.2008.07.017

Alonso M, Dimitrijevic A, Recuero M, Serrano E, Valdivieso F, Lopez-Guerrero JA (2001) Interaction of alpha-2-macroglobulin and HSV-1 during infection of neuronal cells. J Neurovirol 7 (6):556-563

Alvarez J, Austin B, Alvarez A, Reyes H (1998) Vibrio harveyi: a pathogen of penaeid shrimps and fish in Venezuela. Journal of Fish Diseases 21 (4):313-316

Amparyup P, Charoensapsri W, Tassanakajon A (2009) Two prophenoloxidases are important for the survival of Vibrio harveyi challenged shrimp Penaeus monodon. Dev Comp Immunol 33 (2):247-256. doi:10.1016/j.dci.2008.09.003

Amparyup P, Charoensapsri W, Tassanakajon A (2013) Prophenoloxidase system and its role in shrimp immune responses against major pathogens. Fish & shellfish immunology 34 (4):990-1001. doi:10.1016/j.fsi.2012.08.019

Amparyup P, Sutthangkul J, Charoensapsri W, Tassanakajon A (2012) Pattern recognition protein binds to lipopolysaccharide and beta-1,3-glucan and activates shrimp prophenoloxidase system. The Journal of biological chemistry 287 (13):10060-10069. doi:10.1074/jbc.M111.294744

Aoki T, Hirono I, Kondo H, Hikima J, Jung TS (2011) Microarray technology is an effective tool for identifying genes related to the aquacultural improvement of Japanese flounder, Paralichthys olivaceus. Comp Biochem Physiol Part D Genomics Proteomics 6 (1):39-43. doi:10.1016/j.cbd.2010.06.005

Ariki S, Koori K, Osaki T, Motoyama K, Inamori K, Kawabata S (2004) A serine protease zymogen functions as a pattern-recognition receptor for lipopolysaccharides. Proc Natl Acad Sci U S A 101 (4):953-958. doi:10.1073/pnas.0306904101

Armstrong L, Godinho SI, Uppington KM, Whittington HA, Millar AB (2006) Contribution of TNF-alpha converting enzyme and proteinase-3 to TNF-alpha processing in human alveolar macrophages. Am J Respir Cell Mol Biol 34 (2):219-225. doi:10.1165/rcmb.2005-0087OC

Armstrong P (2010) Role of α2-macroglobulin in the immune responses of invertebrates. Invertebr Surviv J 7:165-180

Armstrong PB (2001) The contribution of proteinase inhibitors to immune defense. Trends Immunol 22 (1):47-52

Armstrong PB, Armstrong MT (2003) The decorated clot: Binding of agents of the innate immune system to the fibrils of the limulus blood clot. Biol Bull 205 (2):201-203

Armstrong PB, Levin J, Quigley JP (1984) Role of endogenous proteinase inhibitors in the regulation of the blood clotting system of the horseshoe crab, Limulus polyphemus. Thromb Haemost 52 (2):117-120

Aspan A, Huang TS, Cerenius L, Soderhall K (1995) cDNA cloning of prophenoloxidase from the freshwater crayfish Pacifastacus leniusculus and its activation. Proc Natl Acad Sci U S A 92 (4):939-943

Austin B, Zhang XH (2006) Vibrio harveyi: a significant pathogen of marine vertebrates and invertebrates. Lett Appl Microbiol 43 (2):119-124. doi:10.1111/j.1472-765X.2006.01989.x

Barrera DI, Matheus LM, Stigbrand T, Arbelaez LF (2007) Proteolytic hydrolysis and purification of the LRP/alfa-2-macroglobulin receptor domain from alpha-macroglobulins. Protein Expr Purif 53 (1):112-118. doi:10.1016/j.pep.2006.12.008

Birkenmeier G, Kampfer I, Kratzsch J, Schellenberger W (1998) Human leptin forms complexes with alpha 2-macroglobulin which are recognized by the alpha 2-macroglobulin receptor/low density lipoprotein receptor-related protein. Eur J Endocrinol 139 (2):224-230

Bísaro de Lorenc L, Ramos AM, Sánchez MC, Montenegro R, Chiabrando GA (2005) Structural evaluation of plasma α2-macroglobulin in acute pancreatitis. Clinical Chemical Laboratory Medicine 43 (11):1183-1189

Blackburn MB, Farrar RR, Novak NG, Lawrence SD (2006) Remarkable susceptibility of the diamondback moth (Plutella xylostella) to ingestion of Pir toxins from Photorhabdus luminescens. Entomologia experimentalis et applicata 121 (1):31-37

Bonami JR, Hasson KW, Mari J, Poulos BT, Lightner DV (1997) Taura syndrome of marine penaeid shrimp: characterization of the viral agent. J Gen Virol 78 (Pt 2):313-319

Bonami JR, Trumper B, Mari J, Brehelin M, Lightner DV (1990) Purification and characterization of the infectious hypodermal and haematopoietic necrosis virus of penaeid shrimps. J Gen Virol 71 (Pt 11):2657-2664

Boonyaratpalin S, Supamattaya K, Kasornchandra J, Direkbusaracom S, Aekpanithanpong U, Chantanachooklin C (1993) Non-Occluded Baculo-like Virus, the Causative Agent of Yellow Head Disease in the Black Tiger Shrimp (Penaeus monodon). Gyobyo Ken 28 (3):103-109

Bowman TE, Abele LG (1982) Classification of the recent Crustacea. The biology of Crustacea 1:1-27

Bradford MM (1976) A rapid and sensitive method for the quantitation of microgram quantities of protein utilizing the principle of protein-dye binding. Analytical biochemistry 72 (1):248-254

Buresova V, Hajdusek O, Franta Z, Sojka D, Kopacek P (2009) IrAM-An alpha2-macroglobulin from the hard tick Ixodes ricinus: characterization and function in phagocytosis of a potential pathogen Chryseobacterium indologenes. Dev Comp Immunol 33 (4):489-498. doi:10.1016/j.dci.2008.09.011

Cano-Gomez A, Bourne DG, Hall MR, Owens L, Høj L (2009) Molecular identification, typing and tracking of Vibrio harveyi in aquaculture systems: current methods and future prospects. Aquaculture 287 (1):1-10

Cerenius L, Soderhall K (2011) Coagulation in invertebrates. J Innate Immun 3 (1):3-8. doi:10.1159/000322066

Chaikeeratisak V, Somboonwiwat K, Tassanakajon A (2012) Shrimp alpha-2-macroglobulin prevents the bacterial escape by inhibiting fibrinolysis of blood clots. PloS one 7 (10):e47384. doi:10.1371/journal.pone.0047384

Chaikeeratisak V, Tassanakajon A, Armstrong PB (2014) Interaction of pathogenic vibrio bacteria with the blood clot of the pacific white shrimp, Litopenaeus vannamei. Biol Bull 226 (2):102-110

Chantanachookin C, Boonyaratpalin S, Kasornchandra J, Direkbusarakom S, Ekpanithanpong U, Supamataya K, Sriurairatana S, Flegel T (1993) Histology and ultrastructure reveal a new granulosis-like virus in Penaeus monodon affected by yellow-head disease. Diseases of aquatic organisms 17:145-145

Charoensapsri W, Amparyup P, Hirono I, Aoki T, Tassanakajon A (2009) Gene silencing of a prophenoloxidase activating enzyme in the shrimp, Penaeus monodon, increases susceptibility to Vibrio harveyi infection. Dev Comp Immunol 33 (7):811-820. doi:10.1016/j.dci.2009.01.006

Charoensapsri W, Amparyup P, Hirono I, Aoki T, Tassanakajon A (2011) PmPPAE2, a new class of crustacean prophenoloxidase (proPO)-activating enzyme and its role in PO activation. Dev Comp Immunol 35 (1):115-124. doi:10.1016/j.dci.2010.09.002

Chen J, Chu Y, Cao J, Wang W, Liu J, Wang J (2011) Effects of T-2 toxin and selenium on chondrocyte expression of matrix metalloproteinases (MMP-1, MMP-13), alpha2-macroglobulin (alpha2M) and TIMPs. Toxicol In Vitro 25 (2):492-499. doi:10.1016/j.tiv.2010.12.001

Chen LL, Lo CF, Chiu YL, Chang CF, Kou GH (2000) Natural and experimental infection of white spot syndrome virus (WSSV) in benthic larvae of mud crab Scylla serrata. Diseases of aquatic organisms 40 (2):157-161. doi:10.3354/dao040157

Chen MY, Hu KY, Huang CC, Song YL (2005) More than one type of transglutaminase in invertebrates? A second type of transglutaminase is involved in shrimp

coagulation. Dev Comp Immunol 29 (12):1003-1016. doi:10.1016/j.dci.2005.03.012

Chen WY, Ho KC, Leu JH, Liu KF, Wang HC, Kou GH, Lo CF (2008) WSSV infection activates STAT in shrimp. Dev Comp Immunol 32 (10):1142-1150. doi:10.1016/j.dci.2008.03.003

Cheng W, Tsai IH, Huang CJ, Chiang PC, Cheng CH, Yeh MS (2008) Cloning and characterization of hemolymph clottable proteins of kuruma prawn (Marsupenaeus japonicus) and white shrimp (Litopenaeus vannamei). Dev Comp Immunol 32 (3):265-274. doi:10.1016/j.dci.2007.05.009

Chiang H-C, Lo C-F (1995) Pathogenicity of a baculovirus infection causing white spot syndrome in cultured penaeid shrimp in Taiwan. Diseases of aquatic organisms 23:165-173

Chotigeat W, Deachamag P, Phongdara A (2007) Identification of a protein binding to the phagocytosis activating protein (PAP) in immunized black tiger shrimp. Aquaculture 271 (1):112-120

Chuang WH, Liu PC, Hung CY, Lee KK (2014) Purification, characterization and molecular cloning of alpha-2-macroglobulin in cobia, *Rachycentron canadum*. Fish Shellfish Immunol 41 (2):346-355. doi:10.1016/j.fsi.2014.09.016

Conklin DE (2003) Use of soybean meal in the diets of marine shrimp. Department of Animal Science, University of California Davis, United Soybean Board and American Soybean Association

Craig-Barnes HA, Doumouras BS, Palaniyar N (2010) Surfactant protein D interacts with alpha2-macroglobulin and increases its innate immune potential. J Biol Chem 285 (18):13461-13470. doi:10.1074/jbc.M110.108837

Daniele S, Taliani S, Da Pozzo E, Giacomelli C, Costa B, Trincavelli ML, Rossi L, La Pietra V, Barresi E, Carotenuto A, Limatola A, Lamberti A, Marinelli L, Novellino E, Da Settimo F, Martini C (2014) Apoptosis therapy in cancer: the first single-molecule co-activating p53 and the translocator protein in glioblastoma. Sci Rep 4:4749. doi:10.1038/srep04749

Decha P, Rungrotmongkol T, Intharathep P, Malaisree M, Aruksakunwong O, Laohpongspaisan C, Parasuk V, Sompornpisut P, Pianwanit S, Kokpol S (2008)

Source of high pathogenicity of an avian influenza virus H5N1: why H5 is better cleaved by furin. Biophysical journal 95 (1):128-134

Duchaud E, Rusniok C, Frangeul L, Buchrieser C, Givaudan A, Taourit S, Bocs S, Boursaux-Eude C, Chandler M, Charles JF, Dassa E, Derose R, Derzelle S, Freyssinet G, Gaudriault S, Medigue C, Lanois A, Powell K, Siguier P, Vincent R, Wingate V, Zouine M, Glaser P, Boemare N, Danchin A, Kunst F (2003) The genome sequence of the entomopathogenic bacterium Photorhabdus luminescens. Nat Biotechnol 21 (11):1307-1313. doi:10.1038/nbt886

Egidius E (1987) Vibriosis: pathogenicity and pathology. A review. Aquaculture 67 (1):15-28

Eldred B, Hutton RF (1960) On the grading and identification of domestic commercial shrimps (Family Penaeidae) with a tentative world list of commercial Penaeids. Florida State Board of Conservation, Marine Laboratory,

Ellis AE (1987) Inhibition of the *Aeromonas salmonicida* extracellular protease by alpha 2-macroglobulin in the serum of rainbow trout. Microb Pathog 3 (3):167-177

Elrod-Erickson M, Mishra S, Schneider D (2000) Interactions between the cellular and humoral immune responses in Drosophila. Curr Biol 10 (13):781-784

Fauquet CM, Mayo MA, Maniloff J, Desselberger U, Ball LA (2005) Virus taxonomy: VIIIth report of the International Committee on Taxonomy of Viruses. Academic Press,

Feldman SR, Rosenberg MR, Ney KA, Michalopoulos G, Pizzo SV (1985) Binding of alpha 2-macroglobulin to hepatocytes: mechanism of in vivo clearance. Biochem Biophys Res Commun 128 (2):795-802

Ffrench-Constant RH, Anthony N, Aronstein K, Rocheleau T, Stilwell G (2000) Cyclodiene insecticide resistance: from molecular to population genetics. Annu Rev Entomol 45:449-466. doi:10.1146/annurev.ento.45.1.449

Flegel T (2006) Detection of major penaeid shrimp viruses in Asia, a historical perspective with emphasis on Thailand. Aquaculture 258 (1):1-33

Flegel TW (2007) Update on viral accommodation, a model for host-viral interaction in shrimp and other arthropods. Dev Comp Immunol 31 (3):217-231. doi:10.1016/j.dci.2006.06.009

Flegel TW (2012) Historic emergence, impact and current status of shrimp pathogens in Asia. J Invertebr Pathol 110 (2):166-173. doi:10.1016/j.jip.2012.03.004

Flegel TW, Sritunyalucksana K (2011) Shrimp molecular responses to viral pathogens. Mar Biotechnol (NY) 13 (4):587-607. doi:10.1007/s10126-010-9287-x

Fujimoto K, Okino N, Kawabata S, Iwanaga S, Ohnishi E (1995) Nucleotide sequence of the cDNA encoding the proenzyme of phenol oxidase A1 of Drosophila melanogaster. Proc Natl Acad Sci U S A 92 (17):7769-7773

Fukasawa S, Nakamura K, Miyahira M, Kurata M (1988) Some properties of two proteinases from a luminous bacterium, Vibrio harveyi strain FLN-108. Agricultural and biological chemistry 52 (12):3009-3014

Galliano MF, Toulza E, Gallinaro H, Jonca N, Ishida-Yamamoto A, Serre G, Guerrin M (2006) A novel protease inhibitor of the alpha2-macroglobulin family expressed in the human epidermis. J Biol Chem 281 (9):5780-5789. doi:10.1074/jbc.M508017200

Gillespie JP, Kanost MR, Trenczek T (1997) Biological mediators of insect immunity. Annu Rev Entomol 42:611-643. doi:10.1146/annurev.ento.42.1.611

Gollas-Galvan T, Sotelo-Mundo RR, Yepiz-Plascencia G, Vargas-Requena C, Vargas-Albores F (2003) Purification and characterization of alpha 2-macroglobulin from the white shrimp (Penaeus vannamei). Comp Biochem Physiol C Toxicol Pharmacol 134 (4):431-438

Hall M, Scott T, Sugumaran M, Soderhall K, Law JH (1995) Proenzyme of Manduca sexta phenol oxidase: purification, activation, substrate specificity of the active enzyme, and molecular cloning. Proc Natl Acad Sci U S A 92 (17):7764-7768

Hall M, Söderhäll K (1994) Crayfish α-macroglobulin as a substrate for transglutaminases. Comparative Biochemistry and Physiology Part B: Comparative Biochemistry 108 (1):65-72

Hall M, Soderhall K, Sottrup-Jensen L (1989) Amino acid sequence around the thiolester of alpha 2-macroglobulin from plasma of the crayfish, Pacifastacus leniusculus. FEBS Lett 254 (1-2):111-114

Hall M, Wang R, van Antwerpen R, Sottrup-Jensen L, Soderhall K (1999) The crayfish plasma clotting protein: a vitellogenin-related protein responsible for clot formation in crustacean blood. Proc Natl Acad Sci U S A 96 (5):1965-1970

Han JE, Tang KF, Tran LH, Lightner DV (2015) Photorhabdus insect-related (Pir) toxin-like genes in a plasmid of Vibrio parahaemolyticus, the causative agent of acute hepatopancreatic necrosis disease (AHPND) of shrimp. Diseases of aquatic organisms 113 (1):33-40

Harpel PC (1973) Studies on human plasma α2-macroglobulin-enzyme interactions Evidence for proteolytic modification of the subunit chain structure. The Journal of experimental medicine 138 (3):508-521

Hnasko R, Lin A, McGarvey JA, Stanker LH (2011) A rapid method to improve protein detection by indirect ELISA. Biochem Biophys Res Commun 410 (4):726-731. doi:10.1016/j.bbrc.2011.06.005

Hoffmann R, Baillie GS, MacKenzie SJ, Yarwood SJ, Houslay MD (1999) The MAP kinase ERK2 inhibits the cyclic AMP-specific phosphodiesterase HSPDE4D3 by phosphorylating it at Ser579. EMBO J 18 (4):893-903. doi:10.1093/emboj/18.4.893

Huang CC, Sritunyalucksana K, Soderhall K, Song YL (2004) Molecular cloning and characterization of tiger shrimp (Penaeus monodon) transglutaminase. Dev Comp Immunol 28 (4):279-294

Ishihara M, Kawanishi A, Watanabe H, Tomochika K, Miyoshi S, Shinoda S (2002) Purification of a serine protease of Vibrio parahaemolyticus and its characterization. Microbiol Immunol 46 (4):298-303

Iwanaga S, Lee BL (2005) Recent advances in the innate immunity of invertebrate animals. J Biochem Mol Biol 38 (2):128-150

Jang IK, Pang Z, Yu J, Kim SK, Seo HC, Cho YR (2011) Selectively enhanced expression of prophenoloxidase activating enzyme 1 (PPAE1) at a bacteria clearance site in the white shrimp, Litopenaeus vannamei. BMC Immunol 12:70. doi:10.1186/1471-2172-12-70

Jiravanichpaisal P, Lee BL, Soderhall K (2006) Cell-mediated immunity in arthropods: hematopoiesis, coagulation, melanization and opsonization. Immunobiology 211 (4):213-236. doi:10.1016/j.imbio.2005.10.015

Jittivadhna K (2000) PCR-based Detection of Hepatopancreatic Parvovirus and White-spot Syndrome Virus in Penaeus Monodon. Mahidol University,

Kanost MR (1999) Serine proteinase inhibitors in arthropod immunity. Dev Comp Immunol 23 (4-5):291-301

Kawabata S, Koshiba T, Shibata T (2009) The lipopolysaccharide-activated innate immune response network of the horseshoe crab. ISJ 6:59-77

Kawabata T, Yasuhara Y, Ochiai M, Matsuura S, Ashida M (1995) Molecular cloning of insect pro-phenol oxidase: a copper-containing protein homologous to arthropod hemocyanin. Proc Natl Acad Sci U S A 92 (17):7774-7778

Kim SK, Yang JY, Cha J (2002) Cloning and sequence analysis of a novel metalloprotease gene from Vibrio parahaemolyticus 04. Gene 283 (1-2):277-286

Kitani H (1986) Larval development of the white shrimp Penaeus vannamei BOONE reared in the laboratory and the statistical observation of its naupliar stages. Bulletin of the Japanese Society of Scientific Fisheries 52 (7):1131-1139

Kitani H (1993) Morphology of Postlarvae of the Whiteleg Shrimp Penaeus vannamei. Bulletin of the Japanese Society of Scientific Fisheries 59 (2):223-227

Kitani H (1994) Identification of Wild Postlarvae of the Penaeid Shrimps, Genus Penaeus, in the Pacific Coast of Central America. Fisheries science 60 (3):243-247

Kobayashi M, Johansson MW, Söderhäll K (1990) The 76 kD cell-adhesion factor from crayfish haemocytes promotes encapsulation in vitro. Cell and Tissue Research 260 (1):13-18

Kondo H, Tinwongger S, Proespraiwong P, Mavichak R, Unajak S, Nozaki R, Hirono I (2014) Draft Genome Sequences of Six Strains of Vibrio parahaemolyticus Isolated from Early Mortality Syndrome/Acute Hepatopancreatic Necrosis Disease Shrimp in Thailand. Genome Announc 2 (2). doi:10.1128/genomeA.00221-14

Laskowski M, Jr., Kato I (1980) Protein inhibitors of proteinases. Annu Rev Biochem 49:593-626. doi:10.1146/annurev.bi.49.070180.003113

Lavine MD, Strand MR (2002) Insect hemocytes and their role in immunity. Insect Biochem Mol Biol 32 (10):1295-1309

Leaño EM, Mohan C (2012) Early mortality syndrome threatens Asia's shrimp farms. Global Aquaculture Advocate:38-39

Lee SY, Soderhall K (2002) Early events in crustacean innate immunity. Fish & shellfish immunology 12 (5):421-437

Leu JH, Chen SH, Wang YB, Chen YC, Su SY, Lin CY, Ho JM, Lo CF (2011) A review of the major penaeid shrimp EST studies and the construction of a shrimp transcriptome database based on the ESTs from four penaeid shrimp. Mar Biotechnol (NY) 13 (4):608-621. doi:10.1007/s10126-010-9286-y

Levashina EA, Moita LF, Blandin S, Vriend G, Lagueux M, Kafatos FC (2001) Conserved role of a complement-like protein in phagocytosis revealed by dsRNA knockout in cultured cells of the mosquito, Anopheles gambiae. Cell 104 (5):709-718

Lightner D, Redman R, Bell T, Brock J (1983) Detection of IHHN virus in Penaeus stylirostris and P. vannamei imported into Hawaii. Journal of the World Mariculture Society 14 (1-4):212-225

Lightner DV, Redman RM, Pantoja CR, Tang KF, Noble BL, Schofield P, Mohney LL, Nunan LM, Navarro SA (2012) Historic emergence, impact and current status of shrimp pathogens in the Americas. J Invertebr Pathol 110 (2):174-183. doi:10.1016/j.jip.2012.03.006

Limsuwan C (1991) Handbook for cultivation of black tiger prawns. Tansetakit Co Ltd, Bangkok

Lin YC, Vaseeharan B, Chen JC (2008) Molecular cloning and phylogenetic analysis on alpha2-macroglobulin (alpha2-M) of white shrimp Litopenaeus vannamei. Dev Comp Immunol 32 (4):317-329. doi:10.1016/j.dci.2007.07.002

Lin YC, Vaseeharan B, Ko CF, Chiou TT, Chen JC (2007) Molecular cloning and characterisation of a proteinase inhibitor, alpha 2-macroglobulin (alpha2-M) from the haemocytes of tiger shrimp Penaeus monodon. Mol Immunol 44 (6):1065-1074. doi:10.1016/j.molimm.2006.08.002

Lin Z, Lo A, Simeone DM, Ruffin MT, Lubman DM (2012) An N-glycosylation Analysis of Human Alpha-2-Macroglobulin Using an Integrated Approach. J Proteomics Bioinform 5:127-134. doi:10.4172/jpb.1000224

Lo C, Leu J-H, Ho C, Chen C, Peng S, Chen Y, Chou C, Yeh P, Huang C, Chou H (1996) Detection of baculovirus associated with white spot syndrome (WSBV) in penaeid shrimps using polymerase chain reaction. Diseases of aquatic organisms 25:133-141

Ma H, Wang B, Zhang J, Li F, Xiang J (2010) Multiple forms of alpha-2 macroglobulin in shrimp Fenneropenaeus chinesis and their transcriptional response to WSSV or Vibrio pathogen infection. Dev Comp Immunol 34 (6):677-684. doi:10.1016/j.dci.2010.01.014

Mari J, Poulos BT, Lightner DV, Bonami JR (2002) Shrimp Taura syndrome virus: genomic characterization and similarity with members of the genus Cricket paralysis-like viruses. J Gen Virol 83 (Pt 4):915-926

Marrero A, Duquerroy S, Trapani S, Goulas T, Guevara T, Andersen GR, Navaza J, Sottrup-Jensen L, Gomis-Ruth FX (2012) The crystal structure of human alpha2-macroglobulin reveals a unique molecular cage. Angew Chem Int Ed Engl 51 (14):3340-3344. doi:10.1002/anie.201108015

Martin GG, Omori JEHS, Chong C, Hoodbhoy T, McKrell N (1991) Localization and roles of coagulogen and transglutaminase in hemolymph coagulation in decapod crustaceans. Comparative Biochemistry and Physiology Part B: Comparative Biochemistry 100 (3):517-522

Mayo M (2002) virology division news: ICTV at the Paris ICV: Results of the Plenary Session and the Binomial Ballot. Archives of virology 147 (11):2254-2260

Mayo M (2005) Changes to virus taxonomy 2004. Archives of Virology 150 (1):189-198

Medzhitov R, Janeway Jr CA Innate immune recognition and control of adaptive immune responses. In: Seminars in immunology, 1998. vol 5. Elsevier, pp 351-353

Melchior R, Quigley JP, Armstrong PB (1995) Alpha 2-macroglobulin-mediated clearance of proteases from the plasma of the American horseshoe crab, Limulus polyphemus. J Biol Chem 270 (22):13496-13502

Melo MN, Ferre R, Castanho MA (2009) Antimicrobial peptides: linking partition, activity and high membrane-bound concentrations. Nat Rev Microbiol 7 (3):245-250. doi:10.1038/nrmicro2095

Meyer C, Hinrichs W, Hahn U (2012) Human alpha2-macroglobulin--another variation on the venus flytrap. Angew Chem Int Ed Engl 51 (21):5045-5047. doi:10.1002/anie.201201104

MIYOSHI Si (2006) Vibrio vulnificus infection and metalloprotease. The Journal of dermatology 33 (9):589-595

Monti GE, Frankena K, Engel B, Buist W, Tarabla HD, de Jong MC (2005) Evaluation of a new antibody-based enzyme-linked immunosorbent assay for the detection of bovine leukemia virus infection in dairy cattle. J Vet Diagn Invest 17 (5):451-457

Neitzel J (2010) Enzyme catalysis: the serine proteases. Nat Educ 3:21-25

Pech LL, Strand MR (2000) Plasmatocytes from the moth Pseudoplusia includens induce apoptosis of granular cells. J Insect Physiol 46 (12):1565-1573

Peng S-E, Lo C-F, Liu K-F, Kou G-H (1998) The Transition from Pre-patent to Patent Infection of White Spot Syndrome Virus (WSSV) in Penaeus monodon Triggered by Pereiopod Excision. Fish Pathology 33 (4):395-400

Perazzolo LM, Bachere E, Rosa RD, Goncalves P, Andreatta ER, Daffre S, Barracco MA (2011) Alpha2-macroglobulin from an Atlantic shrimp: biochemical characterization, sub-cellular localization and gene expression upon fungal challenge. Fish & shellfish immunology 31 (6):938-943. doi:10.1016/j.fsi.2011.08.011

Perazzolo LM, Barracco MA (1997) The prophenoloxidase activating system of the shrimp Penaeus paulensis and associated factors. Dev Comp Immunol 21 (5):385-395

Phee BK, Shin DH, Cho JH, Kim SH, Kim JI, Lee YH, Jeon JS, Bhoo SH, Hahn TR (2006) Identification of phytochrome-interacting protein candidates in Arabidopsis

thaliana by co-immunoprecipitation coupled with MALDI-TOF MS. Proteomics 6 (12):3671-3680. doi:10.1002/pmic.200500222

Phuoc LH, Corteel M, Nauwynck HJ, Pensaert MB, Alday-Sanz V, Van den Broeck W, Sorgeloos P, Bossier P (2008) Increased susceptibility of white spot syndrome virus-infected Litopenaeus vannamei to Vibrio campbellii. Environ Microbiol 10 (10):2718-2727. doi:10.1111/j.1462-2920.2008.01692.x

Ponce-Palafox J, Martinez-Palacios CA, Ross LG (1997) The effects of salinity and temperature on the growth and survival rates of juvenile white shrimp, Penaeus vannamei, Boone, 1931. Aquaculture 157 (1):107-115

Powell A, Rowley AF (2007) The effect of dietary chitin supplementation on the survival and immune reactivity of the shore crab, Carcinus maenas. Comp Biochem Physiol A Mol Integr Physiol 147 (1):122-128. doi:10.1016/j.cbpa.2006.12.027

Rao AV (2002) Vibriosis in Shrimp Aquaculture. Neospark Drugs and Chemicals Pvt Ltd

Rattanachai A, Hirono I, Ohira T, Takahashi Y, Aoki T (2004) Molecular cloning and expression analysis of alpha 2-macroglobulin in the kuruma shrimp, Marsupenaeus japonicus. Fish & shellfish immunology 16 (5):599-611. doi:10.1016/j.fsi.2003.09.011

Rehman AA, Ahsan H, Khan FH (2013) alpha-2-Macroglobulin: a physiological guardian. J Cell Physiol 228 (8):1665-1675. doi:10.1002/jcp.24266

Ren L, Emery D, Kaboord B, Chang E, Qoronfleh MW (2003) Improved immunomatrix methods to detect protein:protein interactions. J Biochem Biophys Methods 57 (2):143-157

Sambrook J, Russell David W (1989) Molecular cloning: a laboratory manual. Vol. 3. Cold spring harbor laboratory press,

Savige JA, Paspaliaris B, Silvestrini R, Davies D, Nikoloutsopoulos T, Sturgess A, Neil J, Pollock W, Dunster K, Hendle M (1998) A review of immunofluorescent patterns associated with antineutrophil cytoplasmic antibodies (ANCA) and their differentiation from other antibodies. J Clin Pathol 51 (8):568-575

Schweitzer CE, Feldmann RM (2000) Re-evaluation of the Cancridae Latreille, 1802 (Decapoda: Brachyura) including three new genera and three new species. Contributions to Zoology 69 (4):223-250

Sengprasert P, Amparyup P, Tassanakajorn A, Wongpanya R (2015) Characterization and identification of calmodulin and calmodulin binding proteins in hemocyte of the black tiger shrimp (Penaeus monodon). Dev Comp Immunol 50 (2):87-97. doi:10.1016/j.dci.2015.02.003

Sharon N, Lis H (2004) History of lectins: from hemagglutinins to biological recognition molecules. Glycobiology 14 (11):53R-62R. doi:10.1093/glycob/cwh122

Shike H, Dhar AK, Burns JC, Shimizu C, Jousset FX, Klimpel KR, Bergoin M (2000) Infectious hypodermal and hematopoietic necrosis virus of shrimp is related to mosquito brevidensoviruses. Virology 277 (1):167-177. doi:10.1006/viro.2000.0589

Shinoda S, Miyoshi S-I (2011) Proteases produced by vibrios. Biocontrol science 16 (1):1-11

Sjobring U, Trojnar J, Grubb A, Akerstrom B, Bjorck L (1989) Ig-binding bacterial proteins also bind proteinase inhibitors. J Immunol 143 (9):2948-2954

Smith VJ, Soderhall K (1983) Induction of degranulation and lysis of haemocytes in the freshwater crayfish, Astacus astacus by components of the prophenoloxidase activating system in vitro. Cell Tissue Res 233 (2):295-303

Soderhall K (1999) Invertebrate immunity. Dev Comp Immunol 23 (4-5):263-266

Soderhall K, Aspan A, Duvic B (1990) The proPO-system and associated proteins; role in cellular communication in arthropods. Res Immunol 141 (9):896-907

Soderhall K, Cerenius L (1998) Role of the prophenoloxidase-activating system in invertebrate immunity. Curr Opin Immunol 10 (1):23-28

Somboonwiwat K, Chaikeeratisak V, Wang HC, Fang Lo C, Tassanakajon A (2010) Proteomic analysis of differentially expressed proteins in Penaeus monodon hemocytes after Vibrio harveyi infection. Proteome Sci 8:39. doi:10.1186/1477-5956-8-39

Sottrup-Jensen L (1989) Alpha-macroglobulins: structure, shape, and mechanism of proteinase complex formation. J Biol Chem 264 (20):11539-11542

Sritunyalucksana K, Söderhäll K (2000) The proPO and clotting system in crustaceans. Aquaculture 191 (1):53-69

Sung HH, Chang HJ, Her CH, Chang JC, Song YL (1998) Phenoloxidase activity of hemocytes derived from Penaeus monodon and Macrobrachium rosenbergii. J Invertebr Pathol 71 (1):26-33. doi:10.1006/jipa.1997.4703

Tassanakajon A, Amparyup P, Somboonwiwat K, Supungul P (2010) Cationic antimicrobial peptides in penaeid shrimp. Mar Biotechnol (NY) 12 (5):487-505. doi:10.1007/s10126-010-9288-9

Tassanakajon A, Somboonwiwat K, Supungul P, Tang S (2013) Discovery of immune molecules and their crucial functions in shrimp immunity. Fish & shellfish immunology 34 (4):954-967. doi:10.1016/j.fsi.2012.09.021

Tavares C, Martin JW (2010) Suborder Dendrobranchiata Bate, 1888. Treatise on Zoology–Anatomy, Taxonomy, Biology The Crustacea A 9:99-164

Teo JW, Zhang LH, Poh CL (2003) Cloning and characterization of a metalloprotease from Vibrio harveyi strain AP6. Gene 303:147-156

Tonganunt M, Phongdara A, Chotigeat W, Fujise K (2005) Identification and characterization of syntenin binding protein in the black tiger shrimp Penaeus monodon. J Biotechnol 120 (2):135-145. doi:10.1016/j.jbiotec.2005.06.006

Tran L, Nunan L, Redman RM, Mohney LL, Pantoja CR, Fitzsimmons K, Lightner DV (2013) Determination of the infectious nature of the agent of acute hepatopancreatic necrosis syndrome affecting penaeid shrimp. Diseases of aquatic organisms 105 (1):45-55. doi:10.3354/dao02621

Tyndall JD, Nall T, Fairlie DP (2005) Proteases universally recognize beta strands in their active sites. Chem Rev 105 (3):973-999. doi:10.1021/cr040669e

van Eijk M, van Noorden CJ, de Groot C (2003) Proteinases and their inhibitors in the immune system. Int Rev Cytol 222:197-236

Vargas-Albores F, Hinojosa-Baltazar P, Portillo-Clark G, Magallon-Barajas F (1998) Influence of temperature and salinity on the yellowleg shrimp, Penaeus californieinsis Holmes, prophenoloxidase system. Aquaculture Research 29 (8):549-553

Vazquez-Bader AR, Carrero JC, Garcia-Varela M, Grcia A, Laclette JP (2004) Molecular phylogeny of superfamily Penaeoidea Rafinesque-Schmaltz, 1815, based on

mitochondrial 16S partial sequence analysis. Journal of Shellfish Research 23 (3):911-918

Walker P, Cowley J, Spann K, Hodgson RR, Hall MM, Withyachumnarnkul BB (2001) Yellow head complex viruses: transmission cycles and topographical distribution in the Asia-Pacific region. The New Wave: Proceedings of the Special Session on Sustainable Shrimp Culture, Aquaculture 2001-pages: 227-237

Wang R, Liang Z, Hal M, Soderhall K (2001) A transglutaminase involved in the coagulation system of the freshwater crayfish, Pacifastacus leniusculus. Tissue localisation and cDNA cloning. Fish & shellfish immunology 11 (7):623-637

Westenberg M, Heinhuis B, Zuidema D, Vlak JM (2005) siRNA injection induces sequence-independent protection in Penaeus monodon against white spot syndrome virus. Virus Res 114 (1-2):133-139. doi:10.1016/j.virusres.2005.06.006

Wladyka B, Pustelny K (2008) Regulation of bacterial protease activity. Cell Mol Biol Lett 13 (2):212-229. doi:10.2478/s11658-007-0048-4

Wonteerasupaya C, Vickers JE, Sriurairatana S, Nash GL, Akarajamorn A, Boonsaeng V, Panyim S, Tassanakajon A, Withyachumnarnkul B, Flegel T (1995) A non-occluded, systemic baculovirus that occurs in cells of ectodermal and mesodermal origin and causes high mortality in the black tiger prawn Penaeus monodon. Diseases of aquatic organisms 21 (1):69-77

Wyban J (2007) Thailand's shrimp revolution. Aquaculture Asia-Pacific Magazine 2007:15-18

Yang Y-T, Chen I-T, Lee C-T, Chen C-Y, Lin S-S, Hor L-I, Tseng T-C, Huang Y-T, Sritunyalucksana K, Thitamadee S (2014) Draft genome sequences of four strains of Vibrio parahaemolyticus, three of which cause early mortality syndrome/acute hepatopancreatic necrosis disease in shrimp in China and Thailand. Genome announcements 2 (5):e00816-00814

Yotmanee P, Rungrotmongkol T, Wichapong K, Choi SB, Wahab HA, Kungwan N, Hannongbua S (2015) Binding Specificity of Polypeptide Substrates in NS2B/NS3pro Serine Protease of Dengue Virus Type 2: A Molecular Dynamics Study. Journal of Molecular Graphics and Modelling

Young JH (1959) Morphology of the white shrimp Penaeus setiferus (Linnaeus 1758). US Government Printing Office,

Youtong W, Deachamag P, Phongdara A, Chotigeat W (2011) WSSV: VP26 binding protein and its biological activity. Fish & shellfish immunology 30 (1):77-83. doi:10.1016/j.fsi.2010.09.008

Yu MS, Lee CY (1999) Expression and characterization of the prtV gene encoding a collagenase from Vibrio parahaemolyticus in Escherichia coli. Microbiology 145 (Pt 1):143-150

Zhan W, Wang X, Chi Y, Tang X (2013) The VP37-binding protein F1ATP synthase beta subunit involved in WSSV infection in shrimp Litopenaeus vannamei. Fish & shellfish immunology 34 (1):228-235. doi:10.1016/j.fsi.2012.10.019

APPENDIX

VITA

Mr. Witchanon Wongbaucheun was born in November 15, 1986 in Phetchaburi. He graduated with the degree of Bachelor of Science from the Department of Chemistry, Faculty of Science, Silpakorn University in 2009. He has studied for the degree of Master of Science, Program in Biochemistry and Molecular Biology, Department of Biochemistry, Faculty of Science, Chulalongkorn University since 2010.